Année 2012
Numéro d'ordre : 2012ISAL0123

Thèse

Modèles individu-centrés de l'impact fonctionnel des hétérogénéités de diffusion et de distribution spatiale des protéines de signalisation cellulaire

Présentée devant
L'institut National des Sciences Appliquées de Lyon

Pour obtenir
Le grade de docteur

École doctorale
École doctorale Informatique et Mathématiques (ED512)

Par
Bertrand Caré
Ingénieur INSA Lyon Bioinformatique et Modélisation

Soutenue le 26 novembre 2012 devant la commission d'examen :

Jury MM.

Carson C. Chow	Directeur de Recherche, NIH, Rapporteur
Dirk Drasdo	Directeur de Recherche, INRIA, Rapporteur
Ovidiu Radulescu	Professeur, Université Montpellier 2, Examinateur
Guillaume Beslon	Professeur, INSA Lyon, Examinateur
Christophe Rigotti	Maître de Conférences HDR, INSA Lyon, Directeur de thèse
Hédi Soula	Maître de Conférences, INSA Lyon, Directeur de thèse

Laboratoire de recherche :

Laboratoire d'InfoRmatique en Image et Systèmes d'information
LIRIS CNRS UMR5205

Année 2012
Numéro d'ordre :2012ISAL0123

PhD Thesis

Individual-based models for the functional impact of signalling proteins spatial distribution and diffusion heterogeneity

Présentée devant
L'institut National des Sciences Appliquées de Lyon

Pour obtenir
Le grade de docteur

École doctorale
École doctorale Informatique et Mathématiques (ED512)

Par
Bertrand Caré
Ingénieur INSA Lyon Bioinformatique et Modélisation

Soutenue le 26 novembre 2012 devant la commission d'examen :

Jury MM.

Carson C. Chow	Directeur de Recherche, NIH, Rapporteur
Dirk Drasdo	Directeur de Recherche, INRIA, Rapporteur
Ovidiu Radulescu	Professeur, Université Montpellier 2, Examinateur
Guillaume Beslon	Professeur, INSA Lyon, Examinateur
Christophe Rigotti	Maître de Conférences HDR, INSA Lyon, Directeur de thèse
Hédi Soula	Maître de Conférences, INSA Lyon, Directeur de thèse

Laboratoire de recherche :
Laboratoire d'InfoRmatique en Image et Systèmes d'information
LIRIS CNRS UMR5205

Remerciements

I would like to warmly thank Carson Chow for accepting to review this manuscript and coming from the United States to attend my defence.

Je suspends un moment l'utilisation de l'anglais pour remercier chaleureusement toutes les personnes sans qui ces travaux n'auraient pu voir le jour. Mes pensées vont à eux, et aussi à tous ceux qui, s'ils n'ont peut-être pas tous directement contribué à faire de moi un scientifique, ont en tout cas contribué à mon bonheur par leur soutien et leur amitié ces trois dernières années. A ceux que je viendrais à oublier, je leur demande pardon, s'ils ne se trouvent pas dans ces lignes, ils sont assurément dans mes pensées.

J'aimerais remercier Dirk Drasdo qui a accepté de rapporter ce manuscrit. J'adresse mes remerciements à Ovidiu Radulescu, qui a accepté de prendre part au jury examinant mes travaux.

J'ai eu la chance d'avoir partagé le quotidien de deux équipes, et toute ma gratitude leur est acquise. Merci, donc, aux membres de l'équipe Beagle, du LIRIS et de l'INRIA. Je remercie Hugues Berry et Carole Knibbe, pour m'avoir fait profiter de leur expertise. Je pense également à David Parsons, Gaël Kaneko, Bérénice Batut, Stephan Fischer et Jules Lallouette pour leur sympathie et nos discussions. Je tiens à remercier à Guillaume Beslon, sa passion pour la modélisation du vivant si communicative a eu une influence indéniable sur mon parcours, et merci à lui d'avoir accepté de prendre part à mon jury de thèse.

Merci aux membres de Carmen et du département Biosciences. Je remercie Christophe Soulage et Nicolas Pillon, qui n'ont eu de cesse de parachever mes connaissances en biologie au cours de nombreuses discussions, pour leur amitié et leur aide. Je pense également à Marine Croze et Roxane Vella, ainsi qu'à Cyril Fayard, merci à eux pour ces discussions qui, fussent-elles à propos de science ou non, ont toujours été fructueuses. Je remercie Fabien Chaudier pour sa précieuse aide technique, et sa non moins précieuse sympathie, et je pense aussi à Sandrine Chevaleyre. J'aimerais remercier Hubert Charles, à qui la filière BIM et moi-même devons tant. Je remercie Hubert Vidal pour m'avoir accueilli en Carmen, et pour l'attention qu'il a porté à la modélisation.

J'aimerais également remercier Pascal Calvat et Yonni Cardenas sans qui je n'aurai pu dompter la puissance du Centre de Calcul de l'IN2P3. Je remercie la Région Rhône-Alpes qui a financé ce travail par une bourse du Cluster

ISLE.

J'aimerais exprimer toute ma reconnaissance à Christophe Rigotti, qui a accepté de diriger mes travaux de thèse. Son aide, ses questions toujours pertinentes et sa disponibilité furent d'un précieux secours durant ces trois ans.

Les quelques lignes qui vont suivre n'exprimeront pas assez toute la gratitude et la reconnaissance que j'ai pour Hédi Soula. Merci d'avoir accepté le lourd fardeau de ma formation de chercheur. Je garderai le souvenir de ce qui a été beaucoup plus qu'une direction, une inspiration.

J'aimerais conclure en remerciant Claire, pour son soutien indéfectible, sa patience, son affection. Je remercie mes parents pour leur soutien, ainsi que Sophie et Louis. Enfin, mes remerciements vont à Florent, Cédric, Romain, Jean-Rémi, Jérôme, Nathalie, merci pour tout et le reste.

Abstract

Signalling pathways allow cells to perceive and exchange information under the form of chemical signals. Such a signal generates a response of the cell through the crucial stages of reception and transduction. Different types of protein interact in a structured manner as a cascade of reactions that relay the signal from the exterior to the interior of the cell, notably through the membrane. Signalling proteins are restricted to compartments with different degrees of freedom, and diffuse either in the plasma membrane that is bidimensional interface, or in the cytoplasm which is tridimensional medium. Within these very diffusion spaces, the spatial distributions of signalling proteins are heterogeneous. The mathematical models of signalling pathways dynamics, however, classically assume that signalling proteins are distributed homogeneously.

We developed computational models of biochemical reactions between populations of molecules where the state and the position of each molecule are tracked. Diffusion and reaction between simulated molecules are reproduced based on biophysically accurate stochastic processes. Such granularity allows for the reproduction of heterogeneous spatial distributions and diffusion of signalling proteins as observed in biology, and the investigation of their effect on the functioning of a simulated signalling pathway.

First, we explored the effect of fixed heterogeneous receptor distributions on the extracellular ligand-receptor binding process. In simulation, receptors in clusters presented a decreased apparent affinity compared to the situation where they were distributed homogeneously. Clustering induced a redistribution of binding events that favored rebinding at short time scales at the expense of first passage binding events. Secondly, we explored the transduction stage between receptors and their membrane-bound signalling substrate at the membrane level. Clustering induced a decrease in response as well, and modified the structure of the dose-response relationship. Finally, we implemented a dynamical clustering mechanism in simulation, and reproduced the transduction stage on a membrane presenting non-homogeneous diffusion : restricted zones of low-diffusivity were introduced. When receptors and their substrate were co-clustered, an amplification effect was observed. When only receptors were clustered, the response was attenuated as observed with fixed receptor distributions.

Résumé

Les voies de signalisation cellulaires permettent aux cellules de percevoir et d'échanger de l'information sous la forme de signaux chimiques. Un tel signal génère une réponse de la cellule au travers des étapes cruciales de réception et transduction. Différents types de protéines sont organisés dans une cascade de réactions de proche en proche qui relaient le signal de l'extérieur vers l'intérieur de la cellule, notamment au travers de la membrane. Les protéines de signalisation sont restreintes à des compartiments avec des degrés de liberté différents, et diffusent soit dans la membrane cellulaire qui est bidimensionnelle, soit dans le cytoplasme qui est en trois dimensions. De plus, au sein même de ces espaces, leurs distributions respectives sont hétérogènes. Or l'étude de la dynamique des voies de signalisation repose classiquement sur des modèles mathématiques supposant une homogénéité de distribution spatiale.

Nous avons développé des modèles de réactions biochimiques entre populations de molécules oú l'état et la position de chaque molécule sont caractérisés. La diffusion et les interactions entre molécules simulées sont reproduites sur la base de processus stochastiques issus de la biophysique. Ceci permet de recréer des distributions spatiales et des modes de diffusion hétérogènes tels qu'observés en biologie et d'étudier leur effet sur la dynamique de la signalisation en simulation.

L'exploitation des modèles a été menée sur les différentes étapes de signalisation. Premièrement, l'étude a porté sur l'interaction entre un ligand dans le milieu extracellulaire et des récepteurs membranaires fixes. Lorsque les récepteurs forment des grappes au lieu d'être répartis uniformément, cela provoque une perte de sensibilité globale de l'étage de réception. Deuxièmement, l'analyse a été poursuivie au niveau de l'étage de transduction entre les récepteurs et un effecteur au niveau de la membrane. Là aussi, une distribution en grappe plutôt qu'uniforme des récepteurs provoque une perte de sensibilité. Enfin, l'étude s'est portée sur un modèle intégrant un mécanisme de diffusion non-homogène en mettant en interaction des récepteurs mobiles et leur substrat membranaire. Lorsque des zones restreintes de diffusion ralentie sont définies sur la membrane, deux effets opposés apparaissent sur la dynamique de transduction : un phénomène d'amplification si le ralentissement affecte les deux protéines, et un phénomène de perte de sensibilité si seuls les récepteurs sont ralentis.

Globalement, les résultats illustrent comment les hétérogénéités spatiales modifient les distributions de collision et d'évènements de réaction dans le temps et l'espace à l'échelle microscopique, et comment cela se traduit par un effet sur la dynamique globale de la voie de signalisation à l'échelle macroscopique.

Contents

List of Figures

List of Tables

Introduction

The activity of a living cell consists of a set of functions related to different purposes, such as maintaining its physical integrity, finding energetical and material resources, or proliferating. Within the molecular biology perspective, the cell achieves these functions by modifying the number and/or the state of the chemical compounds that both surround it (ions, nutrients, hormones, toxic chemicals, ...) and compose it (proteins, lipids, DNA, RNA, metabolites, ...). Determining these different molecular species and their respective amounts is a way to depict the state in which the cell is. Combined with knowledge of the interactions between the molecular species that compose and surround the cell, it becomes theoretically possible to infer the evolution of said cell state. The association of the characterized set of molecular species involved in a specific function and the interactions between these species define a pathway.

The combined pathways of a cell constitute the biochemical network describing its operation. Pathways are typically represented as graphs, whose vertices are biomolecules and edges are interactions between biomolecules. This approach inscribes itself in the broader context of biological networks, which themselves emerged from the systems biology paradigm for living systems. As Aderem explains it [Aderem 2005], "*technology development during the 1980s permitted the concepts generated by many years of reductionist inquiry to be analyzed in the context of the entire system*", which is not a mere refutation of the reductionist approach to cell biology, but more of an expression of the potential of systems biology as a holistic paradigm in the resolution of challenging biological questions.

The topological analysis alone of pathways and networks as graphs yielded several particularly insightful results : the small world property in biochemical networks [Barabási 2004], network motifs [Milo 2002], to name a few. On a smaller network scale, another notable achievement is the characterization of the role of feedback loops in regulatory networks [Becskei 2000].

The next logical step in improving a graph as a investigation tool is to introduce quantitative rules behind the edges linking vertices, and numerical quantities behind these vertices. A given cell function's input and output can be seen as numbers of specific molecular species. The proper analysis of this function is enriched by understanding how changes in its input influence its output in a quantitative manner. Concrete examples for this is the analysis of

gene expression data, and pharmacodynamics, whose purpose is to quantify the influence of specific doses of active principles on physiological processes. Another motivation is to improve the predictive value of pathways in the context of wet experimentation. By characterizing the quantitative dynamics of a pathway, it is possible to infer targets for experimental pertubation and predict its quantitative outcome on other nodes of the network, which provides an experimental validation method for the model and new experimental perspectives.

More generally, systems biology helped identifiying characteristics properties of living systems [Aderem 2005], such as *Emergence* – simple deterministic local rules giving unexpected properties to a system, *Robustness* – maintained functional stability in spite of environmental and intrinsic pertubations, and *Modularity* – operation distributed among functional units. A substantial part of the inherent complexity of living systems was therefore addressed by using this approach. However, its extensive use comes with certain *caveats*. While mentioning the representation of biological regulatory systems as networks, Rosenfeld suggests that *"these schematic diagrams, apart from their scientific content and aesthetic appeal, produce an impression of solidity, determinacy and unlimited reusability"* [Rosenfeld 2011]. Lazebnik puts it in a somewhat more offensive manner : *"Biologists summarize their results with the help of all-too-well recognizable diagrams, in which a favorite protein is placed in the middle and connected as everything else with two-ways arrows."* [Lazebnik 2002]. Behind the intent to provoke the reader's reaction, these statements express an actual scientific concern : biochemical networks abstract the physico-chemicals aspects of the cell. The systems biology approach stemmed from the assumption that the problematic complexity of the cell resulted more from the multiplicity of components involved in a function, as well as the multiplicity of their interactions, than from the essence of these interactions itself or their physico-chemical articulations. However, as Weng depicts it in the context of cell signalling [Weng 1999], multiplicity of the proteins invovled and their interactions only makes for the first layer of complexity, the other ones resulting for instance from compartmentalization, scaffold proteins and the specificites of genetic biochemistry. At the light of these considerations, Rosenfeld's conception of the cell sums up the other sources of complexity : *"In a sense, any cell is a vast system of intertwined biochemical reactions in which complex compartmentalization, separation of time scales, spatial heterogeneity and hierarchical structure are the epiphenomena of comparatively simple and universal laws of chemical reactions"* [Rosenfeld 2011]. Biochemical networks address the latter part of this proposition, that is combining the components of the cell using simple and universal laws of chemical

reactions, but are not necessarily taylored for the efficient integration of compartmentalization, separation of time scales, and spatial heterogeneity.

Rosenfeld describes compartmentalization, separation of time scales and spatial heterogeneity as epiphenomena resulting from simple laws of chemical reactions, thus establishing a directed causal relationship between simple biomolecules interactions on one side, and complex physical properties that emerge from these interactions on another side. Another source of complexity comes from the influence of these physical properties on the processes that cause them. Among these properties, spatial heterogeneity, and spatiality more generally, stand as a crucial feature for living systems on multiple scales, including at the subcellular level. Hurtley enumerates various examples of the critical role of spatiality in the proper operation of cells [Hurtley 2009]. More specific examples applied to the problem of biochemical reaction systems given by Neves illustrate the need for spatially-resolved models [Neves 2009]. There is a convergence of studies pointing towards spatial structuration as a prerequisite of the information processing and multitasking capabilities of biochemical pathways [Fisher 2000, Jordan 2000, Graham 2005]. Finally, the temporal dynamics of signalling pathways seem to be highly dependent of the spatial structuration of the cell's signalling systems [Scott 2009, Kholodenko 2006], because this spatial organization determines when and where the physico-chemical interactions between proteins happen.

Cell signalling systems are examples of complex cellular functions, because of their information processing purpose, and their involvement in many other cellular functions such as metabolism, cell fate determination and adaptation to environmental perturbations. The above examples also highlight spatiality as a key factor in cell signalling systems, whose investigation need to rely on multiple scientifics disciplines and led on multiple temporal and spatial scales. How can we explore the role of spatiality in signalling systems ? Direct wet experimentation on living systems aimed at studying spatial heterogeneity in signalling is a difficult – although, as we will see, possible – task. It requires methods for measurement of molecule positions on the nanoscopic scale, and methods for influencing the spatial distributions of these molecules in order to obtain reproductible testable hypotheses. To these requirements adds another one, these experimental methods need not to disrupt the functioning of signalling systems except for the spatial distribution of its molecular effectors, so the observed effect on the pathway does not result from side effects caused by these methods. This work adopts a modelling approach. Using a minimal set of carefully chosen hypotheses that integrates knowledge from biochemistry, cell biology and physics, we can test hypotheses on a idealized, artificial

reproduction of our object of study. We do not intend to use models as merely descriptive imitations of signalling systems, but as interfaces between theory and our object of study that bear mechanistic insights.

Chapter I

Spatially-resolved models for cell signalling.

Contents

This chapter will establish the conceptual, theoretical and methodological bases upon which this thesis is built. Our current understanding of cellular functions is that the cell can be depicted as a vast assembly of interacting biomolecules. The most common representation of such a system is a biochemical network : a graph where biomolecules constitute vertices and interactions constitue edges. Biochemical networks allowed for significant advances in our understanding of cell biology, and we will argue though that several sources of complexity remain untapped by such an approach, in particular, the physical properties of the cellular environment. The introduction of sources of spatial heterogeneity, such as cell compartmentalization and non-homogeneous molecule distributions, will highlight spatiality as a central yet relatively unaddressed feature. This constitutes the motivation of this work.

I.1 Spatially-defined cell signalling systems

Cell signalling is a central mechanism involved in the regulation of many other cellular functions pertaining to different purpose. It also presents the interesting characteristic of being highly spatially structured, and to rely on this spatial organization in order to achieve its complex goals.

I.1.1 Principles and functions of cell signalling

We will detail the principles of cell signalling, the physico-chemical and biochemical aspects of signalling protein and their interactions, as well as the mechanisms governing their diffusion.

Koshland identifies seven core properties that a system needs to implement in order to be labelled as living : program, improvisation, compartmentalization, energy, regeneration, adaptability, and seclusion [Koshland 2002]. Compartmentalization expresses the necessity for such a system to insulate a restricted volume in order to achieve specific functions within this limited volume, in a controlled and physically protected environment. The cell's first and foremost characteristic is that it fulfills this role : the cell defines an inside and an outside. The counterpart of this separation is that, since it isolates a protected internal environment, the processes happening within this volume cannot adapt their functioning according to external perturbations. But the implementation of the other core properties pertaining to living systems, especially adaptability and improvisation, requires the existence of channels through which external signals can be perceived by the internal processes. This is solved by a mechanism called signal transduction [Berg 2002, Alberts 2002], which allows the cell to selectively perceive external chemical signals while maintaining its internal integrity and preserve its inner environment.

The principles of signalling are illustrated on Fig. I.1, and can be decomposed in three essential stages : reception, transduction, and response [Campbell 2007]. A molecular species, the ligand, is present in the external cell medium. The concentration of the ligand encodes a signal. The cell surface is covered with receptors, which are proteins composed of an extracellular domain accessible for ligand species, a transmembrane section, and an intracellular domain. The binding of a ligand molecule to a specific docking site in the extracellular domain triggers a modification of the intracellular domain (reception). This intracellular domain acquires the ability to interact with intracellular proteins and thus simultaneously convert and transmit the external signal inside the cell (transduction). The transduction stage is generally associated with amplification mechanisms. The intracellular signalling stage

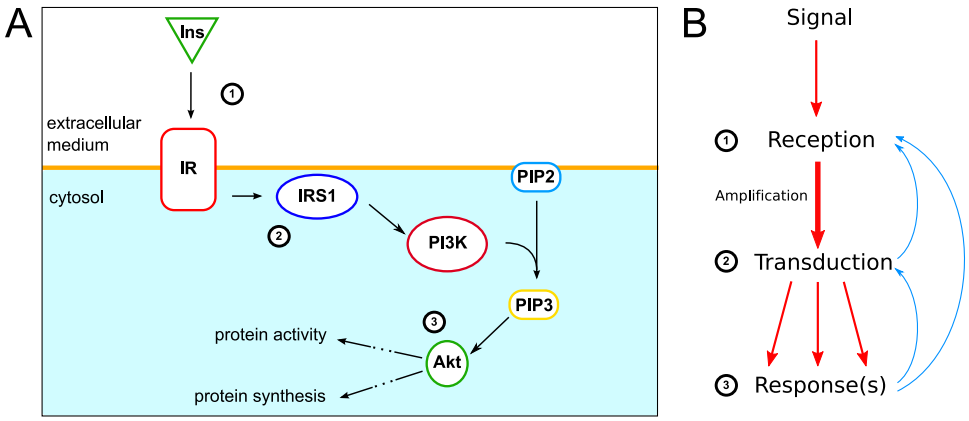

Figure I.1 – The basic functional description of cell signalling illustrated on the Insulin pathway. ***A.*** A chemical signal (here insulin) is located in the extracellular environment. It is perceived by a cell-surface receptor (insulin receptor or IR), which transmits it inside the cell (transduction) by converting it in another internal chemical signal (activation of IRS1) and possibly amplifying it. The internally relayed signal (through PI3K activation then PIP3 production then Akt activation) triggers a response, that is, the initiation, termination, or adaptation of a cellular process. The downstream cascade past Akt was summerized by dotted arrows. A short-term response can be generated in the cytoplasm by modifying protein activity, or in the nucleus by modifying gene expression. ***B.*** Most signalling pathways share the same common succession of steps, though implemented by different proteins. Reception, amplification and transduction can be controlled by feedback from the multiple stages of the signalling cascade (from [Berg 2002]).

involves secondary messengers that relay the signal further inside the cell. Finally, cellular functions are adapted according to this signal, as signalling proteins initiate, terminate, or modify their course (response). Signalling can trigger short-term response by modifying the processes happening in the cytoplasm (the *activity* of proteins), and long-term response by regulating the expression of genes in the nucleus (the *synthesis* of proteins). Feedback loops can exist at the different stages of this mechanism, in order to insure its efficiency. For instance, once the cellular function targeted by the signal has been initiated, negative regulatory feedback can decrease the transduction of the signal, so the cell does not over-respond.

The concentration of signalling proteins in different states along the cascade constitutes the encoding of the signal. If the signalling pathway is considered linear, the encoding is generally monotonic, meaning that the higher the ligand concentration, the higher the number of activated receptors, therefore the higher the number of activated intracellular proteins. This linear picture

however does not hold downstream as feedback links can regulate the upperstream stages of a cascade.

Such signalling systems regulate every function of the cell, from growth and proliferation (such as the Epidermal growth factor / Mitogen-activated protein kinases systems) to intercellular communication through hormones (such as insulin signalling), and they all share the same common functional design as illustrated in Fig. I.1.

I.1.2 Physico-chemical and biochemical aspects of signalling proteins interactions and motion

The first actor of signalling is the transmembrane receptor. Although intracellular receptors do exist and are involved in transduction from the cytoplasm to the nucleus, we will focus on extracellular receptors that transduce the signal from the external bulk into the cell. Such receptors are broadly classified in three classes : ion channel linked receptors, G-protein coupled receptors (GPCR), and enzyme linked receptors [Alberts 2002]. We will insist on the two latter as they are involved in a large set of unrelated biological functions. G-protein coupled receptors and enzyme linked receptors share the common structure mentioned above, as they consist in three domains : an extracellular ligand-binding domain, a transmembrane section, and a intracellular domain. The extracellular domain contains a docking site that is complementary to a specific molecular species.

I.1.2.1 Reception by extracellular ligand-receptor binding.

There is a major structural difference between these two classes at the transmembrane section, as all GPCR have a seven-helix structure that span the membrane whereas the transmembrane section of enzyme linked receptors has no unique characteristic pattern. However, the extracellular ligand binding mechanism is identical for these two families. A ligand molecule binds to a receptor's docking site on its extracellular domain. The molecular structure of the docking site, *i.e.* the positions of its atoms, forms a pocket that geometrically matches the shape of the ligand molecule. On top of the mere geometrical match, the ligand molecule and the docking site also share a compatibility with respect to the physical parameters of their atoms, such as their electrical charge and their Van der Waals interactions [Bergner 2005]. The docking site therefore recognizes a ligand molecule like a lock recognizes a key, which ensures a ligand carrying a signal is identified among the many others chemicals surrounding the cell and triggers the right response. The insertion of ligand

molecule is possible and relatively stable if such insertion decreases the free energy of the ligand-docking site system, and if the free energy barrier can be crossed by molecular structures adjustments of both the ligand molecule and the docking site due to thermal agitation [Leach 2001, Held 2011]. Ligand-receptor binding is not stabilized by the creation of covalent bonds between the receptor and the ligand molecule, so the process is reversible : the ligand molecule eventually leaves the docking site after a time that follows an exponential distribution, in first order approximation. The affinity of a receptor for its ligand can be described as a combination of two factors. First, the free energy barrier between the unoccupied site and the ligand-site complex depicts "how easy" it is for the ligand molecule to get inside the docking site. Second, the energy required to get from the complex conformational state to the unoccupied docking site / free ligand molecule configuration defines "how hard" is it for the ligand molecule to escape. These two factors, not necessarily symmetric, are respectively related to the forward and backward binding reactions rates, which quantify the ligand-receptor couple affinity.

Binding can be seen as a *hand-and-glove* mechanism, where the hand (the ligand molecule) and the glove (the receptor) combine in a mutually adjusting manner allowed by molecular structure flexibility. The conformational state of the extracellular domain modifies the conformational state of the intracellular domain by allosteric modulation [Changeux 2006]. The modified structure of the extracellular domain redefines the physical constraints applied to the whole receptor molecular structure that propagate to the intracellular domain. The new internal structure of the receptor gives it the ability to interact with specific internal proteins, and activates signal transduction. The conformation of the intracellular domain returns to its unactivated state after the ligand molecule has left the docking site. There are also multivalent binding mechanisms involving multiple docking sites, but we restrict the scope of this study to monovalent binding on receptors as monomers containing a single docking site.

I.1.2.2 Transduction by intracellular cascades of phosphorylation.

The mechanism of conformational change generated by ligand binding is the same in both GPCR and enzyme linked receptors. However the transduction mechanism is different. In enzyme linked receptors, binding activates a tyrosine kinase region within the intracellular domain. "Kinase" defines the ability to covalenty add a phospate group (a process called phosphorylation) to a peptide, in this case a tyrosine residue. Such receptors, also referred to as Receptor Tyrosine Kinase, or RTK, constitute the majority of enzyme

linked receptors. The immediate substrate of this tyrosine kinase activity is the receptor's intracellular domain itself, which phosphorylates itself on specific tyrosine residues. This biochemical reaction sets the receptor in an activated state. The newly modified intracellular domain is now recognized by intracellular signalling proteins. This modified target protein relays the signal further by modifying other proteins, and so forth forming a cascade of phosphorylations. The addition of phosphate groups to a protein affects its activity by modifying its molecular structure, thus phosphorylation can either switch on or off its substrate protein depending on the peptide residue where it occurs. Deactivation of the tyrosine kinase activity can be performed by other specialized proteins called phosphatases at the multiple levels of the phosphorylation cascade, notably as part of feedback control loops.

G-protein coupled receptors indirectly transduce the signal by acting on an intermediate specific family of proteins called G-proteins. G-proteins in their inactive state are bound to a small molecule called guanosine-diphosphate (GDP). When a G-protein binds to the intracellular domain of an activated receptor, its GDP molecule is replaced by a guanosine-triphosphate (GTP) molecule. Thus, G-proteins act as molecular switches that are either on (GTP-bound) or off (GDP-bound). Once activated by a receptor, the G-protein diffuses away from it on the membrane and activates a third target protein. A single activated receptor can therefore switch on multiple copies of G-proteins. Once activated by a G-protein, the target protein then produces a secondary messenger : a molecule whose concentration relays the signal by binding onto other proteins deeper in the signalling cascade. It is generally Adenylyl Cyclase which produces the secondary messenger cAMP. As G-proteins are themselves superficially anchored to the membrane, so are their target proteins. There also exists inhibitory G-proteins that, once activated by receptors, inhibit the activity of a target protein. Finally, the GTP molecule bound to an active G-protein can be turned back to a GDP molecule, either by the slow intrinsic hydrolysis activity of the G-protein itself or by extrinsic proteins as part of regulatory feedback control mechanisms. Thus, a G-protein remains in an active state for a limited time, as if the activation followed a countdown, and can only propagate the signal if it encounters its target during the time it stays activated.

Two types of molecular interaction can be identified in signalling : a complexification reaction, where the stabilized assembly of two molecules condition the activity of the complex, and an "activate-and-go" reaction, where a substrate is modified and immediately pursue its diffusion. Reception is a complexification reaction, the ligand-receptor complex remaining active un-

til ligand separation. Transduction by GPCR is an activate-and-go proces. In RTK transduction, both situations are possible depending on the pathway (for example, EGF Receptor transduction is a complexification process [Hlavacek 2003], whereas insulin signalling suggests an activate-and-go process between the insulin receptor and the insulin receptor substrate 1 [Cedersund 2008]).

I.1.2.3 Signalling molecules motion by passive diffusion.

In both reception by ligand binding and transduction by phosphorylation, and as in every protein-protein interaction, spatial proximity of the two interacting molecules is a crucial prerequisite. Outside the cell, ligand molecules typically undergo a passive diffusive motion. Inside the cell, there are several active mechanisms, such as transport along cytoskeleton structures or vesicle secretion, which ensure the transport of freshly synthetized proteins to their correct compartment as well as the targeting of damaged proteins towards the recycling cellular compartments (a process called trafficking). However, once they exit a trafficking process, proteins also undergo a passive diffusive process, which is the principal transport mechanism within and outside the cell. Collisions of solvent molecules (generally water) and other molecules present in the surrounding of a protein provoke its movement in an undirected and apparently random fashion. The term "Brownian motion" describes simultaneously this physical process and its associated mathematical models. The multiple molecular collisions transferring momentum to a molecule occuring without any priviledged direction, the resulting motion of said molecule is isotropical. Two potentially interacting molecules (*e.g.* a ligand molecule and its receptor) first have to encounter following their random trajectories in order for the reaction to occur.

The schematic diagram from figure I.1 can now be enriched by including the mechanisms described above. In spite of their biochemical and structural differences, the two principal signalling system classes (GPCR-based and RTK-based) share the same functional architecture. The figure I.2 include this architecture from which a first order of spatial organization emerges.

The different stages of signalling involves components localized in different parts of the eukaryotic cell. Reception typically occurs on the external side of the cell membrane, transduction occurs on the internal side of the membrane and the fraction of the cytosol that is near this side. Since these stages occur in spatially defined structures, signal transduction has to relay a chemical signal through different cellular compartments presenting specific spatial topologies

and physical properties.

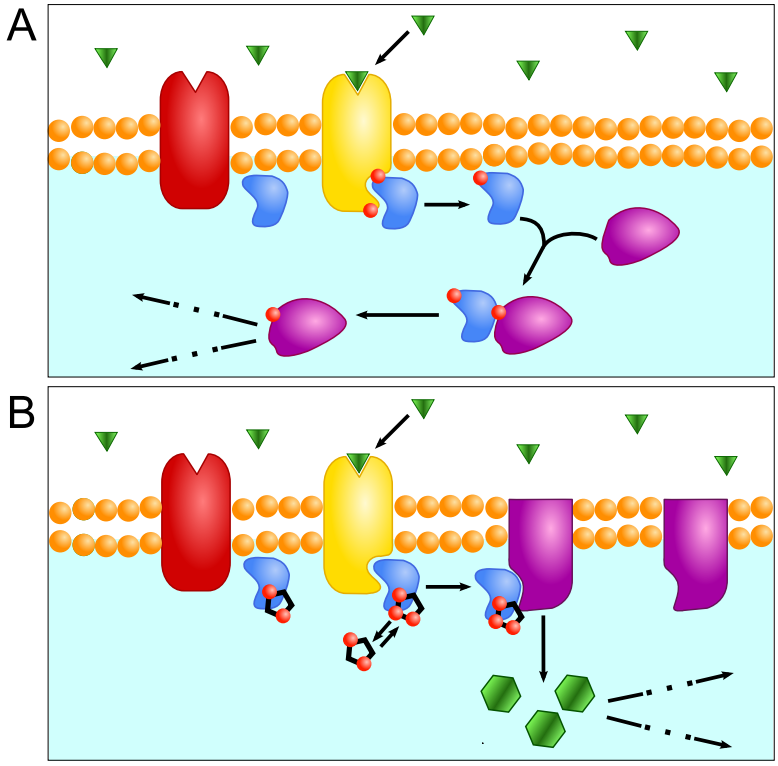

Figure I.2 – Signal transduction mechanism of the two principal signalling pathways classes : RTK-based signalling (***A***) and GPCR-based signalling (***B***). In both cases, the receptor (red globule) is activated by binding of a ligand molecule (green triangle). In RTK-based signalling, the activated receptor (yellow globule) gets the ability to phosphorylate its internal substrate (light blue), which in turn associates with its own downstream substrate (purple) and phosphorylates it. The cascade pursues and branches further downstream until response is generated. In GPCR, the activated receptor provokes the exchange of GDP for GDP in the G-Protein, which in turn activates Adenylyl Cyclase (purple membrane protein), which in turn produces the secondary messenger (green hexagones). Finally, the secondary messenger propagates the cascade downstream.

I.1.3 Spatial organization of cell signalling systems

The cellular compartments present particular geometrical differences, the most striking one being the number of spatial dimensions. The external bulk is a three-dimension space, the membrane is a two-dimension barrier, the cytoplasm is three-dimension space, and deep into it, the nucleus is another three-dimension space protected by another two-dimension membrane. A signalling

system has to consistently transduce a signal from the external bulk to its functional target inside the cell, using signalling proteins that are typically restricted to the compartment to which they belong : ligand in the extracellular bulk, receptors on the membrane, internal effectors in the cytosol, and DNA-interacting proteins in the nucleus. When it is stated that a signal is relayed through these compartments, it denotes that these are not the signalling molecules that are passed from a compartment to another one, but rather that the information they carry that is transmitted. This transmission is realized by chained pairwise interactions between proteins, this chain spanning through the different cellular compartments, such as the membrane and the cytoplasm.

I.1.3.1 Transduction across a structured membrane.

The first physical interface that a signal has to cross is the plasmic membrane. The plasma membrane defines the outside and the inside of the cell. This membrane consists in two layers of specific molecules called phospholipids. These molecules form a class of lipids that are amphiphilic : they are composed of a hydrophilic polar head (generally containing phosphate groups, hence the *phospho-* prefix) to which a hydrophobic tail composed of two fatty acid carbon chains is attached. Phospholipids can be seen as amphiphilic dipoles, and when placed in a polar solvent, they tend to arrange in the form of a symmetric bilayer. Within each layer, the polar heads are oriented towards the polar solvent whereas the hydrophobic tails face the opposite orientation. Two of these layers are superimposed so the hydrophobic side of one layer faces the hydrophobic side of the other, and so that both polar faces are exposed to the polar solvent. This bilayer forms the core structure of the membrane in which proteins such as receptors are plugged. Receptors typically include a hydrophobic transmembrane section that is inserted across the lipid bilayer. Some intracellular signalling proteins, such as G-proteins, are also anchored to the membrane thanks to a covalently attached fatty acid chain. In receptor tyrosine kinase-based signalling, the localization of downstream effectors on the internal side of the membrane is not clearly established, and seems to vary from species to another, even among homologuous protein families [Stenkula 2007].

The membrane is classically described as a fluid mosaic proposed by Singer and Nicholson [Singer 1972], the various proteins and lipids that compose it are maintained by non-covalent interactions, and have a lateral diffusion movement – including receptors spanning the membrane. In this model, the membrane is depicted as a two-dimension hydrophobic solvent on which mem-

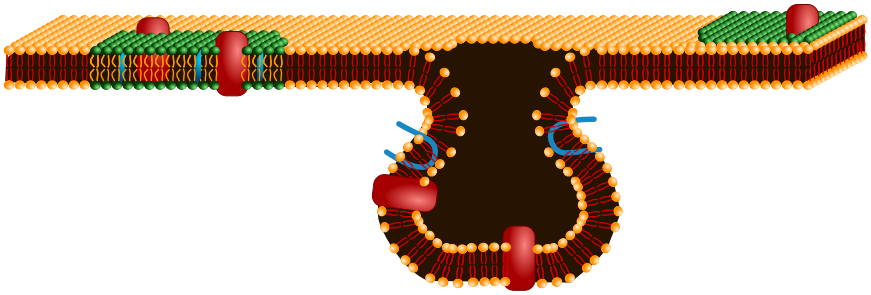

Figure I.3 – Section of membrane showing lipid rafts and a caveola. Lipids forming a raft (in green, on the left) are different from the lipids forming the rest of the membrane (in orange), and they notably include cholesterol (light blue) that increases the local stiffness of the lipid arrangement. On the right, a caveolae is an inward invagination of the membrane stabilized by caveolin (light blue, hairpin-like shape). In both cases, different proteins are concentrated within membrane microdomains (red). The fluid mosaic analogy is nowadays evolving towards a structured, compartmentalized and heterogeneous picture of the membrane.

brane proteins diffuse. The analogy of the membrane as a sea of lipids on which receptors drift laterally suggests that the distribution of the membrane components remains homogeneous by passive diffusion, but this is not the case. Different types of structures exist that organize the spatial distribution of membrane molecules, such as lipid rafts and caveolae. Lipid rafts are mobile subdomains of the membrane characterized by a distinct lipid composition which preferentially includes lipids that locally rigidify the lipid bilayer. These domains integrate receptors and other membrane proteins to form a platform of colocalized macromolecules, so the protein surface density is higher in lipid rafts than in regular parts of the membrane. Caveolae are classically considered to be a subset of lipid rafts. They form small invaginations (“*caves*”) towards the interior of the cell stabilized by a protein called caveolin. They also include a higher concentration of membrane proteins and receptors [Simons 1997, Simons 2000, Foster 2003].

I.1.3.2 Spatial heterogeneity of cell signalling systems

Membrane microdomains are thought to act as signalling platforms, *i.e.* restricted membrane fragments where proteins involved in the same signalling pathway are concentrated, or can be selectively protected and isolated from other membrane proteins [Lingwood 2009, Lingwood 2010]. They also play a role in membrane trafficking, the process by which the cell recycles and transfers its membrane components [Hanzal-Bayer 2007, Simons 2010], and these complex processes are out of the scope of this work. The membrane

Protein	cluster radius	Cell type	Reference
Ras	6-12 nm	BHK cells	[Plowman 2005]
FcεRI	50-100 nm	Mast cells	[Zhang 2006]
GPI-linked	< 5 nm	CHO cells	[Sharma 2004]
β2 receptor	50 nm	H9C2 cells	[Scarselli 2012]
VEGFR2	20-60 nm	HUVE cells	[Lee 2007]

Table I.1 – Membrane protein clusters in different cell types for different signalling systems. Spatial distributions of signalling proteins present various degrees of heterogeneity.

microdomains enriched in membrane proteins modify the picture of a homogeneously covered membrane towards clusters of signalling proteins separated by large portions of low protein density.

Such clustering of receptors and signalling proteins has been showed for different signalling systems, and lipid rafts are not systematically the only source of clustering. Insulin receptors are known to form clusters at the surface of human adipocytes [Gustavsson 1999], along with its first intracellular substrate (IRS1), and such clusters correspond to caveolae [Karlsson 2004]. More generally, GPI-linked proteins anchored to the membrane (such as IRS1) were observed to form clusters as well [Bader 2009, Sharma 2004, Goswami 2008]. β2 adrenergic receptors were also observed to form clusters, in a process that involves the cell cytoskeleton rather than lipid rafts [Scarselli 2012]. The literature spanning multiple cell types and different signalling systems suggests that clustering is a common feature, although not universal (see table I.1 for examples of observed clusters).

Systematic and consensual spatial distributions of signalling proteins are still difficult to find for many systems, and require advanced imagery techniques. Spatial statistics can be applied to the images obtained with sufficiently high resolution (such as in [Almqvist 2004, Lee 2007]) so the individual positions of labelled membrane proteins are accessible. Ripley's K-, L- and H-functions are intuitive indicators of clustering originally designed in order to capture the non-randomness of spatial point patterns [Ripley 1979] (see figure I.4). These indicators were applied to maps of different receptors [Kiskowski 2009, Zhang 2006, Scarselli 2012, Prior 2003].

Different putative mechanisms are proposed to explain the formation and stabilization of such heterogeneous distributions : ligand-induced receptor clustering, membrane protein interactions, adaptor proteins acting as scaf-

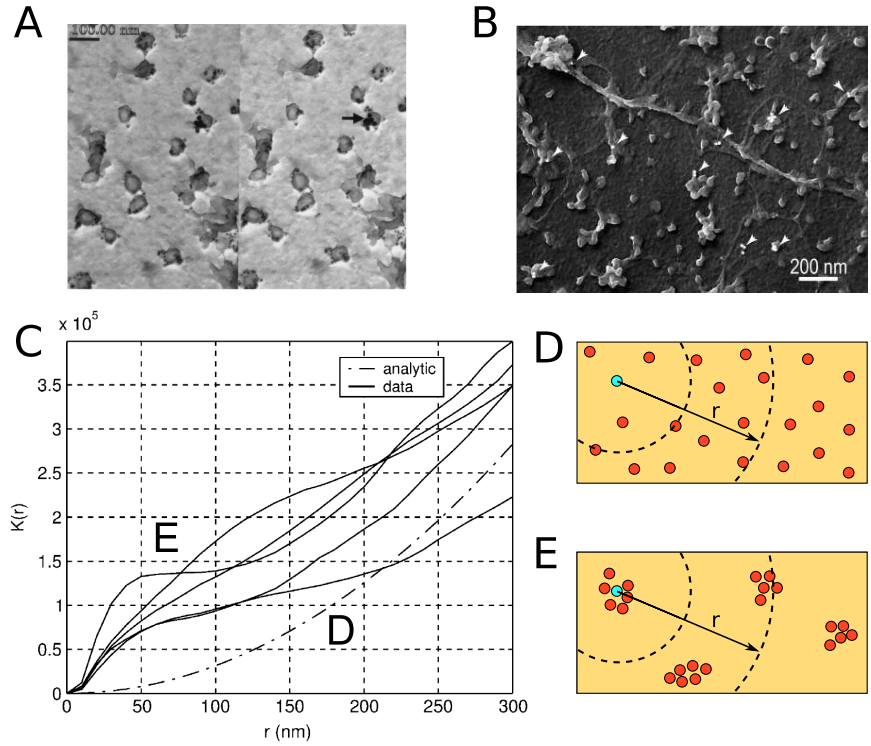

Figure I.4 – ***A.*** Insulin receptor localization in membrane microdomains in the human adipocyte (from [Gustavsson 1999]). ***B.*** Insulin receptor substrate 1 localization in membrane microdomains on the internal side of the membrane ***C.*** Ripley's statistic based on receptor localization : $K(r)$ the average number of receptors found within a radius r from a single receptor, normalized on the global receptor density, computed for the IgE receptor on mastocytes ([Zhang 2006]). ***D.*** If receptors are distributed uniformly, $K(r)$ is proportional to the surface (and thus proportional to r^2). ***E.*** The profile of $K(r)$ is characteristic of clusters of receptors, with a typical bump at r between 50 and 100 nm.

folds [Duke 2009], or non-homogeneous diffusion [Kusumi 1993, Soula 2012], and lipid rafts as seen above [Kusumi 2005]. The initial picture of a generic signalling system as an homogeneous network of interacting proteins is now closer to a heterogeneous, spatially structured assembly (figure I.5) maintained by dedicated mechanisms. We consider a simple, linear, generic pathway composed of a receptor, an intracellular membrane protein and a cytosolic effector, and let aside the complex biochemical interactions such as trafficking, recycling and scaffolding. Similarly, we will consider proteins as monovalent monomers, interacting in a pair-wise manner with a stoichiometry of 1. Is the transmission of the signal affected by a heterogeneous structure compared to a homogeneous one ? The dynamic of the pathway is encoded the form of quantities of signalling proteins activated by different doses of ligand. How will

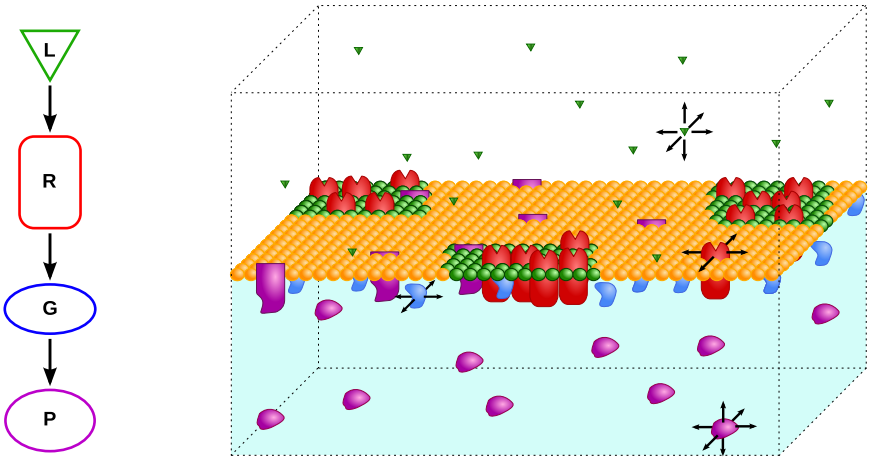

Figure I.5 – Schematic representation of a canonical signalling system including spatial heterogeneity. The inherent simplicity of signalling as a pathway (left) hides the more complex picture of a system organized in space (right), as illustrated on a canonical linear signalling cascade composed of a ligand (green), a receptor (red), a transduction protein (blue) and an intracellular effector (purple). The signal propagates from the external 3-dimension bulk to the 3-dimension cytosol through a 2-dimension membrane, which constitutes a first order of spatial structuration. At the membrane level, a second order of structuration resides in the heterogeneous distributions of signalling proteins, which form clusters of various sizes.

this dynamic be affected by heterogeneous signalling proteins distributions, compared to homogeneous ones ? This constitutes the central interrogation of this work.

I.2 Mathematical and computational models for cell signalling

The behavior of signalling systems can be understood and predicted under the form of intertwined chemical reactions, translated in terms of reaction kinetics of a dynamical chemical system. Formulated as such, the behavior is defined by the quantities of species in their different possible states. We will review the different mathematical models available for the quantitative study of signalling, and how they are generally based on the well-mixed assumption. Then we will establish the microscopic bases on which these macroscopic models are built. Finally, we will see how computational models implementing these microscopic mechanisms are able to accurately reproduce spatially heterogeneous reacton systems without the well-mixed postulate.

I.2.1 Mean-field modelling of biochemical reactions.

We start from dynamical systems of ordinary differential equations, a typically non-spatially resolved formalism that will be helpful to illustrate the global behavior of signalling cascades.

I.2.1.1 Dynamics of a canonical signal transduction pathway.

We can explore the dynamics of a canonical signalling system by obtaining the system of ordinary differential equations that governs it. We first consider the reception stage : a reaction between a ligand and its receptor at the cell surface. A ligand molecule binds to the docking site of a receptor, the pair constitutes a complex. L and R will refer respectively to the ligand and receptor, which combine upon collision to form a complex C, in a reversible manner so a complex C can split back into separate L and R molecules.

$$L + R \underset{k_{f1}}{\overset{k_r}{\rightleftharpoons}} C \tag{I.1}$$

For sake of clarity, we will let aside the vector notation and use individual lowercase letters to represent the number of molecule from each species. The variation of each species amount can be written according to the law of mass action :

$$\begin{aligned} \frac{dl}{dt} &= -k_{f1}lr + k_{r1}c \\ \frac{dr}{dt} &= -k_{f1}lr + k_{r1}c \\ \frac{dc}{dt} &= k_{f1}lr - k_{r1}c \end{aligned}$$

In each of the equation describing a species variation, positive terms represent the generation of the species, and negative terms its consumption. The ligand-receptor interaction is composed of two reactions both occuring simultaneously : ligand-receptor complex formation and breakdown. The velocity of second order ligand-receptor complex formation is proportional to the product of ligand and receptor amounts, and is characterized by an association (or "forward") rate constant k_{f1} expressed in $\#molecules^{-1}.time^{-1}$, whereas the first order complex breakdown is characterized by a dissociation (or "reverse") rate constant k_{r1} expressed in $time^{-1}$. In order to solve for the number of ligand-receptor complexes c, we assume that the global number of receptors r_0 is unchanged, so $r_0 = r + c$. Another conservation law can be assumed for the total ligand concentration $l_0 = l + c$. We insist on the kinetics through

time scales during which the cell does not adapt its signalling system, so the global number of receptors remains the same, and the ligand stimulus is deemed constant, so ligand concentration remains the same. The evolution of the system can be described by a single ordinary differential equation [Lauffenburger 1996] :

$$\frac{dc}{dt} = k_{f1}(r_0 - c)(l_0 - c) - k_{r1}c \tag{I.2}$$

If the number of receptors is small enough compared to the number of ligand molecules, it can be assumed that $l_0 >> c$, which gives :

$$\frac{dc}{dt} = k_{f1}(r_0 - c)(l_0) - k_{r1}c \tag{I.3}$$

With the initial condition $c(t = 0) = c_0$, the transient solution of equation I.3 is :

$$c(t) = c_0 e^{-(k_{f1}l_0 + k_r)t} + (\frac{k_f l_0 r_0}{k_f l_0 + k_r})(1 - e^{-(k_f l_0 + k_r)t}) \tag{I.4}$$

The number of complexes at equilibrium c_{eq} can be obtained by solving the equation I.3 for $\frac{dc}{dt} = 0$, *i.e.* at the steady-state. It yields :

$$c_{eq} = \frac{k_{f1} r_0 l_0}{k_{r1} + l_0 k_{f1}}$$

By posing the dissociation constant $K_{D1} = \frac{k_{r1}}{k_{f1}}$, we obtain :

$$c_{eq}(l_0) = \frac{r_0 l_0}{K_{D1} + l_0} \tag{I.5}$$

The equation I.5 gives the number of receptors occupied at equilibrium when l_0 ligand molecules are applied to r_0 receptors, the ligand-receptor binding being characterized by the dissociation constant K_{D1}. The dissociation constant being the ratio fo k_{r1} to k_{f1}, it is expressed in $\#molecules$. By replacing l_0 by K_{D1} in the equation I.5, we obtain $c_{eq} = \frac{r_0}{2}$: the value of the dissocation constant is the number of ligand molecules needed in order to occupy half of the receptors.

We now have an analytical expression of the number of receptors that a constant dose of ligand will activate. This quantity is a proxy for the cell response induced by such dose. The number of occupied receptors condition the number of intracellular signalling proteins that will be activated. According to the biochemical principles of signalling reviewed in section I.1.1, a canonical transduction stage can be added to the ligand-receptor system by including

two new species : an intracellular protein G that is activated by an occupied receptor C to become an activated molecule of H. This leads to the new reaction network :

$$\begin{aligned} L + R &\underset{k_{f1}}{\overset{k_{r1}}{\rightleftharpoons}} C \\ C + G &\xrightarrow{k_{f2}} C + H \\ H &\xrightarrow{k_{r2}} G \end{aligned} \tag{I.6}$$

This system yields the following variations for each species :

$$\begin{aligned} \frac{dl}{dt} &= -k_{f1} l r + k_{r1} c \\ \frac{r}{dt} &= -k_{f1} l r + k_{r1} c \\ \frac{dc}{dt} &= k_{f1} l r - k_{r1} c \\ \frac{dg}{dt} &= -k_{f2} g c + k_{r2} h \\ \frac{dh}{dt} &= k_{f2} g c - k_{r2} h \end{aligned} \tag{I.7}$$

A new conservation law can be added regarding the total number of intracellular proteins : $g_0 = g + h$. At steady-state, $\frac{dh}{dt} = 0$, and assuming $g_0 >> h$, the same simplification principle as we used to obtain c_{eq} can be used in order get the number of activated intracellular proteins at equilibrium h_{eq}:

$$h_{eq} = \frac{k_{f2} c g_0}{k_{r2} + k_{f2} c}$$

Introducing the dissociation constant $K_{D2} = \frac{k_{r2}}{kr2}$ for the $C + G$ interaction, we obtain :

$$h_{eq} = \frac{c g_0}{K_{D2} + c} \tag{I.8}$$

Since the transduction reaction does not influence the ligand-receptor binding, we can insert the expression for c_eq in place of c in the equation I.10, which yields the number of activated intracellular proteins at equilibrium in function of the initial dose of ligand l_0 :

$$h_{eq} = \frac{\frac{r_0 l_0}{K_{D1} + l_0} g_0}{K_{D2} + \frac{r_0 l_0}{K_{D1} + l_0}} \tag{I.9}$$

This expression can be simplified :

$$h_{eq} = \frac{r_0 l_0 g_0}{K_{D1} K_{D2} + K_{D2} l_0 + r_0 l_0} \tag{I.10}$$

Thus we obtain the number of activated downstream signalling proteins in function of the ligand dose applied. This analytical formulation of the dynamics of transduction gives a first approximation of the cell response. The formulae for receptor occupation and intracellular protein activation can be rendered dimensionless and expressed as fractions of the total molecules numbers for each type. We pose the normalized variables $l^* = \frac{l_0}{K_{d1}}$, $c^* = \frac{c_{eq}}{r_0}$, $h^* = \frac{h_{eq}}{g_0}$, the parameter $r^* = \frac{r_0}{K_{d2}}$, and obtain :

$$c^* = \frac{l^*}{1+l^*} \tag{I.11}$$

$$h^* = \frac{r^* l^*}{1+l^*(r^*+1)} \tag{I.12}$$

The curves corresponding to equations I.11 and I.12 are called doses-responses curves and represent the equilibrium dynamics of the signalling system (see figure I.6. They characterize the relation between a ligand dose and the response at equilibrium measured respectively at the reception stage and the transduction stage.

The analytical formulations provide helpful parameters that characterize the dose-response relationship. The classical example of such parameters is the *effective dose 50%* (ED50), or *effective concentration 50%* (EC50) depending on the unit used for the input stimulus. It is the ligand quantity that generates half of the response. The ED50 can be measured on experimental doses-responses in order to compare the response of a signalling system in different conditions. One can note that doses-responses curves following equation I.5 and I.10, the ED50 is equal to respectively K_{D1} and K_{D2}. So this parameter gives also access to the kinetics parameters of the signalling pathway.

In the $L + R \rightleftharpoons C$ reaction, the dose-response curve presents a saturation plateau with the asymptotic value r_0, and the dissociation constant K_{D1} only defines the "speed" at which the plateau is reached. This defines the affinity of the reaction : the lower K_{D1}, the fewer the ligand molecules required to generate a given response, and therefore the higher the affinity. The situation is different for the transduction reaction $C + G \rightleftharpoons C + H$, because of the parameter $r^* = \frac{r_0}{K_{D2}}$: the dissociation constant K_{D2} defines simultaneously the saturation plateau value and the affinity of the reaction.

A notable contribution to the study of reaction networks was done by Feinberg, based on the pioneer work of Horn and Jackson [Horn 1972], who devel-

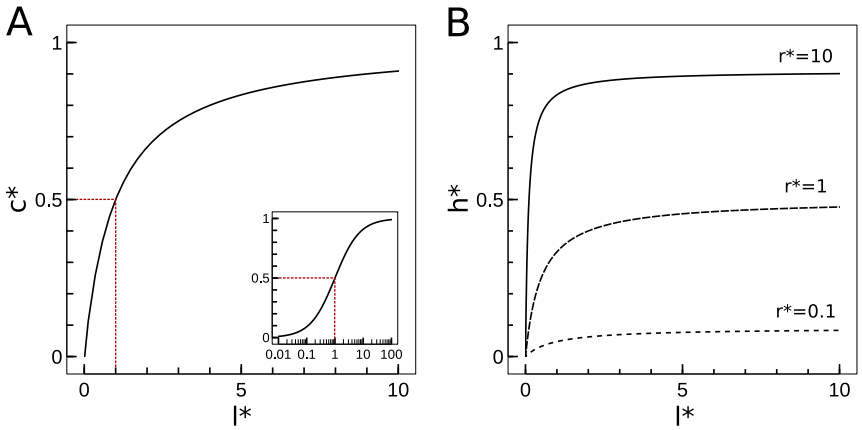

Figure I.6 – Doses-responses curves at the reception stage and transduction stage of a generic signalling pathway. ***A.*** Fraction of bound complexes $c^* = \frac{c_{eq}}{r_0}$ in function of normalized ligand dose ($l^* = \frac{l_0}{K_{D1}}$). The dose $l^* = 1$, or $l_0 = K_{D1}$, is the EC50 or ED50 (red dashed line). The inset shows the same curve in a semi-logarithmic scale, a representation commonly found in pharmacodynamics. ***B.*** Fraction of activated intracellular proteins $h^* = \frac{h_{eq}}{g_0}$ in function of normalizd ligand dose for different values of the parameter $r^* = \frac{r_0}{K_{D2}}$

opped a consistent mathematical theory chemical reaction networks (CRNT) [Feinberg 1987, Feinberg 1989]. This theory provided two theorems, the deficiency zero theorem and the deficiency one theorem, that state the conditions for the existence, uniqueness and stability of fixed points in reaction networks. Remarkably, these conditions are irrespective of the values of kinetic parameters, and only depend on the algrebraic structure of the reaction network and the molecule complexes space. In our simple case, the steady-states described by equations I.10 and I.5 are unique and asymptotically stable, and the response measured in terms of R occupation or G activation follows an increasing monotonous function of ligand stimulation.

The analytical formulations derived in this section are only valid for homogeneous, well-mixed reaction systems. We will not use them to investigate spatial heterogeneity, but rather as a reference when analyzing the global behavior of our simulated signalling systems with different signalling proteins distributions. ODE systems are typically continuous and deterministic tools. However, they neglect the intrinsic stochastic nature of chemical reactions. Before addressing spatial models, it will be useful to define the stochastic counterparts of deterministic models.

I.2.1.2 Non-spatial stochastic simulation algorithm for chemical kinetics

The fluctuations in small numbers of molecules may give rise to qualitative behaviors unforeseen by mean-field formalisms [Erban 2009]. Molecules come in integer numbers, which might be of importance when considering biological reactions, some of which involving small number of molecules. Molecules also react independently of each other : when a molecule of species A reacts with a molecule of species B, there is no clear physical mechanism that implies that the individual reaction has a direct effect on the fate of another molecule of A – or another molecule B. Gillespie proposes a formalism developped in order to get closer to the physical dynamics and the stochastic nature [Gillespie 1977] of biological reactions. Given a set of N molecular species in a fixed volume V, interacting through M reaction channels. A reaction channel describse a single instateneous physical event that changes the number of molecules at least one species. There are two kinds of such events : bimolecular reactions and unimolecular reactions. All other types of reactions can be decomposed in steps linked by such elementary reactions.

A reaction occurs when two molecules collide and react, reactive collisions being separated in time by many non-reactive collisions. Such reaction events are 1) occuring in integer numbers between individual molecules and 2) occuring randomly given the randomized molecule positions velocities. Instead of describing the state of the system by characterizing the position, velocity and type of each molecule in V, Gillespie defines the state of the system by setting the random variable $\mathbf{X}(t) = (x_1(t), x_2(t), ..., x_i(t))$, each x_i being a random variable of the number of molecules of the i^th species. We will refer to a realization of $\mathbf{X}(t)$ by lowercase letters, such as $\mathbf{x}$. Thus, rather than treating each molecular species as averaged populations of molecules over V, each species will be treated as an integer random variable. The transition between two states of the system will be characterized non-deterministically by a reaction *probability* rather than a reaction *rate*. In addition to the state vector, Gillespie introduces :

- a propensity function $a_j(\mathbf{x})$: the probability of a reaction event j between the i_{th} and the k_{th} species occuring in the infinitesimal time dt is given by $a_j(\mathbf{x})dt = c_j x_i x_k dt$.

- a stage change vector $\nu_j \in \mathbb{N}^N$: the reaction j induces the state change $\mathbf{x} \to \mathbf{x} + \nu_j$.

- the "grand probability function" $P(\mathbf{x}, t) \triangleq Prob\{\mathbf{x}(t) = \mathbf{x} | \mathbf{X}(t_0) = \mathbf{X}_0\}$,

that is the probability to be in state $\mathbf{x}$ at t given that the system was in state $\mathbf{X}_0$ at t_0.

This set up leads to the derivation of the chemical master equation (CME), that is the equation describing the evolution fo the grand probability function :

$$\frac{\partial P(\mathbf{X}, t|\mathbf{X}_0, t_0)}{\partial t} = \sum_{j=1}^{M} [a_j(\mathbf{X} - \nu_j) P(\mathbf{X} - \nu_j, t|\mathbf{X}_0, t_0) - a_j(\mathbf{X}) P(\mathbf{X}, t|\mathbf{X}_0, t_0)] \tag{I.13}$$

The first term of the sum in the equation above represents the transition of others states to the state j. The second term describes the transition from the state j to others states. The CME is exact, but often intractable. However, Gillespie proposes a procedure that constructs the probabilistic realizations of $\mathbf{X}(t)$ using a Monte Carlo method. The general principle is the following : the time τ to the next reaction and the index j of that reaction are drawn from properly defined random variables. Hence, the trajectory of $\mathbf{X}(t)$ is produced by random individual reactions. If the τ interval is split into n discrete steps, then the probability that a reaction R_j occurs at a time $t+\tau$, given $\mathbf{X}(t) = x$, is the probability of the event "*no reaction occured at each of these discrete steps* and *the reaction R_j occured after these n steps* :

$$p(\tau, j|\mathbf{x}, t)d\tau = (1 - a_0(\mathbf{x})\frac{\tau}{n})^n a_j(\mathbf{x})d\tau$$

The first factor of the right hand side product correspond to the event "no reaction occured" and is equal to $1 - \sum_{k=1}^{M} a_k(\mathbf{x})$. We set $a_0(\mathbf{x}) = \sum_{k=1}^{M} a_k(\mathbf{x})$ for sake of readability. The second factor to the event "the reaction R_j occured". By taking the limit when $n \to \infty$, the probability of these combined events becomes :

$$p(\tau, j|\mathbf{x}, t)d\tau = e^{-a_0(\mathbf{x})\tau} a_j(\mathbf{x}) = a_0(\mathbf{x}) e^{-a_0(\mathbf{x})\tau} \frac{a_j(\mathbf{x})}{a_0(\mathbf{x})} \tag{I.14}$$

With this expression, we can now implement the general principle stated above in order to recreate trajectories of $\mathbf{X}(t)$. The Gillespie algorithm is therefore the following :

1. At the time t and the state $\mathbf{x}$, evalute each $a_j(\mathbf{x})$, and their sum $a_0(\mathbf{x})$.

2. According to equation I.14, draw the next-reaction time τ using the expression $\tau = \frac{1}{a_0} ln(\frac{1}{1-u_1})$ and u_1 a number drawn from a unit-interval uniform random variable.

3. Draw the index for the reaction to be executed by taking the smallest integer j satisfying $\sum_{k=1}^{j} a_k(\mathbf{x}) > u_2 a_0(\mathbf{x})$, u_2 being another number drawn from a unit-interval uniform random variable.

4. Replace $t \leftarrow t + \tau$ and $\mathbf{x} \leftarrow \mathbf{x} + \nu_j$

5. Return to step 1 or end the simulation, depending on the stopping conditions.

This constitutes the basic stochastic simulation algorithm (SSA). It is in essence a Markovian model that simulates a discrete random walk in the state space according to probability distributions derived from the propensities of the reactions. The advantage of the SSA is that it derives directly from the same core premises than the CME, and thus shares its exactness. The τ are not time-approximation comparable to the Δt of a ODE numerical simulation, but are exactly derived from the stochastic definition of chemical reactions established by Gillespie. However, this exactness requires a compromise at the expense of computing speed. The relative slowness of the SSA comes from the fact that each individual reaction of the system is computed, and each of these reactions involves random number generation. The number of iterations of the simulation depends on the propensities of the reactions : if their combined propensity $a_0(\mathbf{x})$ is high, then the drawn τ values will be low in average, and the simulation of long times will generate a huge number of iterations. Diverse improvements were proposed, whose common purpose generally being to reduce the number of iterations simulated while maintaining an acceptable exactness. The most notable is probably the τ-leaping technique [Gillespie 2007], which consists in realizing multiple reactions at each τ incrementation, and will not be described here.

Although the SSA provides a framework that includes the stochastic nature of biochemical reactions, it does not address the spatial aspects of reaction systems. It still holds the assumption of a well-mixed medium where populations of molecules, although discrete, are still homogeneously distributed. This assumption has ramifications in the CME model : although molecules are treated individually, they have no memory of their reaction history; and collisions occur between molecules that undergo an implicitly "memoryless diffusion". This results in exponential distributions of reaction times. However, if spatial homogeneity cannot be assumed, the exponential dependence of reaction times may not hold [Dobrzynski 2008] : the probability of a molecule to react should depend on its previous positions, velocities, and reaction history, because it may condition its probability to collide with a reaction partner. We

propose to review the microscopic physical mechanisms that rule molecule motion and reaction, in order to reimplement them in spatially-resolved models.

I.2.2 Formalisms for molecule motion and interaction.

The macroscopic models seen above revealed themselves unsuitable for implementing the specific spatial configurations of signalling systems. These models described above use parameters – mainly reaction rates and diffusion coefficients – that are the macroscopic formulation of what is really the combination of distinct microscopic processes. In the eventual purpose of recreating these processes for individual molecules, we propose to review them, starting by introducing Brownian motion as the basis for diffusion.

I.2.2.1 Microscopic basis of diffusion by Brownian motion

Let us consider a molecule as a punctual particle of mass m whose center of mass' position is $\mathbf{x}$. The particle is surrounded by comparatively smaller molecules of the solvent that create a friction force. In addition, collisions of solvent molecules with the particle generate random forces applied to its motion. The motion of the particle is described by Langevin dynamics :

$$m\frac{d^2\mathbf{x}}{dt^2} = -\lambda m\frac{d\mathbf{x}}{dt} + \nu(t) \tag{I.15}$$

The friction term is $\lambda m\frac{d\mathbf{x}}{dt}$, and states that friction generates a force proportional to the particle's velocity. The term $\nu(t)$ represents the random forces applied to the particle by solvent molecules. The random collisions on the particle that have no priviledged direction, and their contribution on the particle motion can be assumed to follow $\nu(t)$, a Gaussian decorrelated stationary random process. When the dynamics is set in the over-damped regime, the acceleration term can be neglected in front of the friction term, and gives the equation of Brownian dynamics :

$$\lambda m\frac{d\mathbf{x}}{dt} = \nu(t) \tag{I.16}$$

We can note that the motion has a zero net consumption of energy : solvent molecules provide the energy for the particle motion by collision, and also consume it by friction. We can specify the term $\nu(t)$. Since the random collisions have no priviledged direction, $E[\nu(t)] = 0$. Additionally, if we assume that the collisions are not correlated in time nor direction, the autocovariance of the process is $cov(\nu(t), \nu(t-t')) = \kappa^2\delta(t-t')$, where δ is the Dirac δ function. If

we also assume that at equilibrium the particle velocities follow the Maxwell-Boltzmann distribution of variance $\frac{k_bT}{m}$, we can identify $\kappa = \sqrt{2k_bTm}$. In these conditions, the equation can be rewritten :

$$\frac{d\mathbf{x}}{dt} = \sqrt{\frac{2k_bT}{\lambda m}}\mathbf{W}(t) \tag{I.17}$$

$\mathbf{W}(t)$ being a Wiener process whose expectation is zero, and autocorrelation function is $< W(t_1)W(t_2) >= \min(t_1, t_2)$. The equation I.17 constitutes the Brownian dynamics of the particle. We can note that the Einstein relation appears in the random collisions term, thus we can set the diffusion coefficient $D = \frac{k_bT}{\lambda m}$. The equation can be rewritten as a stochastic differential equation :

$$d\mathbf{x} = \sqrt{2D}d\mathbf{W}(t) \tag{I.18}$$

The motion of the particle can be understood as a random walk of increments drawn from a Gaussian distribution, whose variance is proportional to the diffusion coefficient of the particle. It is related to its macroscopic formulations by the diffusion coefficient, as established by Einstein's relation. The diffusion coefficient defines the variance of the amplitude of the random particle displacement. The mean square displacement (MSD) of the particle obeying Brownian motion is defined as the distance between its position at a time t and its initial position at $t = 0$:

$$\langle(\mathbf{x}(t) - \mathbf{x}(0))^2\rangle = 2dDt \tag{I.19}$$

With d being the spatial dimensionality.
We can dervie the macroscopic manifestation of Brownian motion as the Fokker-Planck equation : the probability density function to find a particle at a position $\mathbf{x}$:

$$\frac{\partial\rho(\mathbf{x}, t)}{\partial t} = \mathrm{div}(\nabla(D\rho)) \tag{I.20}$$

Where $\rho(\mathbf{x}, t)$ is the probability to find a particle at the position $\mathbf{x}$ at a time t. With this macroscopic manifestation of Brownian motion for a population of particles, it is possible to combine reaction kinetics and diffusion in the same macroscopic formalism called reaction-diffusion models. Reaction-diffusion models manipulate concentrations of molecules that are not only a function of time, but also of spatial coordinates. For a multiple-species reaction system, the concentrations of each species still constitute the components of the vector $\mathbf{q}$. But the variations of this vector follow a partial differential equation of the generic form :

$$\frac{\partial\mathbf{q}}{\partial t} = \underbrace{D\Delta\mathbf{q}}_{Diffusion} + \underbrace{R(\mathbf{q})}_{Reaction} \tag{I.21}$$

The matrix D is a diagonal matrix composed of diffusion coefficients for each species, Δ is the Laplace operator. The first term of the right hand side constitutes the contribution of diffusion to the variations of species concentrations. The second term is the contribution of reactions between molecules to the variations of concentrations. If the diffusion term is zero, then the equation reduces to a simple non-spatial ordinary differential equation, and the concentration variations are only due to reation kinetics. On the contrary, if the reaction term is nonexistent, then the equation describes a purely diffusive process.

This class of models constitutes the principal deterministic formalism for spatially-defined reaction systems. They were used notably by Kholodenko to explore how signalling cascades are built on gradients of signalling molecules, around the concept of protein activity gradient [Kholodenko 2006, Kholodenko 2009]. This illustrates the notion that signalling is not just a matter of how many signalling proteins are active, but also of where are these active proteins located in the cell.

These models manipulate molecule distributions that can be heterogeneous under the form of gradients, which is suitable for spatial distributions that are continuous. For spatial distributions such as the ones illustrated in I.1.3.2, the heterogeneous yet continuous molecule distribution hypothesis can not hold. Therefore, we will not directly use reaction-diffusion models, but reimplement its microscopic diffusion mechanism, Brownian motion, in computational models for individual molecules.

I.2.2.2 Space-dependent reaction rates and reaction-limited versus diffusion-limited processes

The reaction rates are macroscopic parameters that hide what is really a two-step microscopic process. We will take the example of a bimolecular reaction between a ligand L and a receptor R forming a complex C, described by the formula $L + R \underset{k_f}{\overset{k_r}{\rightleftharpoons}} C$. The forward reaction requires that two molecules collide, and the frequency of such an event can be represented by a transport rate constant k_+. Then the actual physical interaction occuring after collision of the two molecules can be represented by an intrinsic reaction rate constant k_{on}. The overall macroscopic reaction rate k_f is there the combination of these two-steps. Linderman & Lauffenberger [Lauffenburger 1996] sum up the formulations of k_f that arise in different situations :

a. If the ligand L and the receptors R diffuse freely in three dimensions in a solution, then $k_f = \frac{k_{+(bulk)}k_{on}}{k_{+(bulk)} + k_{on}}$. Here $k_{+(bulk)} = 4\pi Ds$ where s is the minimal distance between molecules for the binding to occur, and D is the sum of the diffusion coefficients of R and L.

b. If L still diffuses freely in a three-dimension bulk but receptors are placed on the surface of spherical cell of radius a, then $k_f = \frac{k_{+(cell)}k_{on}}{k_{+(cell)} + rk_{on}}$. Here, $k_{+(cell)} = 4\pi Da$, and r is the number of free receptors.

c. If both L and R diffuse in a two-dimension space (such as the membrane), then $k_f = \frac{k_{+(mem)}k_{on}}{k_{+(mem)} + k_{on}ln(\frac{b}{s})}$. This time, $k_{+(mem)} = 2\pi D$, b is half the average distance between two ligand molecules, and s is still the minimal interaction distance.

These formulations were mainly obtained thanks to the works of [Shoup 1982, Berg 1977, Zwanzig 1991, Goldstein 1995], who used anlysis of flux of molecules in different cellular geometrical conditions. The expressions of k_f share a similar structure that reveals the contribution of diffusion to the forward reaction rate. According to the relative values of k_+ and k_{on}, the reaction can be termed diffusion-limited (or diffusion-controlled) or reaction-limited (or reaction-controlled) :

- if $k_+ >> k_{on}$, then $k_f \sim k_{on}$: the transport rate is fast compared to the intrinsic reaction rate, the latter being the limiting step. The process is termed reaction-limited.

- if $k_+ << k_{on}$, then $k_f \sim k_+$: the transport rate is slow compared to the intrinsic reaction rate, so the process is diffusion-limited.

The classification of a given signalling pathway reception stage, or transduction stage, as a diffusion or a reaction-limited process is not always clear. The comparison of k_+ and k_{on} relies on the accurate determination of various parameters such as the number of protein copies per cell, diffusion coefficients in *in vivo* media, which is often difficult experimentally. The determination of k_{on} itself can be problematic, since the measurement method generally estimates k_f, and not k_{on}. The reaction regime of a signalling pathway involving the same receptor may differ from one cell type to another, which do not share the same physical properties or protein composition (Wiley showed this for the EGF binding to its receptors in [Wiley 1988]).

We can make another remark about these attempts to characterize the contributions of diffusion and intrinsic bimolecular reaction mechanism to the overall forward rate. They include the geometrical aspects of the compartments in which the proteins are distributed, *i.e* the transport rate differs whether the reaction occurs within the membrane, or between receptors on the membrane and ligand in the three-dimension bulk. The transport rate derivation, as a rate of encounter, requires the assumption of a well-mixed medium. When this situation cannot be assumed, a solution is to let the microscopic diffusion process generate molecule trajectories, and then execute reaction events as molecules collide.

I.2.3 Spatially-resolved computational models

The deterministic ODE models, the stochastic chemical master equation, or the reaction-diffusion partial differential equation, are based on parameters that are the macroscopic manifestation of microscopic processes. In non-spatial models, the reaction rates are set assuming spatial homogeneity leading to exponential distributions of next reaction times. In reaction-diffusion systems, the diffusion coefficients describing the macroscopic evolution of molecular densities are derived from Brownian dynamics. However, the spatial organization of cell signalling systems does not correspond to these derivations, because of the geometrical differences between the external cell medium, the membrane, and the cytosol, and because of the heterogeneity of spatial distribution of signalling proteins within the membrane, especially at the reception and transduction stage.

Thus, models integrating the spatial properties of signalling systems requires a finer granularity because the well-mixed assumption is no longer valid. Computer simulations offer a way to meet this requirement. Rather than manipulating averaged variables whose evolution is ruled by macroscopic parameters, it is possible to reproduce the microscopic behavior of the components of a signalling system, even in large populations, and observe the simulated global behavior of the system. Individual-based computational models offer the possibility to rigorously reproduce microscopic processes on large molecule populations, in heterogeneous geometrical and individual distributions, and stand as particularly suitable tools for our investigation. The simulation implementation of such models takes the form of Monte Carlo algorithms that intrinsically include the stochastic nature of the microscopic processes they emulate. Such simulation techniques give access to the global dynamics of the system at the macroscopic scale that can be compared to ODEs or stochastic

non-spatial models. Computational models also give access to the behavior of the system at the scale of individuals, for instance under the form of empirical probability distributions of events, spatial densities at high granularity, and characteristic times distributions. The principle is to take advantage of the computer's ability to repeat numerous simple instructions reproducing the microscopic behavior of individuals, rather than compute general equations reproducing the macroscopic behavior of averaged populations. In this paradigm, the system can be simulated with the adequate granularity.

I.2.3.1 Mesoscopic finite volumes methods

When faced with a system whose spatial homogeneity cannot be assumed, a natural way to account for it is to decompose the geometrical space of the system in finite subvolumes. Their size can be set so homogeneity can be assumed within each subvolume. This is the core principle behind mesoscopic finite volume models. The global volume in which reactions occur is projected on a lattice. Within a given node (or subvolume), since homogeneity is assumed, the local evolution of the molecules populations can be numerically solved either according to a local ODE system, or with a SSA. With ODE, the concentration of the species in the node are scalars, and their evolution is determined according to reactions rates observing the law of mass action. Transfer of molecule is achieved by computing the fluxes between adjacent subvolumes. The numerical parameters ruling the evolution of individual subvolumes are derived from the macroscopic parameters according to the discretization parameters in time and space, mainly the time step of the numerical solver, and the characteristic length of the lattice. The *Virtual Cell Project*, or VCell, is a simulation framework using subvolumes [Schaff 1997, Schaff 2000]. VCell allows for the definition of a model of a system of interest that is implemented in different simulation methods. The geometry of cell can be defined manually or from reconstructed from image data. Species and reactions are mapped to the compartments, which are discretized in computational subvolumes. The software reconstructs the PDE and ODE equations from the physiological and geometrical model defined by the user, and applies numerical solvers. Another approach is to use stochastic algorithm derived from Gillespie's work in each subvolume. In each subvolume, molecules come in integer numbers, and the local chemical master equation is solved numerically with a SSA. Diffusion is treated as a reaction event and included in the SSA by computing the probabilities of molecules jumping to an adjacent subvolume. The *mesoscopic reaction diffusion simulator* (MesoRD) implements this class of method [Hattne 2005].

The development of mesoscopic finite volumes methods present non-trivial computational challenges, because it is aimed at simulating systems at heterogeneous time and spatial scales. The ODE/PDE requires the use of particularly stable numerical solvers, so the behavior of the subvolumes remains consistent at the global level. Implicit integration schemes guarantees stability, but come at the cost of iterative methods. Explicit schemes require sufficiently small time and space-sampling so qualitatively unrealistic behaviors are avoided. The definition of geometrical compartments also poses the question of how to treat the interfaces that separate them, as these interfaces introduce discontinuities. This is addressed by the use of advanced numerical integrations techniques, and VCell now offers eight different solvers [Cowan 2012]. Stochastic algorithms present the advantage of being exact as they derive from the chemical master equation, but become prohibitively slow when they include diffusion across numerous subvolumes. This is addressed by optimized simulations techniques such as the next subvolume method in MesoRD [Elf 2004]. It consists in reducing the computational cost by only recalculating reaction probabilities in subvolumes that underwent a state update, and keeping the subvolumes sorted in a tree by order of which one will most probably host the next reaction-diffusion event. The complexity of mesoscopic finite volumes methods scales typically linearly with the number of subvolumes, but advanced optimizations techniques such as the next subvolume method scales logarithmically.

I.2.3.2 Lattice individual-based models

In lattice individual-based, a computational mesh represents the volume of the simulated system. This mesh, or lattice, consists of a set of discrete coordinates that molecules can occupy. It can be understood as a finite volume method with a spatial sampling so small that subvolumes have the size of one molecule. At the scale of individual molecules, the determinism of the macroscopic simulation methods is replaced by probabilistic realizations of Monte Carlo methods. Events are assigned a probability to which a randomly drawn number in the unit interval is compared, determining its outcome. Diffusion is reproduced as a discrete random walk on the lattice, by allowing molecules to jump from their lattice node to an adjacent one. For a molecule with a macroscopic diffusion coefficient D in motion on a lattice of characteristic length l with a time-sampling of intervals Δt, we can define the jumping probabilities

:

$$p(\textit{each of the adjacent nodes}) = \frac{D\Delta t}{l^2} \quad \text{(I.22)}$$

$$p(\textit{stay in place}) = 1 - \frac{2nD\Delta t}{l^2} \quad \text{(I.23)}$$

Here, n is the dimensionality of the lattice. One may note that in order for the probabilities to sum up to 1, we have the condition $\frac{2nD\Delta t}{l^2} \leq 1$, which leads to $\frac{\Delta t}{l^2} \leq \frac{D}{2n}$. In other terms, the time and space-samplings are coupled and must be set carefully so the probabilities.

Reactions occur when two potentially interacting molecules are deemed close enough to each other. Depending on the model definition, this can be between two molecules located on adjacent nodes, or sharing the same node if the model ignores steric hindrance and allows for two molecules to occupy the same node. The definition of a biologically relevantmicroscopic reaction probability between two molecules based on the macroscopic reaction rate is a non-trivial task. As seen in I.2.2.2, the macroscopic reaction rate is the manifestation of a transport process combined with an association process. In individual-based models, the transport process is explicitly recreated by diffusion, and the reaction probability should actually characterize the association process. For two species A and B present in numbers N_A and N_B respectively in a total simulation volume V_T that is well-mixed, the number of potentially reacting pairs is :

$$N_P = \frac{N_A N_B V_C}{V_T}$$

V_C is the characteristic volume in which two molecules must be contained in order to react. Each of the pairs has a probability p to react, so the number of pairs that will react is pN_P.
The macroscopic representation of the same process is characterized by a reaction rate k_{macro} that we try to relate to the probability p. During a time Δt, the number of reactions is :

$$N_R = \frac{k_{macro} N_A N_B \Delta t}{\mathcal{A} V_T}$$

With $\mathcal{A}$ being Avogadro's number. Therefore, since $N_R = pN_P$, we obtain that $p = \frac{k_{macro}\Delta t}{\mathcal{A} V_C}$.
The decoupling between reaction and diffusion in two separate microscopic processes allows for the recreation of heterogeneous spatial configurations

while maintaining the validity of the simulation scheme. Lattice individual-based models generally scale linearly with the number of lattice nodes.

Lattice models are at the core of GridCell [Boulianne 2008], a simulator for complex reactions in three-dimensional biological systems. Spatiocyte is another example of microscopic lattice simulation algorithm [Arjunan 2010] which was included in the E-Cell initiative among other modelling algorithms [Tomita 1999]. Aside from these attempts to provide a generic framework for cell biology modelling, microscopic lattice algorithms are often implemented in *ad hoc* simulations for specific case studies. For instance, Berry demonstrated the effect of macromolecular crowding on michaelian reaction kinetics [Berry 2002] using a lattice model with volume exclusion. Linderman et al implemented lattice models for the study of membrane compartmentalization in G-protein signalling systems [Mahama 1994, Shea 1998, Fallahi-Sichani 2009].

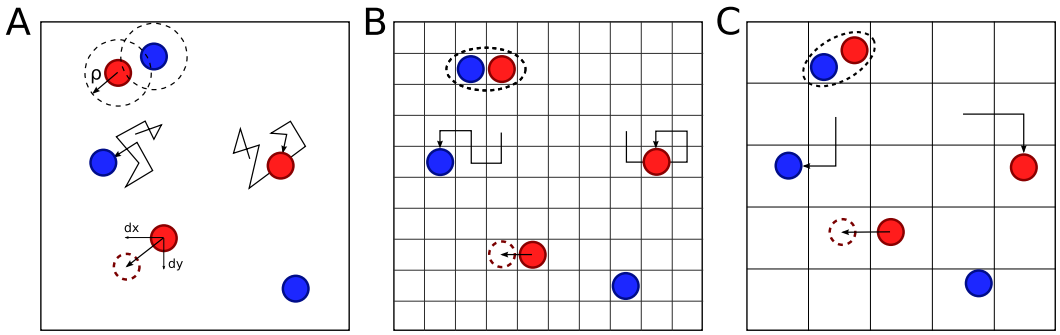

Figure I.7 – Schematic of simulation algorithms for off-lattice models (***A.***), microscopic lattice models (***B.***) and mesoscopic finite volumes models (***C.***) for bimolecular reactions (blue and red spheres). ***A.*** In off-lattice models, the simulated molecule jumps every Δt time step by increments on its degrees of freedom, these increments drawn from a normal distribution whose variance is $2D\Delta t$. Reaction occurs probablistically between two partners closer than a reaction radius (circled with dashes). ***B.*** In microscopic lattice models, molecule positions are discrete. Reaction occurs using Monte Carlo methods between two partners that are on adjacent nodes. Trajectories are discrete jumps between adjacent nodes. ***C.*** In mesoscopic finite volumes models, the subvolumes either contain discrete populations of molecules, or continuous concentrations (not represented). Reaction occurs between molecules contained in the same subvolume (using SSA for discrete molecule populations, or ODE for continuous concentrations). Motion of molecules is determined by stochastic realizations of the RDME for discrete populations, or by solving the flux according to reacton-diffusion PDE between subvolumes. Adapted from [Burrage 2011].

I.2.3.3 Off-lattice individual-based models

Lattice models are based on discretization of time and space. Off-lattice individual-based models track the position of every molecule with trajectories that are not discretized in time or in space (but become discrete when these models are implemented in simulation on computational systems) . The coordinates of a molecule are real numbers, and their evolution is ruled by an approximation of Brownian motion in a time-discrete random walk. The computational implementation of the Brownian dynamics seen in I.2.2.1 using the Euler-Maruyama method [Higham. 2001] gives the motion of a simulated molecule at position $\mathbf{X}(t)$:

$$\mathbf{X}(t+\Delta t) = \mathbf{X}(t) + \sqrt{2D\Delta t}\zeta \tag{I.24}$$

Where D is the diffusion coefficient, Δt the simulation time step and ζ is a vector of the same dimensionality as the position $\mathbf{X}$, whose components are independently drawn in zero-mean and unit variance normal distribution. This process preserves the linearity of the mean square displacement with respect to time and the macroscopic properties of populations of molecules diffusing homogeneously.

In this simulation context, a reaction event occurs whenever two potentially interacting molecules are at a distance inferior to a binding radius, as proposed by Andrews & Bray [Andrews 2004]. The relation between the radius ρ, the diffusion coefficients D_A and D_B of two interacting species, and the macroscopic reaction rate is given by the formula $\rho = \dfrac{k_{macro}}{4\pi(D_A + D_B)}$. In the case of proteins, the diffusion coefficient is around $10\mu\text{m}^2.\text{s}^{-1}$, and reaction rates are typically around $10^6\text{M}.\text{s}^{-1}$. This leads to binding radii of around 10^{-11}m, which is smaller than the actual physical molecule radius, and is unrealistic [Erban 2009]. The binding radius should also be greater than the diffusion step $\sqrt{2D\Delta t}$, which imposes a time step below the nanosecond. Erban & Chapman developped the $\lambda - \bar{\rho}$ model in order to circumvent these limitations. The binding radius ρ, within which a reaction event is certain to happen, is replaced by a reaction radius $\bar{\rho}$ within which a reaction event happens at a rate λ. It becomes possible to use larger reaction radii, and thus larger time and space samplings, which reduces the computational cost. The reaction model is executed using Monte Carlo methods (as is diffusion), the rate λ defining a probability of reaction p_λ. In practice, the neighbourhood of the molecule in which reaction may occur is not restricted to spheres or disks [Dudko 2004]. The simulated molecules can be assumed punctual, so that the model ignores volume exclusion and trajectory intersection, but

collision still has to be searched for in order to generate reaction events. Releasing the spatial discretization constraint presents a major downside : the detection of collision, or proximity, between molecules cannot be performed node-wise. Thus, the complexity of off-lattice algorithms scales quadratically with the number of simulated molecules. However, optimization techniques can be implemented in order to decrease the computational cost of the search for reaction partners, such as spatial partitionning.

The most notable simulators implementing off-lattice individual algorithms are Smoldyn [Andrews 2010, Andrews 2012], MCell [Stiles 2001, Kerr 2008], and ChemCell [Plimpton 2005]. These simulators are designed to be used as generic simulation framework for arbitrary cellular geometries, and come with visualization tools. Off-lattice models are also developped as *ad hoc* investigation models. Morelli & ten Wolde explored the effect of spatial and temporal noise on an system of antagonistic enzymes [Morelli 2008]. The use of off-lattice individual-based model allowed them to measure the microscopic spatial properties of the system in a way that mean-field formalism cannot apprehend, by definition.

I.3 Local Conclusion

Cell signalling systems are complex cascades of proteins interacting by specific biochemical processes, principally complexification and phosphorylation. They are functionally organized as the succession of a reception stage between a ligand and a receptor, a transduction stage between a receptor and an intracellular protein, and a response stage by cascades of biochemical reactions. The amounts of signalling proteins in active or inactive state at the different stages of the cascade define the encoding of the signal. Cell signalling systems exhibit spatial heterogeneities of different orders : they relay a signal through compartments with different geometries and dimensionalities, and within these compartments, the distributions of signalling proteins is not homgeneous, but take the form of clusters.

Our objective is to investigate the dynamics of a generic linear signalling system where spatial homogeneity cannot be assumed. The outline of our study follows the structure of a generic linear pathway. We will first develop an off-lattice individual-based model of the reception stage between an extracellular ligand and membrane receptors. We will use this model to test the effect of heterogeneous distributions of fixed receptors on binding at equilibrium in chapter 2, measuring the apparent affinity of the reaction and ex-

ploring different diffusion regimes. In chapter 3, we will extend the study of ligand-receptor interaction by taking advatange of the simulation framework to measure empirical binding events waiting times distributions, and how a spatial correlation in receptor positions induces a temporal correlation in receptor activation. In chapter 4, we will then present another individual-based, on-lattice computational model to investigate the effect of heterogeneous distributions on the transduction stage between clusters of fixed receptors and their downstream membrane protein substrate. In chapter 5, we will add to our transduction model a non-homogeneous diffusion mechanism that reproduces dynamical heterogeneous protein distributions instead of fixed ones, and investigate its effect depending on diffusion.

Chapter II

Extracellular ligand-receptor binding under fixed heterogeneous receptor distributions

Contents

Highlights

► Simulation of activation by ligand molecules of receptors in fixed heterogenous distributions (clusters). ► Dose-response curve parameters compared with overlapping clusters, contiguous clusters, or homogeneously spread receptors. ► Clustering decreases the apparent affinity of the system of receptors. ► Clustering favors rebinding but decreases initial binding events leading to an overall impaired response.

II.1 Introduction

The global study follows the functional structure of signalling pathways, and thus starts with the reception stage, where extracellular ligand molecules bind to membrane receptors, initiating the cell response. The first part of our study focuses on the effect of heterogeneous receptor distributions on the response of a pathway, measured as the number of occupied receptors. Before presenting the publication that summarizes our findings in the next section, we introduce the general approach and the experimental setups.

II.1.1 Outline

The response initiated by a signalling pathway is triggered by the presence of ligand molecules perceived by membrane receptors, which is a reversible binding reaction. At this initial reception stage, the response can be estimated as the number of ligand-receptor complexes, considering that the more there are occupied (and therefore activated) receptors, the stronger the response. Transduction and downstream signalling effectors are excluded from this present chapter, which only focuses on reception on the extracellular face of the membrane.

At constant concentration of ligand molecules, the number of occupied receptors reaches a dynamical equilibrium defined by the balance of two opposite reactions : ligand-receptor complex association and dissociation (as seen in I.2.1.1). The reaction rates of these two opposites reactions relate the number of occupied receptors obtained with a given ligand concentration, under the form of dose-response curves. Dose-response curves constitute the main investigation tool of this chapter, as they summarize the global behavior of the reception stage for vast ranges of ligand stimulation. The characteristics of the curve can be directly related to the parameters defining the ligand-receptor interaction. The publication presented hereafter typically used the slope at origin of the curve and the half maximal efficient concentration (EC50), that is the amount of ligand required to occupy half of the total available receptors. These characteristics can be estimated on dose-response curves for different experimental setups, and give a quantitative grasp on the apparent affinity of the ligand-receptor interaction.

The aim of this first study is to compare the dose-response curves of the same system of receptors under different spatial distributions, using the characteristics of the curves to determine the apparent affinity of the ligand-receptor system. The core principle that ligand-receptor binding can only occur if a ligand molecule is located in the immediate vicinity of a receptor introduces the notion of *affinity zone*. From this notion, three degrees of spatial correlation for receptor positions were considered :

1 - No spatial correlation
Receptor positions are not correlated, the affinity zone of each receptor is independent and different from the affinity zones of the other ones.

2 - Over stacked receptors
Receptor positions are correlated, they are grouped in clusters within which they share the same affinity zone.

3 - Contiguous receptors
Receptor positions are correlated, they constitute clusters of adjacent affinity zones that are nevertheless different, or partially overlapped.

The case 1 corresponds to the classical picture of well mixed reactions systems described in I.2.1.1, and was used as the control case to which the dose-response curves for cases 2 and 3 where compared. An analytical formulation of receptor occupation at equilibrium for the case 2 was derived inspired from multi-sites binding kinetics [Juska 2008] adapted to the affinity zone scheme (equation 5 in publication 1, page 3). This layout can be understood as the "worst-case scenario" of spatial correlation, with receptors so close that the total effective target area for ligand molecules is dramatically reduced. For these two first cases, an off-lattice individual-based computational model (as seen in I.2.3.3) based on the affinity zone scheme was also used to obtain dose-response curves from simulation. As no analytical formulation could be developped for the case 3, the same computational model was used to obtain dose-response curves. In this case, spatial correlation in receptor positions is introduced while preserving the total target area.

II.1.2 Computational model

We developped a computational model based on the principle that reaction and diffusion are recreated separately and microscopically for each individual molecule. Thus, the well mixed assumption is no longer required and the reversible binding reaction can be recreated with heterogeneous receptor distributions.

The model presented in the publication is an off-lattice individual based model (as seen in I.2.3.3), with the parameters illustrated on figure II.1 (an extension of figure 2 in publication 1 page 5).

A total simulation time is discretized in steps dt. The simulated environment consists in a 2-dimension plane of surface $S_T = 2 \times L \times H$. Each of the N_l ligand molecules is a punctual particle with position in real coordinates $(x_l, y_l) \in [-L; L] \times [0; H]$. Toric boundary conditions are set at $x_l = L$ and $x_l = -L$, the upper and bottom boundaries ($y_l = 0$ and $y_l = H$) are reflective barriers. The bottom boundary corresponds to the membrane, where receptors are set. Motion of each ligand molecule is achieved using the approximated Brownian random walk procedure described in I.2.3.3, with a diffusion coefficient D. Ligand molecule positions are initialized randomly and uniformly in the medium.

The r_0 receptors are defined as a position on the membrane x_r, around which a reactangular box of width $2 \times l_r$ (defined as b in the publication) and height h_r is set. This area (of surface $S_R = 2 \times l_r \times h_r$ constitutes the affinity zone. The parameter Cl gives the number of clusters to be created, each containing $n = r_0/Cl$ receptors. The simulation calculates the size of a cluster, each composed of n receptors with a spacing $2 \times spa$ (defined as r in the publication), and splits the total length of the membrane in possible slots for each cluster. Depending on the parameter t_{init}, the clusters are arranged periodically with equal spacing, or irregularly by randomly choosing a slot for each cluster. The same initialization procedure is used for homogeneous receptor distributions, which is the special case $Cl = r_0$. Receptors are immobile and stay at their initial position during the simulation.

At each time step, each ligand molecule located in the affinity zone of a free receptor has a probability $p_1 = k_1 dt$ to bind and thus form a ligand-receptor complex, rendering the receptor unavailable for other ligand molecule. The ligand molecule is labelled as unavailable for other receptors as well and immobilized. At each time step, each ligand-receptor complex has a probability $p_{-1} = k_{-1} dt$ to unform, the ligand molecule starts off its diffusion again from the position $x_l = x_r, y_l = rel$. The parameter rel was generally set to h_r, so the ligand molecule is released at the edge of the affinity zone. This was implemented to address the unbinding radius problem that arises in off-lattice bimolecular reaction systems [Erban 2009], that is the bias towards immediate rebinding of a just-released ligand molecule. The simulation also allows for negative value of the parameter rel, which forces the ligand molecule to be released at a random height $y_l \in [0; |rel|]$. It was used in publication 1 to investigate clustering with binding events decorrelation.

The simulation consists in alternative stages of diffusion, then reaction, until completion. The number of molecules in each state is tracked for every time step. Additionally, the occurences of specific events were also tracked, such as ligand-receptor encounter events, individual binding events, and consecutive binding events of the same ligand molecule, but such data will be analyzed in the chapter III and was not used in this chapter.

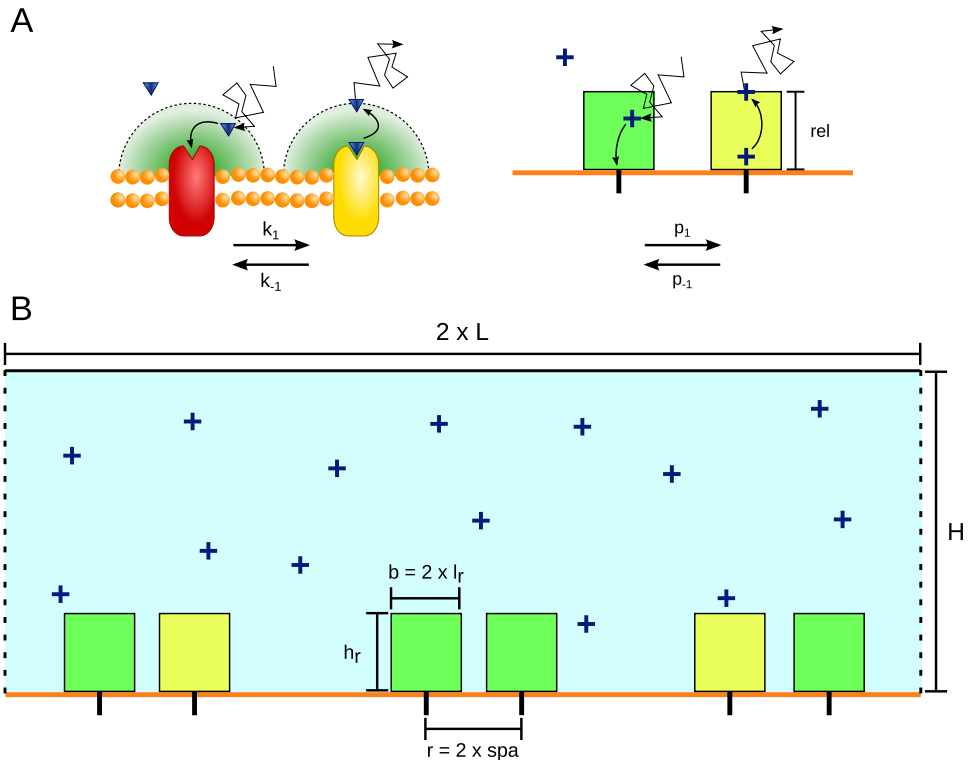

Figure II.1 – ***A.*** The affinity zone scheme. The vicinity of a receptor forms a continuum in which reaction is more likely to occur as the ligand molecule approaches the receptor binding site (left). This was implemented in the simulation (right) by defining an affinity zone in which a ligand molecule has a constant probability p_1 to bind, and 0 outside. Unbinding of a ligand molecule occurs with probability p_{-1}, the ligand molecule starting off its motion at a height *rel* from the membrane (here $rel = h_r$). ***B.*** Schematic of a simulated environment illustrating the meaning of the parameters.

Publication 1

Impact of receptor clustering on ligand binding

Bertrand R. Caré and Hédi A. Soula

BMC Systems Biology 2011, **5**:48

Caré and Soula *BMC Systems Biology* 2011, **5**:48
http://www.biomedcentral.com/1752-0509/5/48

BMC Systems Biology

RESEARCH ARTICLE Open Access

Impact of receptor clustering on ligand binding

Bertrand R Caré[1,2,3*] and Hédi A Soula[2,3*]

Abstract

Background: Cellular response to changes in the concentration of different chemical species in the extracellular medium is induced by ligand binding to dedicated transmembrane receptors. Receptor density, distribution, and clustering may be key spatial features that influence effective and proper physical and biochemical cellular responses to many regulatory signals. Classical equations describing this kind of binding kinetics assume the distributions of interacting species to be homogeneous, neglecting by doing so the impact of clustering. As there is experimental evidence that receptors tend to group in clusters inside membrane domains, we investigated the effects of receptor clustering on cellular receptor ligand binding.

Results: We implemented a model of receptor binding using a Monte-Carlo algorithm to simulate ligand diffusion and binding. In some simple cases, analytic solutions for binding equilibrium of ligand on clusters of receptors are provided, and supported by simulation results. Our simulations show that the so-called "apparent" affinity of the ligand for the receptor decreases with clustering although the microscopic affinity remains constant.

Conclusions: Changing membrane receptors clustering could be a simple mechanism that allows cells to change and adapt its affinity/sensitivity toward a given stimulus.

Background

The binding kinetics between cell surface receptors and extracellular biomolecules are critical to all intracellular and intercellular activity. Modelling and predicting of receptor-mediated cell functions are facilitated by measurement of the binding properties on whole cells. Therefore, these measurements, however elaborate, have been based on the ground of chemical enzyme/substrate formalism [1-4]. Such formulations were derived from the law of mass-action that evaluates local reaction rates from averaged chemical species densities over the medium volume. Mass-action laws are mean-field approximations because they evaluate local reaction rates on the basis of average values of the reactant density over a large spatial domain. In addition, it amounts to assume that ligand/receptor interactions are independent [5,6].

These assumptions may fail in real biological systems, in particular considering membrane receptors which are restricted to only 2 of the 3 spatial dimensions [7,8]. The effect of binding kinetics for membrane-restricted receptors (on spherical cells) has already been investigated by Berg and Purcell [9]. This study focused on the spatial restriction of receptors to a 2D support while interacting with bulk ligand diffusing in a 3 D medium, and resulted in an expression for reaction rate coefficients as non-linear functions of cell surface receptor density. This pioneer study has been enriched by further works towards reversibility and rebinding [10], receptor density [11], time dependency [12], and gradient sensing capabilities [13,14]. Taking a step further, the spatial organization of receptors on the membrane itself should also be taken into account. At first glance, since membrane receptors are bound to the cell membrane that allows a lateral degree of freedom, one would expect a simple (and homogeneous) distribution of receptors on the membrane. Indeed, cell membrane is composed of a mixture of phospholipids in a fluid phase and as such, in the classical fluid-mosaic model of membrane [15], membranes components undergo isotropic random movement akin to Brownian motion [16,17]. In this model, the resulting equilibrium distribution of components - among them receptors - is therefore homogeneous. Recently, however, this picture has evolved considerably towards a non-homogeneous distribution of the usual components of cell membranes [18-21].

* Correspondence: bertrand.care@insa-lyon.fr; hedi.soula@insa-lyon.fr
[1]Université de Lyon, Laboratoire d'InfoRmatique en Image et Systèmes d'information, CNRS UMR5205, F-69621, France
[2]Université de Lyon, Cardiovasculaire Métabolisme et Nutrition, Inserm UMR1060, F-69621 Villeurbanne Cédex, France
Full list of author information is available at the end of the article

BioMed Central

© 2011 Caré and Soula; licensee BioMed Central Ltd. This is an Open Access article distributed under the terms of the Creative Commons Attribution License (http://creativecommons.org/licenses/by/2.0), which permits unrestricted use, distribution, and reproduction in any medium, provided the original work is properly cited.

Indeed, more and more evidence points towards the existence of micro-domains enriched in various lipids such as cholesterol as well as other proteins. In particular, receptor colocalization in lipid rafts and other membrane structures have been reported in cells [22-24].

This localization and clustering may have a dramatic influence on signalling. This influence remains, however, unclear as literature reports contradictory effects of clustering/declustering on signalling (see e.g. [23,25]). This is probably due to the method of destroying cholesterol-rich domains via methyl-β-cyclodextrin which may have other effects than simply unclustering membrane receptors, and alter signalling functions.

In any case, the impact of an inhomogeneous receptor density *on* the membrane itself has been only studied recently. Only few theoretical contributions have been reported in some specific cases: : bacteria sensitivity [26] and chemotaxis [27], G-protein activation [28], simple model of trans-phosphorylation (implying two receptors only) [29].

In addition, several more detailed studies illustrate the possible effect of receptor clustering on receptor binding by inducing enhanced rebinding or ligand receptor switching [30-33], or enhancing encounter probability of activated receptors with submembranar signalling proteins such as in GPCR signalling pathways [34].

Notably [32] proposes that clustering provides higher rebinding capabilities and therefore helps to obtain a better response - i.e. more binding events. However, another analysis [35] proposes that the forward rate constant is diminished when receptors are clustered, providing in that case less binding events. Both effects counteract themselves, and the final output remains to be studied.

Considering ligand-receptor binding as a diffusion-limited reaction [9,10], we investigated how receptor distribution may impact this primordial step of signalling, ligand binding to receptor extracellular domain. We will restrict ourselves to ligand-receptor binding probabilistic mechanisms at the early stage of signalling, that is, without considering specific biological/biochemical interactions between receptors themselves, nor between receptors and internal signalling proteins, but only the spatial aspects of ligand-receptor interaction at cell surface. We place this study in the context of generic clustering of receptors that cover the whole cell surface.

In order to investigate the effects of receptor clustering on ligand binding, we present two joint approaches of ligand receptor binding at equilibrium when receptors are organized in clusters at cell surface. We consider three membrane receptor layouts illustrating three degrees of spatial correlation. These layouts, for two of which a simple ODE description is available, are studied in the context of ligand-receptor reversible binding. The three layouts are investigated following computer based simulations conjointly with an ODE formalism, the latter adapted to include spatial characteristics of receptor organization.

Ligands are assumed to diffuse freely above the membrane without interaction except when they can bind stochastically to receptors. Receptors are modelled as still positions on the membrane. Ligand-receptor complex formations are stochastic events occurring whenever a ligand is near enough a free receptor. More precisely, it occurs whenever the ligand lies in a defined area above the receptor position. This area is called the *affinity zone*. This simple binding model can be implemented into both an ODE formalism and computer simulations in to investigate the effects of spatial correlation on total receptor occupation. It allows fast computation and exploration of various receptor configurations together with an analytic formulation of receptor occupation. Using constant reaction rates (which can be easily related to simulation parameters), we compare the amount of complex binding at equilibrium between these different layouts. We show that, contrary to intuition, clustering decreases the overall binding activity: the number of complexes at equilibrium for equal ligand concentration are lower in the clustered case than in the homogeneous case. This drop in the so-called "apparent" affinity increases with clustering as dose-response curves are increasingly shifted to the right.

Methods

We describe below the three possibilities of spatial correlation we have chosen to investigate. For each, we present the assumptions made in order to model them properly, the simple analytical formulation we derived whenever it was possible, and the corresponding individual-based model used in simulation. As mentioned in introduction, we consider monovalent ligands reversibly binding to monovalent receptors which are independent from each other.

No spatial correlation

The first layout consists of receptors homogeneously set on the membrane, which stands as a reference configuration of homogeneously spread receptors on the cell membrane. The classical approach to model ligand-receptor interaction is through reaction mechanism akin to enzymatic reactions. In the case of monovalent receptors, the most simple model remains the classical Ligand-Receptor Binding Equilibrium equation:

$$L + R \underset{k_{-1}}{\overset{k_1}{\rightleftharpoons}} C \tag{1}$$

where L will be the ligand and R the receptor. When docked, the ligand forms with the receptor a complex C.

The reaction is reversible with the forward rate constant k_1 and backward rate constant k_{-1}.

The further steps involve some generally implicit assumptions: the complex concentration variation will be the sum of two parts. The negative rate of complex dissociation will be k_{-1} times the complex number. The statistical process underneath this assumption relies basically upon a time independent (exponential) undocking probability [36].

On the other hand, the complex formation equation is based on what is called *the law of mass action* which states that the rate of a reaction is proportional to the product of the concentrations of the reactants. In essence, this law simply states that the reaction rate is proportional to the *rate of encounter* of reactants in the medium. This rate of encounter is itself proportional to the joint probability to find both reactants in the same vicinity. These probabilities are in the case of homogeneous medium the respective concentrations. As [7] have pointed out, this formulation is correct whenever the medium is well-stirred and isotropic with respect to diffusion. In addition, one must assume that particles are independent from each other. Note that in that case, at equilibrium, the relation is well known [5]

$$c = \frac{r_0 l}{\kappa + l} \tag{2}$$

where lower case indicates quantities of corresponding species. The total number of receptors will be denoted as r_0 and $\kappa = \frac{k_{-1}}{k_1}$ is the dissociation constant. Variables can be made dimensionless via $l^* = l/\kappa$ and $c^* = c/r_0$. Note for later that we have two ways to retrieve the dissociation constants: first, using the EC_{50} (efficient concentration 50) that is the amount of ligand needed to generate occupation of half the receptors at equilibrium. In this case, this amount is κ (and therefore 1 in the dimensionless version). Otherwise, we can also use the slope at origin $c'(0) = \frac{r_0}{\kappa}$ (also equals 1 in the dimensionless version).

Over stacked receptors

Spatial correlation of receptors should in itself modify Eq. 2, as the joint probability to find both reactants in the same vicinity is no longer independent for close receptors. Thus, we first propose an extreme case that has an analytical derivation. Let us assume we have r_0 receptors which are divided among clusters of size n - there are r_0/n such clusters. We will suppose that receptors inside these clusters are so close together that the area in which ligand binding may occur is the same for each receptor of a cluster. In other words, each receptor of a cluster interacts with ligand localized in the exact same portion of the extracellular vicinity, and clusters of size n can be seen as receptors with n sites. With this assumption, the ODE describing the equilibrium saturation rate of receptors is a special case of equations considering clusters of size n as virtual macromolecules with n docking sites, as seen in [36-38]. This simple trick allows us to compute the number of sites occupied c. Indeed, let us name C_i ($i \leq n$) a cluster with i sites occupied ($C_0 = R$, R being a cluster with no receptors occupied). The lower case letters, c_i, will denote the numbers of clusters C_i. We discard the transitions for more than one site at a time, yielding only constants for transition between C_{i-1} and C_i ($i \geq 1$)

$$L + C_{i-1} \underset{k_{-i}}{\overset{k_i}{\rightleftharpoons}} C_i \tag{3}$$

At this point we simply partitioned the number of clusters r_0/n by their amount of occupied sites i $\left(\sum_{i=0}^{n} c_i = r_0/n\right)$. Therefore the total number of sites occupied (and of bound ligands) will be $c = \sum_{i=1}^{n} ic_i$, since there are i occupied sites per C_i.

From this we can derive a set of ODE's that describe the evolution of concentrations of these components, where we can assume a homogeneous medium. At equilibrium, we obtain a very general formula

$$c = \frac{r_0}{n} \frac{1}{\sum_{i=0}^{n} \frac{l^i}{\prod_{j=1}^{i} \kappa_j}} \left(\sum_{i=1}^{n} i \frac{l^i}{\prod_{j=1}^{i} \kappa_j} \right) \tag{4}$$

where we can relate simply the different association/dissociation constants. We assume that a receptor with i occupied sites is i times more likely to release one of its cognate molecules than a receptor with only 1 site occupied. Indeed, we have $k_i = k_1$ but $k_{-i} = ik_{-1}$, so $\kappa_i = i\kappa_1$. Due to the shared affinity zone, we will assume in this model that the potential to bind a free site will be independent of the number of free sites. Therefore the on rate k_i will be equal to k_1 because it defines the transition from $L + C_{i-1}$ to C_i through binding of 1 ligand to 1 site. This event happens with the same probability as the transition $L + R$ to C_1. Then getting rid of the 1 subscript ($\kappa = \kappa_1$)

$$\prod_{j=1}^{i} \kappa_j = i\kappa^i$$

and

$$c = \frac{r_0}{n} \sum_{i=1}^{n} \Phi_i^n \left(\frac{l}{\kappa}\right) \tag{5}$$

with

$$\Phi_i^n(x) = \frac{x^i}{(i-1)\left(\sum_{j=0}^{n} \frac{x^j}{j}\right)} \tag{6}$$

Several theoretical dose-response (for dimensionless ligand dose $l^* = \frac{l}{\kappa}$ and normalized responses $c^* = \frac{c}{r_0}$) curves for different values of n are displayed on Figure 1-A.

In the dimensionless case (c^* versus l^*) the slope at the origin is $1/n$ yielding an apparent affinity of n. Even if we cannot simply find the EC_{50}, we can note that when $n \gg 1$, we can approximate the value by ignoring terms of order greater than one. It first yields that $\sum_{j=0}^{n} \frac{\left(\frac{l}{\kappa}\right)^j}{j} \sim 1$ and $\sum_{i=1}^{n} \frac{\left(\frac{l}{\kappa}\right)^i}{(i-1)} \sim 1$. So finally, whenever $n \gg 1$, the dimensionless efficient concentration is

$$EC_{50} \sim \frac{n}{2} \tag{7}$$

The real EC_{50} obtained by numerical computation is compared to Eq. 7 on Figure 1-B. The previous approximation is correct even for low n. The very first

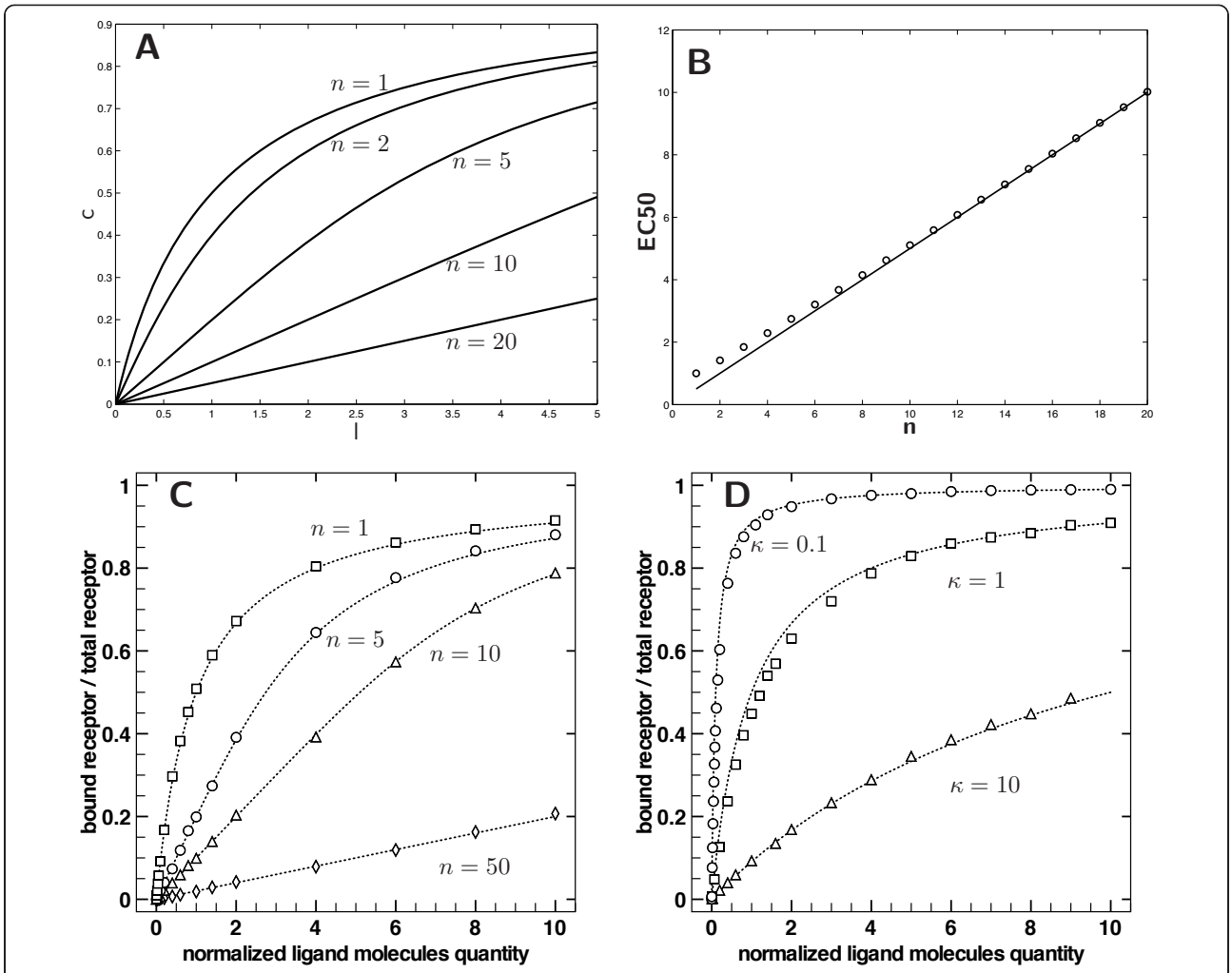

Figure 1 Model validation and clusters of over stacked receptors. A) Dose response for reference size $n = 1$ (no cluster) and various cluster sizes $n \in \{2, 5, 10, 20\}$. The curves have the same saturation value (*lim* $c = 1$ when $l \to \infty$). The slope at the origin is $1/n$ and the $EC_{50} \approx n/2$. B) Efficient concentration according to the degree of clustering. The line is $EC_{50} = n/2$ and the circles are the solution of $1/2 = \frac{1}{n}\sum_{i=1}^{n} \phi_i^n(l)$ using Eq. 4. C) Results for normalized receptor binding with $\kappa = 1$ and for $n \in \{1, 5, 10, 50\}$ sites by receptor (respectively squares, circles, triangles, diamonds) compared to theoretical dose response according to Eq. 4 (dashed lines) with same n. D) Results of normalized receptor binding for three experiments (circles: $\kappa = 0.1$, squares: $\kappa = 1$, triangles: $\kappa = 10$) compared to theoretical dose responses for respective κ according to Eq. 2 (dashed lines).

conclusion to this analysis is that receptor binding dependence can impede or at the least modify dramatically the overall response. Using the same microscopic characteristics (i.e. binding affinity) but with different macroscopic structure, one can create a new *apparent* affinity which is, depending on how it is measured, n using the slope or $n/2$ using the EC_{50}. The local conclusion of this simple analysis is that we can expect modification of the receptor occupation at equilibrium whenever the spatial configuration of the receptors is changed. Introducing correlations in the probabilities of encounter by spatial organization modifies the receptor occupation. In addition, the apparent affinity seems to decrease with the clustering of receptors.

By overstacking affinity zones, even partially, this configuration creates a "strong" spatial correlation which influences dramatically the complex formation rate: within a cluster of receptors, the occupation of a receptor affinity zone is directly dependent of the occupation of affinity zones of the other receptors, since they are totally or partially the same. In order to address the issues stated above, we now propose to investigate what may happen if affinity zones remain distinct from each other inside a cluster of receptors, but "weak" spatial correlation is still induced by placing receptors contiguously. We propose to examine this case using a simulation framework, as no simple mathematical derivation could be obtained.

Contiguous receptors

We introduce in this section a particle simulation framework that was used to detect the effect of clustering, by modelling clusters of receptors with contiguous but non-overlapping affinity zones. This configuration is taken to be the opposite extreme of over stacked receptors in terms of spatial configuration. That is, within a cluster, receptors are still close to each other, but the presence of ligand in the vicinity of one receptor does not influence the binding of a ligand with receptors of the same cluster: their affinity zones are contiguous.

The simulation is restricted to a 2D environment, and a 1D membrane. Ligands are particles in a 2D environment (see Figure 2). The cell membrane is the bottom segment of this environment. Particles of ligand undergo a 2D Brownian motion in the over-damped regime. Explicitly, using the Euler formalism, the equations of movement are

$$\begin{pmatrix} x(t+dt) \\ y(t+dt) \end{pmatrix} = \begin{pmatrix} x(t) \\ y(t) \end{pmatrix} + \sqrt{Ddt} \begin{pmatrix} Z_1 \\ Z_2 \end{pmatrix} \quad (8)$$

where Z_i, $i = 1, 2$ are two independent random numbers drawn from a normal distribution of zero mean and variance 1. D is the diffusion coefficient and dt is the time step for integration. Vertical cylinder boundary conditions are applied for the diffusion; bottom and top segment are bouncing and uncrossable boundaries. The lateral segments are connected: particles that go through one side appear on the other side. To avoid too much transient dependence, initial positions of particles are homogeneous (chosen randomly with uniform probability).

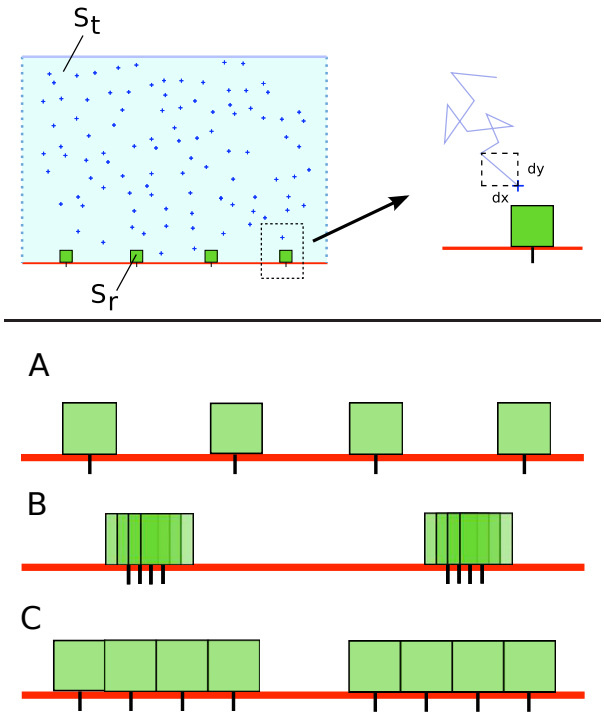

Figure 2 Simulation environment. Top panel: On the left is a cartoon view of the 2D membrane of area S_t. Ligand particles are crosses, and the green boxes are receptors (of affinity zone S_r). Receptors are fixed, and ligands undergo a 2D Brownian motion. Bottom panel: cartoon view of the different experiments performed. The spatial configuration of the receptors is modified and the computation of the occupation is performed. Three spatial configuration are tested: A) Evenly spaced receptors - homogeneous repartition. B) Over stacked receptors: the clusters are evenly spaced, but contain a certain number of sites C) Non-overlapping spatial configuration. The affinity zones are contiguous but do not overlap. Clusters of n receptors are evenly placed on the membrane.

Receptors are punctual but localized only on the bottom line of the environment area. Their diffusion is neglected and they will therefore remain at their initial position throughout the simulations. To simulate docking, we chose a very simple formalism: each receptor has an affinity zone - a square above its position - where there is a constant probability p_1 for a ligand to bind whenever it is found itself in. Of course, a ligand can only bind to a free receptor. No binding event can

occur for an already bound receptor. In addition, the bound ligand cannot diffuse as long as it stays bound. Finally, when formed, the complex has a constant probability to dissociate p_{-1}. Upon dissociation, the ligand molecule resumes its Brownian approximated motion, starting from the center of upper edge of the affinity zone it just left. This is to avoid bias in rebinding events; the probability at the next time step for the ligand to return into the affinity zone or to move away will be equal.

Using this formalism, it is very simple to relate the parameters of the simulation with the association constant of the ligand/receptor binding. Indeed, at equilibrium, the number of receptor-ligand complexes that are dissociating per time step is equal to $p_{-1}c$.

Assuming the classical framework [5,39], the rate of binding will be the product of three terms: the number of free available receptors - r; the probability to find a ligand in the affinity zone - that is lS_r/S_t with l as the number of free ligands, S_r and S_t the surface of the affinity zone and the environment respectively; and finally the probability to bind - p_1.

This produces the relation (since what comes out must be equal to what comes in at equilibrium), and using $r = r_0 - c$

$$p_{-1}c = \frac{S_r p_1}{S_t} rl = \frac{S_r p_1}{S_t} (r_0 - c)\, l$$

to obtain the classical equation:

$$c = \frac{r_0 l}{\kappa + l}$$

with

$$\kappa = \frac{S_t p_{-1}}{S_r p_1} \tag{9}$$

Eq. 9 allows a direct comparison with the dissociation constant. It relates simply with docking and undocking probability plus what we called before the affinity zone: the surface available for binding.

Results

Unless otherwise specified, the parameters are identical for all simulations. The simulations were performed for a sufficient number of time steps to ensure equilibrium was reached, which is around 10^3 for the selected parameters. The number of receptor is fixed and is $r_0 = 500$. Similar runs were performed with $r_0 \in \{1000, 2000, 5000, 10000\}$, showing no qualitative or quantitative differences with $r_0 = 500$. Thus, the latter value for r_0 was chosen to limit finite-sized effects and computational time. The time step dt is equal to 10^{-2} and $D = 1$. All the results displayed below are normalized on the × axis (ligand molecules) with respect to a reference dissociation constant $\kappa = 5.10^5$ (using a space ratio $S_T = 5.10^5 S_R$) by taking a constant ratio $p_{-1}/p_1 = 1$ with $p_1 = p_{-1} = 0.1$. The results obtained would have to be considered within the correct regime of reaction, that is reaction-limited or diffusion-limited. As the simulated reaction is either one or the other possibility, results cannot be interpreted in the same way. Our concern being the effect of the spatial organization of receptors on binding at equilibrium, we would like to make sure that we simulated ligand-receptor binding in the diffusion-limited regime, so the observation of an effect of clustering can specifically be related to diffusion and geometrical aspects. In order to check whether the simulations were reaction-limited or diffusion-limited, we compared the average mean first passage time (MFPT) of a ligand molecule in a receptor affinity zone to the reaction time-scale.

A diffusion time scale several orders of magnitude larger than the reaction one characterizes diffusion-limited reactions. An estimation of the average MFPT can be obtained using the asymptotic formula from [40] for r_0 traps of surface area S_r which are located on the boundary of a 2D medium of surface area S_t : $MFPT = \frac{S_t}{2\pi D r_0} \log\left(\sqrt{\frac{S_t}{S_r}}\right)$, and gives for our standard set of parameters a MFPT value of approximatively 418. Using the same simulation environment, we also computed first passage times (FPT) of ligand molecules to receptors. The experimental mean first passage time was obtained by non-linear regression of an exponential probability density function with these simulated first passage times. It yields an MFPT estimate of 1267 ± 18 time steps. Both these estimations being consistent and far larger than the reaction time scale, the following results are valid in the context of diffusion-limited reactions but their significance cannot be assured in the reaction-limited case, which would require a dedicated and separate study.

Finally, the number of occupied sites at equilibrium is computed throughout all simulations, and displayed normalized with respect to $r_0 = 500$.

No spatial correlation: homogeneous receptor distribution

In the case of evenly distributed receptors (see Figure 2-B top for a cartoon of possible configurations, and Figure 1-D for measurements of receptor occupation), the simulation framework behaves as expected. In particular, the behavior of the particles system is consistent with Eq. 2 and κ following Eq. 9 (in the Models section presented above). Three different values for κ are used; $\kappa = 1$ is the reference simulation

($\kappa = 5.10^5$, $p_1 = p_{-1} = 0.01$). The two others values for κ are $\kappa = 10$ (using $p_{-1} = 0.1 = 10p_1$) and $\kappa = 0.1$ (using $p_{-1} = 0.001 = p_1/10$). The results for the several runs are displayed on Figure 1-D. The dashed lines are curves according to the theoretical function (Eq. 2 using the numerical values of the simulation parameters S_r, S_t and the binding properties).

To obtain a good approximation of the slope at origin and the EC_{50}, more runs were necessary for low concentrations and for values near expected the EC_{50} (i.e 1, 0.1). But, all in all, the minimal number of runs is 10 for any given concentration and parameters set. Due to their smallness, error bars are actually negligible - the radius of data points is larger.

As the figures show it and for each parameter set tested, the particles simulation framework is consistent with the predicted behavior: a curvilinear Michaelian-type curve with the correct affinity κ - using the simulation parameters S_r, S_t, p_1 and p_{-1}).

Over stacked receptors

Spatial correlation in the case of receptors with stacked affinity zones - Figure 1-C - is also checked with the analytical formula Eq.5. Here again, using the predicted affinity κ is consistent with the theoretical formulation, as the Eq. 5 is mathematically equivalent to Eq. 2 for $n = 1$.

Three degrees of spatial correlation implied by over stacked receptors ($n \in \{1, 5, 10, 50\}$) are investigated and compared to the control case $n = 1$. Note that the control is of course the same for $\kappa = 1$ on Figure 1-D. Results are averaged values for five runs (Figure 1-B circles). The dashed lines are theoretical values obtained via Eq. 5. Here again, simulations perfectly match the theory in all cases.

Simulations were in perfect agreement with the mathematical derivations presented in the Models section for both type of layouts (as in Figure 1). Simulations of evenly dispatched receptors follows the classical Ligand-Receptor binding equilibrium equation. When over stacked in clusters of various sizes, the proposed equation 5 and the simulations match. Simulations for the latter case will act as a worst case scenario for clustering of receptors. Indeed, this will be the worst situation as regards to affinity zone availability. It should be expected therefore that the ligand receptor binding would be overlap-dependent. The overall binding should increase as the affinity zone is made available and the overlap is decreasing. The maximal effect would therefore be operating for contiguous but non-overlapping affinity zones.

Contiguous receptors

We present in Figure 3 the results of the dose response curves using the third layout - adjacent receptors whose affinity surfaces do not overlap within a cluster.

The dose response curves are compared, all other parameters being equal, to the control case where receptors are homogeneously spread. In Figure 3-A, a comparison of two experimentally obtained dose response curves is displayed. The number n refers to the number of receptors per cluster, the total number of receptors remaining equal to $r_0 = 500$. So $n = 1$ refers to no clustering and is the Michaelian dose response Eq. 2, and $n = 100$ refers to clusters of size 100 (as defined in Figure 2-B). Figure 3-A and 3B thus show how response is modified by clustering: the EC_{50} has increased and the response always lies below the control one, in a weaker but similar way than in the over stacked case seen previously.

Figure 3-B is a close-up view of the origin of the Figure 3-A graph. The slopes at origin clearly differ. The apparent dissociation constant computed from the start of the curve is greater in the clustering case, showing strong clustering effect at low ligand concentrations. For all clusters sizes, the slope at the origin as well as the EC_{50} can be estimated respectively by linear regression and non-linear least square fitting. For the slopes at origin, simple linear regressions of occupation rate against dose were performed, using values between 0 and 0.05κ. On the other hand, EC_{50} were estimated by fitting data using Hill functions - a widely used model for non-Michaelian kinetics $-\ c(l) = \dfrac{r_0 l^\alpha}{\kappa^\alpha + l^\alpha}$. The parameters to be adjusted are κ and α yielding an estimate of EC_{50}.

EC_{50} and slope at origin obtain via fitting are displayed in Figure 3-C and Figure 3-D respectively as a function of cluster size n in semi-logarithmic scale. For both parameters and for all cluster sizes, the values are normalized by the control case ($n = 1$).

The graph Figure 3-C shows that EC_{50} gradually increases with cluster size until a plateau is reached at around 170% of the control value. Similarly the slope at origine decreases down to 50% of the control value. Observing dose response curves from similar experiments, but with increasing cluster size, leads to observing different affinities for the ligand for receptors at a global scale, whereas the intrinsic affinity of each individual receptor remained equal. The saturation at high cluster sizes is merely due to the fact that no more clustering can be induced once extreme cluster sizes are reached, which are limited by the fixed number of receptors.

The Hill coefficient α is classically considered as a reflection of cooperativity in enzymatic reactions. In our case, we observed an increasing α with cluster size until saturation under 20% (data not shown). One can note that Hill function is not an appropriate qualitative model for the curves obtained, as slopes at origin are non-zero, but in our case it merely serves as a

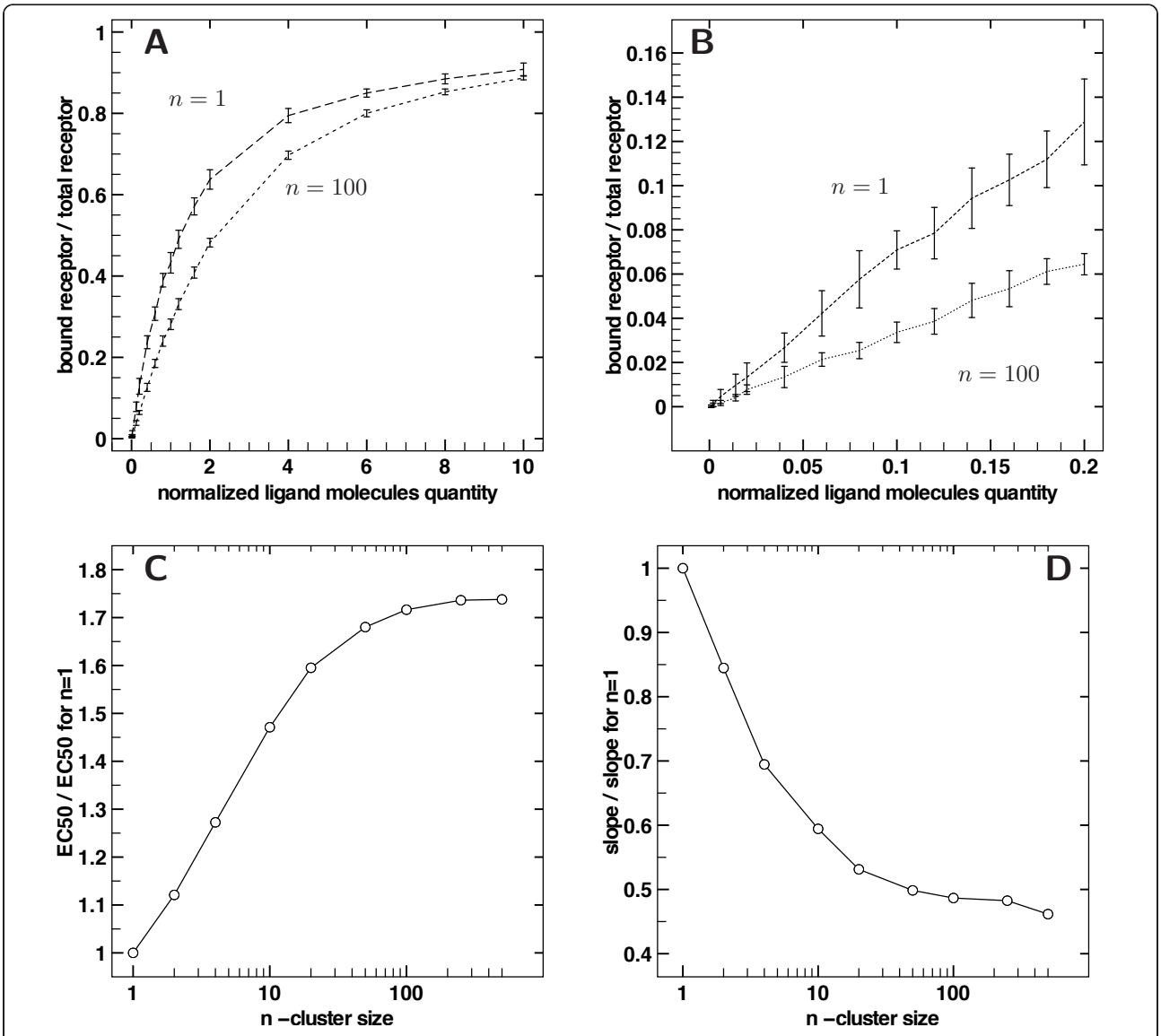

Figure 3 Effect of clustering for contiguous receptors. A) Dose response for $n = 1$ (control) and $n = 100$ receptors per cluster. Error bars are ± standard deviation. B) Close-up of A for $l \leq 0.2$. Error bars are ± standard deviation. C) Ratio of fitted EC_{50} to control EC_{50} (i.e. for $n = 1$) with increasing cluster size, with contiguous receptors, in semi-logarithmic scale. D) Ratio of fitted slope at origin to slope at origin for $n = 1$, with increasing cluster size, with contiguous receptors, in semi-logarithmic scale.

mathematical support for EC_{50} estimation. The very slight variation of Hill coefficient can hardly support any qualitative or quantitative conclusions about clustering effect in the contiguous receptors case, as the Hill function is not pertinent here as a mechanistic model.

Clustering enhances response by increased rebinding

Intuitively, receptor clustering should induce two opposite effects that counter themselves: enhanced rebinding to close receptors, but decreased ligand-receptor encounter probability. In other words, when receptors are clustered, ligands spend on average more time diffusing before encountering a receptor. Indeed the membrane is not evenly covered and has large receptor-free zones. On the other hand, once bound a ligand will be released in a richer receptor area when receptors are clustered thereby allowing a greater rebinding probability. In order to explore the effect of this rebinding, we perform the following experiment: instead of releasing a ligand at the edge of its former cognate receptor affinity zone when it undocks, the ligand is relocated randomly within the entire medium.

By imposing this random repositioning of ligands after unbinding, the simulation bypasses the potential effect

of rebinding, as ligands are on average reinjected quite far from the membrane.

Receptor occupation is then only caused by spatial and temporal independent complex formation. Comparison between dose response curves in such a case and standard simulations may then qualitatively illustrate the part of response alteration which is only due to clustering-enhanced rebinding.

Dose response from such simulations are compared with the standard simulations presented so far i.e. the simulations described in the previous section) for the same clustering (i.e. same n), in Figure 4.

As mentioned above, the effect of random reinjection strongly affects the receptor occupation even in the unclustered case. Since black bars are increasing with clustering, removing rebinding events has a stronger importance the more the receptors are clustered. It was expected since ligands have a higher probability to rebind when receptors are available in the vicinity. Moreover white bars show that the impact of clustering can be greatly increased via random reinjection when normalized by unclustered case (up to ten times the EC_{50} as compared to results in Figure 3-C). In that case the forward rate decrease observed via clustering is not counterbalanced anymore by the greater rebinding dynamics of the clusters. This experiment showed that the decrease in the forward rate due to clustering is stronger than the rebinding gain obtained with closer nearby receptors.

Clustering through partially overlapping receptors

Between clusters of over stacked receptors and clusters of adjacent receptors, we investigate an intermediate scenario, in which clusters are composed of receptors with partially overlapped zones. Responses are computed for a single dose $l \in \{0.5\kappa, 1\kappa, 2\kappa\}$, with clusters of n = 100 receptors progressively overlapping, as the cartoon Figure 5-B pictures. Figure 5-A displays the fraction of occupied receptors at equilibrium in function of intra-cluster overlap, each line corresponding to a given dose l as mentioned above.

As the overlap increases, at fixed number of receptors set in a fixed number of clusters, the effective surface covered by receptors decreases, and so decreases the receptor occupation at equilibrium, from 0% to 100% overlap within a continuum. When in clusters, receptors can possibly share a common affinity zone with some of its neighbors. The decreases in apparent affinity is therefore more pronounced in that case. A similar behavior was observed for each cluster size tested.

Spreading of receptors

On the other side, we simulated situations where the affinity zone width (b) remained constant but the distance between receptors r increased. This could represent a situation where the receptors are still clustered but use a larger space than their binding radius. This layout is depicted on Figure 6-A. We tested two values for the ratio r/b with $r > b$. Note that previously r/b was

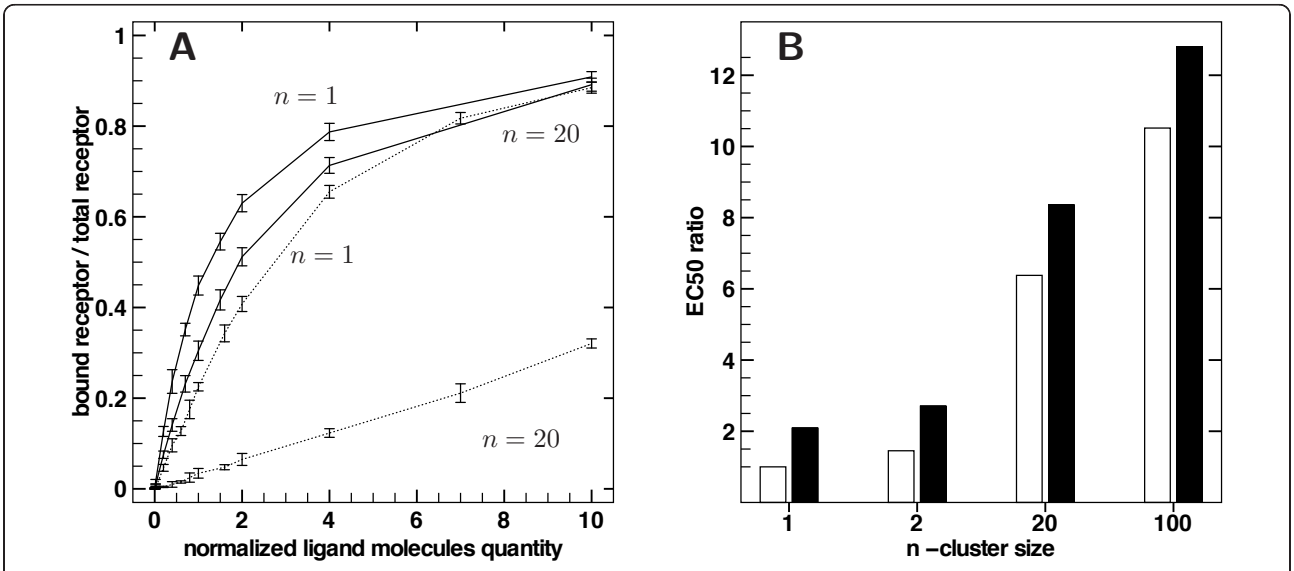

Figure 4 Effect of rebinding on receptor occupation at equilibrium. A) Comparison of dose response curves between n = 1 and n = 20 when ligand is dropped at the edge of affinity surface when unbound (solid lines - standard simulations) or ligand randomly reinjected in bulk when unbound (dashed lines). B) Black bars: ratio obtained with the same layout but using E_{50} obtained with random reinjection normalized by E_{50} obtained with normal reinjection. White bars: ratio obtained for random reinjection using EC_{50} computed for various cluster sizes normalized by E_{50} with no clusters (n = 1).

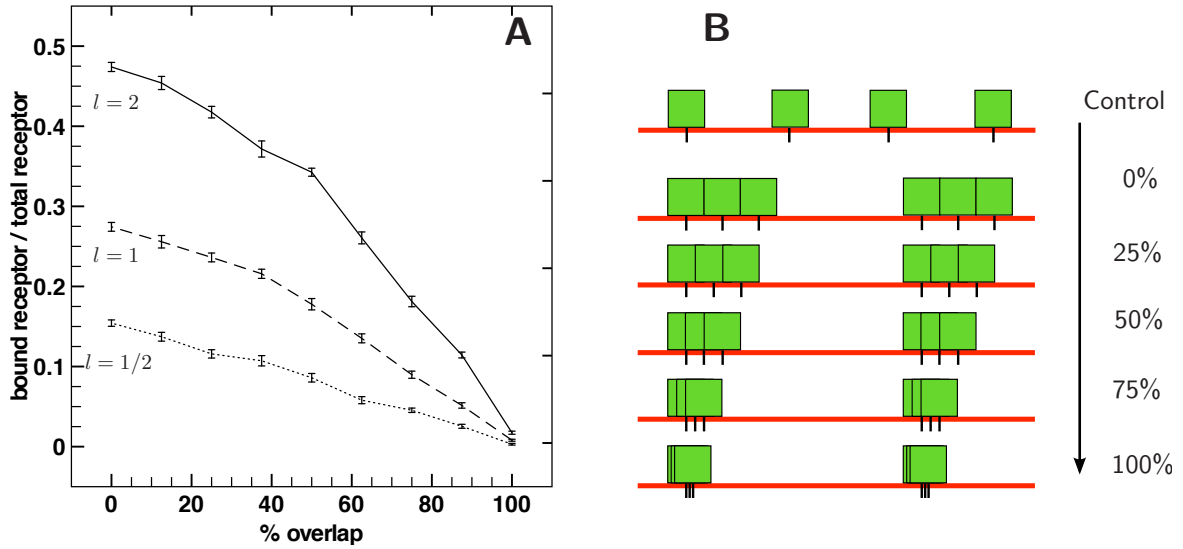

Figure 5 Receptor occupation when affinity surfaces partially overlapped within a cluster. A) Comparison of occupation as a function of relative overlap of affinity surfaces. On a single curve, points correspond to the same experiment, for a fixed ligand concentration, but with varying overlap. Error bars are ± standard deviation. B) Cartoon representing increasingly overlapped receptor affinity surfaces within clusters.

always ≤ 1 with equality occurring in the contiguous case. Figure 6-B displays the impact on EC_{50} ratios compared to control (for n = 100). The effect of clustering decreases whenever receptors are farther away inside a cluster. Intuitively, this could have been expected since the total zone covered by the receptors is much wider and counteracts the clustering effect as receptor positions tend to become homogeneous.

Ligand diffusion

The simulations were so far performed with ligand diffusion coefficient D = 1. Results suggest that the mean time between receptor-ligand encounters is affected by clustering, as receptors positions are correlated, but diffusion itself also affects characteristic times. Simulations were run with diffusion coefficients between 0.01 and 10 (for all the following experiments we used $dt = 10^{-4}$),

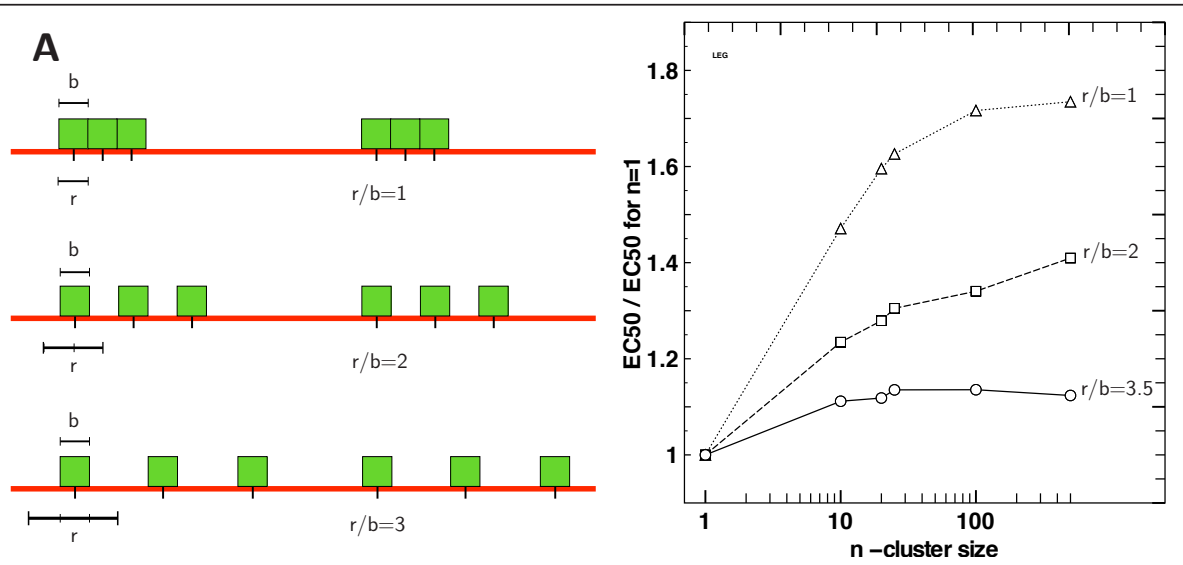

Figure 6 Receptor spacing, affinity zone size and clustering. A) Cartoon representing clusters of receptors with different receptor size width (r) on affinity zone width (b) ratio. A fixed affinity zone as it was used in simulation with a increasing receptor width leads to an increasing r/b ratio and therefore to sparser clusters of receptors. B) Ratio of fitted EC_{50} to control EC_{50} (i.e. for n = 1) with increasing cluster size, with contiguous receptors and with respect to receptor width on affinity zone width ratio. The scale is semi-logarithmic.

still comparing homogeneous receptor spacing and receptor clustering. After having checked that the equilibrium is reached, we could observe that the receptor occupation in function of the dose decreased, but still reached the same saturation value. We then compared apparent affinities in function of cluster size. Figure 7 shows the comparison of EC50 (obtained via fit) between the clustered and unclustered case. A decrease of D yields an amplification of the effect of clustering on response. On the other hand, increasing D leads to a much smaller impact on apparent affinities. Slow diffusing ligand molecules will take a longer time to go from a receptor to another than fast diffusing ligand molecules, meaning that two receptors will be "seen" farther from each other by slow diffusing ligand molecules. As expected changing D modifies the degree of spatial correlation between receptors, and therefore influences the effect of clustering, as it is only based on the geometry of the system. Spanning three degrees of magnitude of the diffusion does not change the results qualitatively.

Conclusions

The presented computational model transcribes the necessity of proximity for reactants to interact and combines it with the probabilistic nature of biochemical reactions at microscopic scale. The use of approximated Brownian motion in real coordinates and binding through affinity surfaces in a continuous medium allows the investigation of ligand-receptor reactions at microscopic scale and potentially reduces latent finite size effects of discrete lattices simulations. Modelling receptor as affinity zones with probabilistic binding allows to directly relate simulation parameters with ODE formalism.

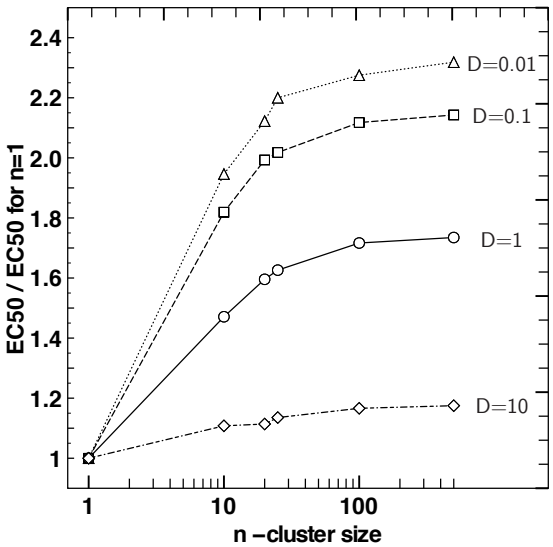

Figure 7 Clustering effect with different ligand diffusion coefficients. Ratio of fitted EC_{50} to control EC_{50} (i.e. for n = 1) with increasing cluster size, with contiguous receptors and with respect to the ligand coefficient diffusion used in simulation. The scale is semi-logarithmic.

Several configurations are explored by means of simulations. First, the model was validated for homogeneous receptor repartition by checking simulation concordance with the classic Michaelian equation. Two extreme cases of clustering were then tested, inducing spatial correlation either considering two possibilities. Within a cluster, receptors could be so close to each other that they interact with ligand particles contained exactly in the same area. Or alternatively, receptor affinity zones could simply be adjacent without overlapping. For receptors with stacked affinity zones, simulations still match the mathematical description.

For contiguous receptors, as no simple mathematical formulation is available, simulations are the only way to explore the potential effect of clustering. Some additional experiments are also performed to study more specifically some local aspects of ligand-receptor interaction, such as rebinding or the effect of partial receptor overlap.

Results suggest some insights about the receptor colocalization effects on ligand-receptor binding, observed on membrane receptors occupation. The ligand-receptor encounter probability is lower when receptors are clustered, because an inhomogeneous membrane covering leads to depleted zones and highly concentrated zones which both contain the same concentration of ligand. Thus, ligand molecules roaming in such depleted zones do not encounter receptors and actual reacting quantities are decreased compared to what is assumed to interact in homogeneous configuration. But, receptor clustering also increases the rebinding probability, in accordance with previous works [32]. These two opposite effects yield a dynamic chemical equilibrium for receptor occupation which differs from the one predicted by reaction rate equation under homogeneous dilution assumption. Simulations suggests that the enhanced rebinding cannot overcome the decreasing effect of spatial segregation and leads to a decreased apparent affinity of the global set of receptors. Nevertheless, the decreasing effect of spatial segregation may be progressively compensated as ligand concentration reaches high levels, since in a ligand-saturated medium, ligand-receptor encounter probability converges to one. Finally, both effects combine in a non-trivial and dose-dependent manner, and give an altered response, which cannot be characterized by the theoretical dissociation constant, and whose shape cannot be described by a classical Michaelian ODE.

Lipid rafts and other membrane structuring components could then serve as signalling modulators by

adapting cell sensitivity through receptor clustering. A single kind of receptor could be declined in various apparent affinities by dynamic clustering, and thus be sufficient to give the cell some flexibility in terms of signal response, whereas producing several different types of receptor with different affinities would consume a lot more resources.

Individual-based simulations provide insights into how spatial configuration of complex systems impact the processes they generate. They produce valuable results at both spatio-temporal microscopic scale - e.g. first-time encounter probability, ligand-receptor residence time, average distance travelled between rebinding events distributions - and macroscopic scale, such as receptor occupation at equilibrium, or pharmacodynamic dose-response. Individual-based models also allow for more complete implementations of the biological reality of the studied phenomena. For example, receptor diffusion could be allowed, or receptors could be set in clusters whose size is drawn from pertinent distribution laws, such as normal, exponential or power laws. Simulations would then provide valuable results on the robustness of observed effects of clustering towards realistic and noisy spatial configurations.

Results suggest that receptor clustering has an impact on signalling by itself, without incorporating any specific receptor-receptor interactions in the model. However, it should be interesting to explore specific biological interactions with the model, such as receptor transphosphorylation, hetero/homodimeric receptors or allosteric competition between binding sites, which could be easily implemented and experimented. Simulations could be used to study more complex signalling systems such as G-Protein-based pathways and would inspire useful intuitions for biological experiments, as they provide insights on the functional impact of spatial configurations on the mechanics of signalling.

Acknowledgements
BC holds a fellowship from la Région Rhône-Alpes. We gratefully acknowledge support from the CNRS/IN2P3 Computing Center (Lyon/Villeurbanne - France), for providing a significant amount of the computing ressources needed for this work. We thank Andrew Fowler for his critical reading of the manuscript.

Author details
[1]Université de Lyon, Laboratoire d'InfoRmatique en Image et Systèmes d'information, CNRS UMR5205, F-69621, France. [2]Université de Lyon, Cardiovasculaire Métabolisme et Nutrition, Inserm UMR1060, F-69621 Villeurbanne Cédex, France. [3]EPI BEAGLE, INRIA Rhône-Alpes, 69603 Villeurbanne, France.

Authors' contributions
BC helped to design the study, performed the simulations, analyzed the simulation data and drafted the manuscript. HS conceived the study, analyzed the data and drafted the manuscript. All author read and approved the final manuscript.

Received: 21 May 2010 Accepted: 31 March 2011
Published: 31 March 2011

References

1. Heffetz D, Yehiel Z: **Receptor Aggregation Is Necessary for Activation of the Soluble Insulin Receptor Kinase.** *J Biol Chem* 1986, **261**:889-894.
2. Flörke RR, Schnaith K, Passlack W, Wichert M, Kuehn L, Fabry M, Federwisch M, Reinauer H: **Hormone-triggered conformation changes within the insulin-receptor ectodomain: requirement for transmembrane anchors.** *Biochem J* 2001, **360**:189-198.
3. Changeux JP, Edelstein SJ: **Allosteric Receptors after 30 Years.** *Neuron* 1998, **21**:959-980.
4. Greenfield D, McEvoy AL, Shroff H, Crooks GE, Wingreen NS, Betzig E, Liphardt J: **Self-Organization of the Escherichia coli Chemotaxis Network Imaged with Super-Resolution Light Microscopy.** *PLoS Biology* 2009, **7**:6.
5. Murray JD: *Mathematical Biology: I. An Introduction* Springer; 2002.
6. Gillespie DT: **Stochastic simulation of chemical kinetics.** *Annual review of physical chemistry* 2007, **58**:35-55.
7. Berry H: **Monte Carlo Simulations of Enzyme Reactions in Two Dimensions: Fractal Kinetics and Spatial.** *Biophys J* 2002, **83**:1891-1901.
8. Kholodenko BN, Hoek JB, Westerhoff HV: **Why cytoplasmic signalling proteins should be recruited to cell membranes.** *trends in Cell Biology* 2000, **10**:173-178.
9. Berg HC, Purcell EM: **Physics of Chemoreception.** *Biophys J* 1977, **20**:193-219.
10. Goldstein B, Dembo M: **Approximating the Effects of Diffusion on Reversible Reactions at the Cell Surface: Ligand-Receptor Kinetics.** *Biophys J* 1995, **68**:1222-1230.
11. Erickson J, Goldstein B, Holowka D, Baird B: **The effect of receptor density on the forward rate constant for binding of ligands to cell surface receptors.** *Biophysical Journal* 1987, **52.**
12. Zwanzig R, Szabo A: **Time dependent rate of diffusion-influenced ligand binding to receptors on cell surfaces.** *Biophys J* 1991, **60**:671-678.
13. Endres RG, Wingreen NS: **Accuracy of direct gradient sensing by single cells.** *Proc Natl Acad Sci USA* 2008, **105(41)**:15749-15754.
14. Endres R, Wingreen N: **Accuracy of direct gradient sensing by cell-surface receptors.** *Prog Biophys Mol Biol* 2009.
15. Singer SJ, Nicolson GL: **The Fluid Mosaic Model of the Structure of Cell Membranes.** *Science* 1972, **175**:720-731.
16. Saffman PG, Delbrück M: **Brownian motion in biological membranes.** *Proc Natl Acad Sci USA* 1975, **72(8)**:3111-3.
17. Chung I, Akita R, Vandlen R, Toomre D, Schlessinger J, Mellman I: **Spatial control of EGF receptor activation by reversible dimerization on living cells.** *Nature* 2010, **464**:783-787.
18. Simons K, Ikonen E: **Functional rafts in cell membranes.** *Nature* 1997, **387**:569-572.
19. Simons K, Toomre D: **Lipid Rafts and Signal Transduction.** *Nature Reviews* 2000, **1**:31-41.
20. Simons K, Vaz WLC: **Model systems, lipid rafts, and cell membranes.** *Annu Rev Biophys Biomol Struct* 2004, **33**:269-95.
21. Brown DA, London E: **Functions of Lipid Rafts in Biological Membranes.** *Annual Reviews of Cell and Developmental Biology* 1998, **14**:111-36.
22. Gustavsson J, Santiago P, Karlsson M, Ramsing C, Thorn H, Borg M, Lindroth M, Peterson KH, Magnusson KE, Stralfors P: **Localization of the insulin receptor in caveolae of adipocyte plasma membrane.** *FASEB Journal* 1999, **13**:1961-1971.
23. Parpal S, Karlsson M, Thorn H, Strålfors P: **Cholesterol Depletion Disrupts Caveolae and Insulin Receptor Signaling for Metabolic Control via Insulin Receptor Substrate-1, but Not for Mitogen-activated Protein Kinase Control.** *J Biol Chem* 2001, **276.**
24. Lee S, Mandic J, Vliet KJV: **Chemomechanical mapping of ligand-receptor binding kinetics on cells.** *Proc Natl Acad Sci USA* 2007, **104(23)**:9609-14.
25. Vitte J, Benoliel AM, Eymeric P, Bongrand P, Pierres A: **Beta-1 integrin-mediated adhesion may be initiated by multiple incomplete bonds, thus accounting for the functional importance of receptor clustering.** *Biophys J* 2004, **86(6)**:4059-74.
26. Bray D, Levin MD, Morton-Firth CJ: **Receptor clustering as a cellular mechanism to control sensitivity.** *Nature* 1998, **393**:85-88.
27. Mello BA, Shaw L, Tu Y: **Effects of Receptor Interaction in Bacterial Chemotaxis.** *Biophys J* 2004, **87**:1578-1595.

28. Mahama PA, Linderman JJ: **A Monte Carlo Study of the Dynamics of G-Protein Activation.** *Biophys J* 1994, **67**:1345-1357.
29. Wanant S, Quon MJ: **Insulin Receptor Binding Kinetics: Modeling and Simulation Studies.** *Journal of theoretical Biology* 2000, **205**:355-364.
30. Shea LD, Linderman JJ: **Calculation of Diffusion-Limited Kinetics for the Reactions in Collision Coupling and Receptor Cross-Linking.** *Biophys J* 1997, **73**:2949-2959.
31. Shea LD, Linderman JJ: **Compartmentalization of Receptors and Enzymes Affects Activation for a Collision Coupling Mechanism.** *Journal of theoretical Biology* 1998, **191**:249-258.
32. Gopalakrishnan M, Forsten-Williams K, Nugent MA, Täuber UC: **Effects of receptor clustering on ligand dissociation kinetics: theory and simulations.** *Biophys J* 2005, **89(6)**:3686-700.
33. Ghosh S, Gopalakrishnan M, Forsten-Williams K: **Self-consistent theory of reversible ligand binding to a spherical cell.** *Phys Biol* 2007, **4**:344-354.
34. Fallahi-Sichani M, Linderman JJ: **Lipid Raft-mediated Regulation of G-Protein Coupled Receptor Signaling by Ligands which Influence Receptor Dimerization: A Computational Study.** *PLoS ONE* 2009, **4**:8.
35. Goldstein B, Wiegel FW: **The effect of receptor clustering on diffusion-limited forward rate constants.** *Biophys J* 1983, **43**:121-5.
36. Juska A: **Minimal models of multi-site ligand-binding kinetics.** *J Theor Biol* 2008, **255(4)**:396-403.
37. Weiss JN: **The Hill equation revisited: uses and misuses.** *FASEB* 1997, **11**:835-841.
38. Tanford C, Reynolds JA, Johnson EA: **Thermodynamic and kinetic cooperativity in ligand binding to multiple sites on a protein: Ca2+ activation of an ATP-driven Ca pump.** *Proc Natl Acad Sci USA* 1985, **82**:4688-4692.
39. Linderman JJ, Lauffenburger DA: *Receptors: models for binding, trafficking, and signaling* Oxford University Press; 1993.
40. Coombs D, Straube R, Ward MJ: **Diffusion on a Sphere with Localized Traps: Mean First Passage Time, Eigenvalue Asymptotics, and Fekete Points.** *SIAM Journal on Applied Mathematics* 2009, **70**:302-332.

doi:10.1186/1752-0509-5-48
Cite this article as: Caré and Soula: **Impact of receptor clustering on ligand binding.** *BMC Systems Biology* 2011 **5**:48.

Submit your next manuscript to BioMed Central and take full advantage of:

- **Convenient online submission**
- **Thorough peer review**
- **No space constraints or color figure charges**
- **Immediate publication on acceptance**
- **Inclusion in PubMed, CAS, Scopus and Google Scholar**
- **Research which is freely available for redistribution**

Submit your manuscript at
www.biomedcentral.com/submit

BioMed Central

II.3 Discussion

Receptor clustering was implemented two different classes of layouts, by grouping contiguous adjacent affinity zones or by stacking affinity zones in over stacked clusters, and dose-response curves in these situations were compared to curves from a homogeneous receptor distribution. Clustering induced a dramatic decrease in the apparent affinity of the receptors to their ligand : less receptors are occupied, and thus more ligand molecules are required to generate the same response. Increasing the degree of spatial correlation (by distributing the same number of receptors in fewer clusters) increases this effect. Faster ligand diffusion regimes mitigate this effect, whereas slower diffusion regimes accentuate it. Changing the diffusion regime amounts to expand or contract distances, thus likely modifying the degree of spatial correlation "perceived" by the ligand molecules.

In the case of over stacked receptors, the effect on the response is mainly explained by the reduction of the global effective target area. This somewhat artificial layout has no real biological counterpart, and principally acts as a limit case of clustering. In the computational model, when a ligand molecule is located in the affinity zone of several over stacked receptors, only a single binding event is allowed, the probabilistic draw is not multiplied. This matches the single transition rates of the ODE model of the over stacked case, but it is less realistic than more detailed derivations using binding combinatorics for multi-site ligands [Juska 2008]. However, clustering affects the response even in the contiguous receptors case when the target area is preserved and when each receptor binding is treated individually and independently. The simulated medium is in two dimensions, over a 1-dimension membrane. The dimensionality conditions the recurrence of a Brownian motion as well as the mean-first passage time to given targets [Montroll 1956, Holcman 2008]. Notably, in dimension 2, the Brownian motion is recurrent whereas in dimension 3 it is transient. Our results may not be therefore directly transposable to a 3-dimension medium over a 2-dimension membrane, even if a small return to origin or a greater mean-first passage time would be expected to increase the effect of clustering.

The effect of clustering appears as the combination of two counterbalancing phenomena that decrease the overall apparent association rate. Rebinding is favored by clustering, but initial binding is impaired. Since rebinding is conditionned by the ligand molecule finding a receptor to begin with, the decreasing effect of clustering on initial binding overcomes the enhancing effect of rebinding. It is possible to use the computational framework to measure in

simulation the distributions of individual binding events. The next chapter explores the effect of clustering from an event-driven approach in order to complete the global preliminary study presented so far.

Chapter III

Ligand-receptor binding events spatio-temporal analysis

Contents

Highlights

► Simulation of activation by ligand molecules of receptors in fixed heterogenous distributions (clusters) as in chapter 2. ► Binding events were tracked individually and sorted out in rebinding events or initial binding events. ► The distributions of time between consecutive binding events are modified by clustering which favors short rebinding times.

III.1 Introduction

The study presented in this chapter is based on the same ligand-receptor binding model than in chapter II, but instead of observing the effect of clustering on doses-responses curves, we investigate how clustering modifies the spatio-temporal distributions of binding events.

III.1.1 Outline

The results presented in the previous chapter suggest that two counterbalancing effects arises from heterogeneous receptor distributions. Clustering seemed

to enhance receptor occupation by rebinding, but also to decrease initial (or first) binding. The computational framework can be exploited to measure in simulation the distribution of binding events in time and space, at the scale of molecules that can be tracked and identified individually. The current chapter presents an analysis of the effect of clustering on such individual events, using the same model as in the previous chapter II. This completes the investigation of the effect of clustering, which was previously approached from the perspective of cell response at equilibrium, and now explored in terms of spatio-temporal dynamics. Using the computational framework, the ligand-receptor interaction can be reproduced as it would happen in an idealized yet accurate experimental environment. The simulation provides a controlled environment in which the microscopic behavior of individual components of the system can be examined.

The focus was set on the spatio-temporal redistributions of binding events induced by clustering. The study was restricted to a system of receptor submitted to a single constant dose of ligand. The receptors were distributed in contiguous clusters of different sizes. The applied ligand stimulation was set at a level where the divergence between simulated doses-responses curves and their theoretical counterparts appeared maximal, near the dissociation constant.

The behavior of this experimental set up was investigated through different aspects. We examined the transient phase, the temporary stage before receptor occupation reaches equilibrium. Then we tracked the binding events occuring for each individual ligand molecules. This gave access to the empirical distributions of waiting times between binding events, which was used to propose an quantitative insight on how clustering redistributes the contribution of rebinding and initial binding. As these results showed that the spatial correlation in receptor seemed to induce a temporal correlation in receptor activation, this aspect was investigated using the autocorrelation of the receptor activation signal for different degrees of clustering.

Thus, the publication 2 presented further approaches the effect of clustering by exploiting the possibilities offered by computational models in terms of capturing the microscopic, individual properties of a system in order to understand its observed macroscopic emergent properties.

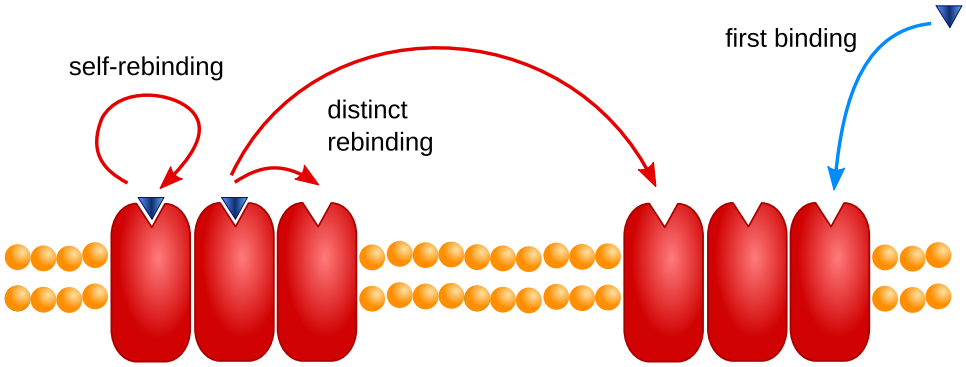

Figure III.1 – Each individual binding event can be sorted in different classes, by keeping track of the binding history of individual ligand molecules. Rebinding events (red arrows) can be sorted in self-rebinding – consecutive rebinding to the same receptor, and distinct rebinding – consecutive binding to another receptor. First binding events (blue arrow) are also tracked. The homogeneous case is treated the same way, as a special case of clustering with size n=1.

III.1.2 Binding events classification

The binding events were sorted in different types illustrated on figure III.1. Each binding event generated an output entry indicating the time at which it occured, the time since the previous binding event, the index of the involved ligand molecule, the index of the receptor. This yielded the complete binding history of individual ligand molecules and receptors.

Such data were pooled from identical simulation set ups, and used for a first binary classification of such events in rebinding and first (initial) binding. The contribution of each was normalized to the global number of binding events, since in our previous work we showed that clustering decreases the receptor occupation.

The analysis was pushed further by sorting rebinding events in self-rebinding (a ligand molecule binds twice to the same receptor) and distinct rebinding (a ligand molecule binds twice to two different receptors). In distinc rebinding, no difference is made between two receptors of different clusters, or two receptors of the same cluster. The homogeneous case is treated as a special case of clustering defined by a cluster size $n = 1$. The effect of clustering was explored in terms of number of events of each type, additionnally, the time spent between consecutive binding events was also exploited.

In parallel to the initial binding versus rebinding classification, the binding history data were also decomposed in terms of unique binding : the ratio

of the total number of binding events to the number of different individual ligand molecules that generated receptor occupation.

Publication 2

The Effect of Membrane Receptor Clustering on Spatio-temporal Cell Signalling Dynamics

Bertrand R. Caré and Hédi A. Soula

Proceedings of the 9th International Conference on Information Processing in Cells and Tissues 2012, *LNCS* **7723**:50-61

The Effect of Membrane Receptor Clustering on Spatio-temporal Cell Signalling Dynamics

Bertrand R. Caré[1,3] and Hédi A. Soula[2,3]

[1] Université de Lyon,
Laboratoire d'InfoRmatique en Image et Systèmes d'information, CNRS UMR5205,
F-69621 VILLEURBANNE
bertrand.care@insa-lyon.fr
[2] Université de Lyon,
Cardiovasculaire, Métabolisme, Diabétologie et Nutrition, Inserm UMR1060,
F-69621 VILLEURBANNE
hedi.soula@insa-lyon.fr
[3] EPI BEAGLE INRIA

Abstract. Membrane receptors allow the cell to respond to changes in the composition of its external medium. The ligand-receptor interaction is the core of the signalling process and may be greatly influenced by the spatial configuration of receptors. As growing pieces of evidence suggest that receptors are not homogeneously spread on the cell surface, but tend to form clusters, we propose to investigate the implication of receptor clustering on ligand binding kinetics using a computational individual-based model. The model simulates the activation of receptors distributed in clusters or uniformly spread. The tracking of binding events allows the analysis of the effect of receptor clustering through the autocorrelation of the receptor activation signal and the empirical time distributions of binding events, which are still unreachable with in vitro or in vivo experiments. Results show that the apparent affinity of clustered receptors is decreased. Additionally, receptor occupation becomes spatially and temporally correlated, as clustering creates platforms of coherently activated receptors. Changes in the spatial characteristics of a signalling system at the microscopic scale globally affect its function in time and space.

Keywords: cell signalling, receptor, ligand, clustering, pathway, binding, kinetics, equilibrium, autocorrelation, individual-based model, computational biology.

1 Introduction

In cell signalling, most models describe the ligand as an external stimulus and the receptor as the binding target, based on the ground of chemical enzyme/substrate formalism [1, 2]. Such formulations are based on the law of mass-action, which evaluates local reaction rates from averaged chemical species densities over the medium volume. The law of mass-action is a mean-field approximation since it

M.A. Lones et al. (Eds.): IPCAT 2012, LNCS 7223, pp. 50–61, 2012.
© Springer-Verlag Berlin Heidelberg 2012

estimates local reaction rates on the basis of average values of the reactants densities over a large spatial domain. In addition, it amounts to assume that ligand-receptor interactions are independent with respect to time and space [3, 4].

In biology, these assumptions can be questioned, in particular when considering membrane receptors which are restricted to only 2 of the 3 spatial dimensions [5, 6]. On the specific case of membrane-restricted receptors (on spherical cells), the expression for reaction rate coefficients is a non-linear function of cell surface receptor density [7]. This pioneer study has been enriched by further works towards reversibility and rebinding, [8], receptor density [9], time dependency [10], and gradient sensing capabilities [11, 12].

Furthermore, the spatial organization of receptors *on the membrane itself* should also be taken into account. At first glance, since membrane receptors are bound to the cell membrane that allows for lateral degrees of freedom, one would expect a simple (and homogeneous) distribution of receptors on the membrane. Indeed, cell membrane is composed of a mixture of phospholipids in a fluid phase and as such, in the classical fluid-mosaic model of membrane [13], membranes components undergo isotropic random movement akin to Brownian motion [14, 15]. In this model, the resulting equilibrium distribution of components – and receptors among them – is therefore homogeneous. Recently, however, this picture has evolved considerably towards a non-homogeneous distribution of the usual components of cell membranes [16, 17, 18, 19, 20]. More and more evidence points towards the existence of micro-domains enriched in various lipids, such as cholesterol, as well as other proteins, such as receptors. In particular, receptor colocalization in lipid rafts and other membrane structures have been reported [21, 22, 23]. This specific localization and clustering may have a dramatic influence on signalling. This influence however remains unclear as literature reports contradictory effects of clustering/declustering on signalling (see e.g. [24, 25, 22]). The method used to disrupt the clusters of receptors may have significant side-effects on the cell signalling system.

On the modelling side, the impact of an inhomogeneous receptor density *on* the membrane itself has been studied only recently. Only few theoretical contributions have been reported in some specific cases : bacteria sensitivity[26] and chemotaxis [27], G-protein activation [28], simple model of trans-phosphorylation (implying two receptors only) [29]. In addition, several more detailed studies illustrate the possible effect of receptor clustering on receptor binding by inducing enhanced rebinding and ligand receptor switching [30, 31, 32, 33], or enhancing encounter probability of activated receptors with submembranar signalling proteins such as in GPCR signalling pathways [34]. Notably [32] proposes that clustering provides higher rebinding capabilities and therefore helps to obtain a better response – i.e. more binding events. However, another analysis [8] proposes that the forward rate constant is diminished when receptors are clustered, providing in that case less binding events. Both effects counteract themselves, and the final output remains to be studied.

In a previous paper, we investigated how receptor distribution may impact the primordial step of signalling that is ligand binding to receptor extracellular

domain [35]. We showed that in the case of a diffusion-limited reaction, receptor clustering impairs the sensitivity of the signalling system. While conserving the microscopic binding properties, the apparent affinity of a receptor for its ligand diminishes with clustering. We showed that this effect is based on spatial features and is diffusion-dependent. In the limit of high diffusion this impairment vanishes, whereas low diffusion amplifies it.

We present in this article a detailed study on how this effect takes place in terms of binding. Intuitively two effects are in action. Clustered receptors are "harder to find", as it diminishes their probability to be found by ligand molecules. In the other hand, when receptors are clustered, they are more likely to be found by a ligand that has been released by another nearby receptor. In other words, more rebinding events are expected in the clustered case. Obviously these two effects counter themselves and the outcome is not intuitively clear. Additionnaly, we show in this article several properties of the binding kinetics of receptors depending on their spatial configuration. Especially, we investigated not only how clustering affects the global amount of activation resulting from ligand stimulation, but also how the temporal dynamics of receptor activation changes with clustering, which translates a spatial correlation into a temporal one.

2 Models

As already mentioned, mathematical models of binding kinetics generally rely on the law of mass action. In the case of a correlated receptor spatial configuration, this hypothesis breaks down. In order to investigate this issue, we developped a simulation engine where the spatial characteristics of real signalling systems arises naturally by using an individual-based model. This simulation engine is defined and described in detail in another article [35] that we briefly describe here as well. The engine computes the equation of movement of punctual particles in a 2-dimension space with cylindric boundary conditions on the x-axis, and closed boundary on the y-axis, the membrane being at $y = 0$. This space is used to describe the extracellular medium. The membrane is the bottom line of the 2-dimension space. Receptors are positioned on the membrane and do not move during simulation, assuming that receptor diffusion is negligible compared to ligand diffusion. Ligand molecules are punctual particles which undergo a classical 2-dimension Brownian motion in the extracellular space. As mentioned above, motion is forbidden beneath the membrane or through the upper part of the simulation space. However, particles going through one lateral boundary appear across the other. Ligand molecules undergo Brownian motion in the overdamped regime via an explicit Euler scheme of step dt :

$$x(t + dt) = x(t) + \sqrt{Ddt}Z_1$$
$$y(t + dt) = y(t) + \sqrt{Ddt}Z_2$$

with D being the simulated ligand diffusion coefficient, and $Z_{1,2}$ are random values drawn from a normalized Gaussian variate. Binding can occur whenever

a ligand molecule is in the 'affinity zone' of a unoccupied receptor – a fixed square above the position of the receptor. If the receptor is free – not already bound to a ligand – binding can occur with a given probability p_1. Finally, an already bound ligand molecule can be released at the border of the affinity zone with a probability p_1 at each time step.

We studied two kinds of receptor spatial configurations in these simulations. The first is a reference – control – receptor distribution, in which they are uniformly spread on the 1-dimension membrane – referred hereafter as to the homogeneous distribution, or unclustered receptors case. The clustered case is obtained by positioning receptors next to each other – with adjacent but non-overlapping affinity zones – by groups of n. These clusters are then uniformly spaced. Most simulations will then compare several cluster sizes (various n) to the control. Note that the control case describes this reaction :

$$L + R \underset{k_{-1}}{\overset{k_1}{\rightleftharpoons}} C \tag{1}$$

and [35] showed that we can relate reaction rates to the binding/unbinding probabilities via :

$$k_{-1} = p_{-1}$$
$$k_1 = \frac{p_1 S_r}{S_t}$$

with S_r being the area of the affinity zone and S_t the total area of the extracellular medium.

3 Results

Unless stated otherwise, the number of receptors for each simulation run was $N_r = 500$, the number of ligand molecules $N_l = 4.10^5$, $k_1 = k_{-1} = 10.0$, $dt = 10^{-3}$ giving $p_1 = p_{-1} = 10^{-2}$. The surface of each affinity zone was $S_r = 0.4$ and the total medium surface $S_t = 2.10^5$. The ligand diffusion coefficient was $D = 1.0$. The cluster size is noted n, $n = 1$ referring to the case of homogeneously spread receptors.

3.1 Transient Phase

Our previous results only dealt with receptor occupation at equilibrium, i.e. the average number of ligand-receptor complexes after the simulation reached a stationay state. The transient solution should yield the same result : clustering decreases the overall responses. As shown in Fig. 1 the fraction of occupied receptors through time was also cluster-dependent. The figures show a similar initial activation rise. Indeed, initially, ligand molecules were positioned uniformly, and since the global surface covered by receptor affinity zones was unchanged by clustering, the initial probability for a ligand to be in an unoccupied receptor

was equal no matter the cluster size. Quickly afterwards though, binding events began to decline steadily whenever receptor were clustered. This shows that the actual binding history for ligand molecules in the vicinity of receptor must be taken into account in order to understand this shift in complexation.

3.2 Binding Events Analysis

The occurence of specific events was tracked during simulation runs. The simulation yielded simultaneously the number of binding events and the number of ligand-receptor encounter events that took place at each time step. Binding events fell into two categories: the first binding events and the rebinding events. The former refers to ligand molecules binding to a receptor for the first time, from the ligand point of view. The latter refers to ligand molecules binding to a receptor for at least the second time, from the ligand point of view.

The relative contribution of binding events of each kind versus cluster size is reported on Fig. 2. In order to avoid any bias due to the decreasing in receptor occupation with clustering, the number of events were normalized on the total number of binding events recorded. As clustering increases, the contribution of first binding events dropped dramatically, while the amount of receptor activation due to rebinding increased. First binding events occured less often if receptors were clustered, but clustering was favorable to rebinding. This suggests that most of the receptor activation was performed by a small contingent of ligand that kept on rebinding.

By computing the ratio of the number of rebinding events to the number of first binding events versus cluster size (see Fig. 3), we obtained the average number of times a ligand molecule rebound to a receptor. As expected this ratio increased with cluster size. By having access to the index of each ligand molecule that generated a binding event, we also obtained the number of unique ligand molecules that had contributed to the total number of binding events. This gives an estimate of the average number of binding events generated by a single ligand molecule according to the cluster size – Fig. 3. Both curves have a similar trend : in the clustered case, receptor activation was induced through constant rebinding by the same set of ligands. Indeed, a high number of unique rebinding indicates a small contingent of ligand molecules involved in the signal. This put a strong emphasis on dependence on the binding history of ligands. On the other hand, in the unclustered case, most binding was performed by 'fresh' ligands newly coming from the medium, whereas rebinding was marginal.

3.3 Ligand Temporal Dynamics

The simulation also provided the time a ligand molecule had to wait between two consecutive binding events. Here, "consecutive" is defined in the ligand molecule referential. Consecutive binding events, that is, rebinding events, were sorted out in two classes : rebinding by a ligand molecule to the same receptor (self-rebinding) and rebinding by a ligand molecule to a different receptor (distinct rebinding). It was thus possible to investigate the qualitative effects of receptor

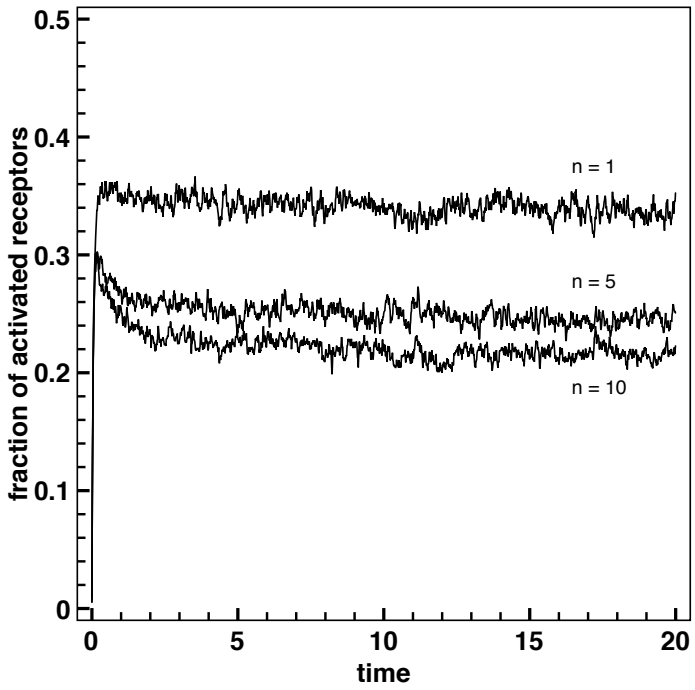

Fig. 1. Fraction of activated receptors versus time for various cluster sizes. The graph shows the signals of receptor activation for a single simulation run with the same parameters except the receptor clusters size. Clustering decreased the receptor activation at equilibrium.

clustering on the temporal dynamics of binding. Fig. 4 shows the mean time between rebinding events sorted in the two types mentioned above, plus the mean time of all rebinding times indifferently, for different cluster sizes. As expected, the time to rebind to another receptor decreased with clustering - since there were other receptors available in the vicinity when they were clustered. In the unclustered case, rebinding to another receptor was a marginal event, as suggested by its longer mean time (one order of magnitude above the others) and its quasi-inexistent influence on the overall rebinding time. Additionally, we noted that the self rebinding time also decreased with clustering, making the self-rebinding more frequent in the clustered case. This could be explained by the fact that, in the unclustered case, a bound receptor could be readily reoccupied by a new ligand molecule. We also had access to inter and intra-cluster rebinding times. Inter-cluster rebinding refers to rebinding of a ligand molecule to a receptor belonging to another cluster, unlike intra-cluster rebinding where rebinding occur to a receptor of the same cluster. Simply put, in the clustered case, there were no rebinding events (during simulation time) between clusters. All rebinding occured within the same cluster. As for the unclustered case, each receptor is a single cluster and we already mentioned that inter-cluster rebinding was extremely marginal.

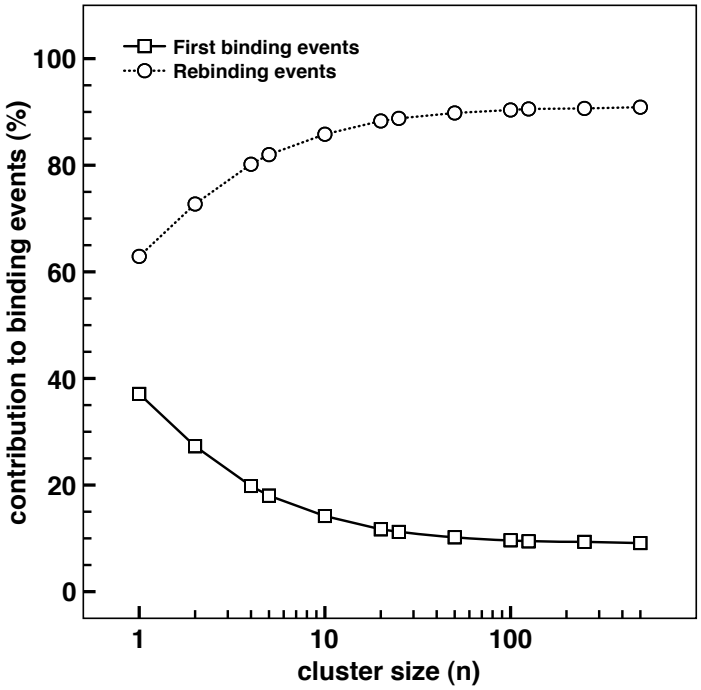

Fig. 2. Relative contribution of binding events from different types to the total binding. Binding events were splitted in two distinct types : the first binding type, i.e. when a ligand molecules bound to a receptor for the first time, and the rebinding type, i.e. when a ligand bound to a receptor and had already been bound in the past to any receptor.

3.4 Receptor Temporal Dynamics

From a receptor point of view, the change in the temporal dynamics of rebinding suggests that the spatial correlation of positions should induce a temporal correlation of activation. In order to investigate this coupling, the activation signal of each receptor was tracked for each time step in the form of a binary signal (0 : free, 1 : occupied by ligand). This signal was then averaged for 10 neighboring receptors. For all n, it simply means we sorted by groups of the 10 closest receptors. The autocorrelations of such signals were computed and are compared in Fig. 5 (dashed lines) with the autocorrelation of a spatially uncorrelated signal (solid line, $n = 1$). The autocorrelation is the correlation of the signal with itself shifted by a lag. Let $x(t)$ being a signal, we simply computed the following expression, the average being taken over the entire time course :

$$ac(lag) = \langle (x(t) - \bar{x})\,(x(t + lag) - \bar{x}) \rangle$$

The theoretical autocorrelation for binding events was expected to follow an exponential decay. Indeed, the curve for $n = 1$ presented a classical exponential decay. The correlation of the activation signal decreased with time. However, as clustering was introduced, the half-time of this decay increased. This means that the activation state of receptors correlated with their past state for a longer time

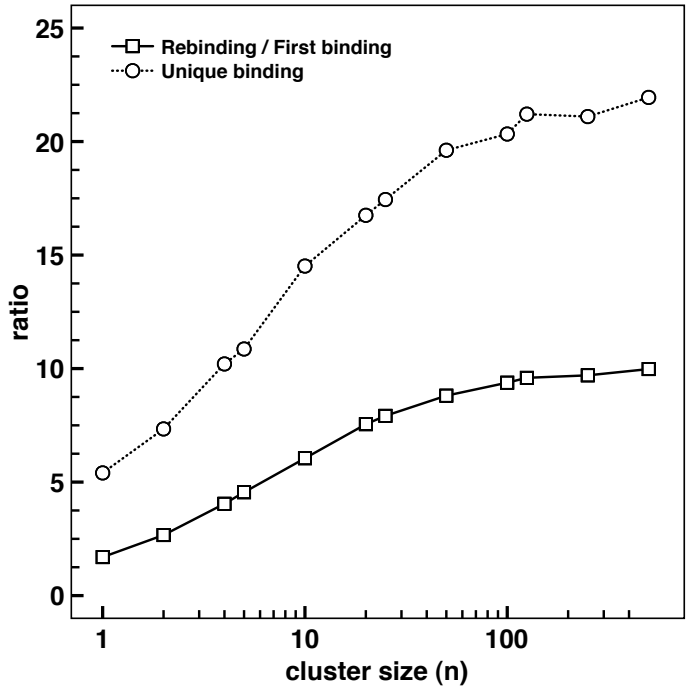

Fig. 3. Squares, solid line : ratio of rebinding events to first binding events (squares, solid line) versus cluster size. A ratio of 5 indicates that, in average, 5 out of 6 binding events occured through rebinding. Circles, dashed line : ratio of the number of individual ligands involved in binding events to the total number of binding events versus cluster size. In this case, a ratio of 5 means that, over the course of the simulation, a unique ligand molecule generated in average 5 binding events on its own (ignoring the ligand molecules that never bound to a receptor).

with clustering than in the unclustered case. The autocorrelation profiles suggest that the temporal correlation of the activation state of adjacent receptors was stronger with clustering.

Clustering introduced a spatial correlation on receptor activation, shown by an increase in rebinding events at the expense of first binding events. Globally, the fraction of activated receptors, at equal ligand stimulation, was decreased, as rebinding did not overcome the loss of encounter events between ligand molecules and receptor. The effect of clustering also appeard on the temporal dynamics of the receptor system, as the activation state of receptors correlated more with its past value. This illustrates how the spatial correlation of receptors translates into a temporal correlation of their binding with the ligand.

4 Discussion

A computational model was used to recreate ligand-receptor binding under specific spatial configurations similar to the ones observed experimentally. This kind of model allows for a detailed analysis of signalling systems, as each individual binding event can be tracked.

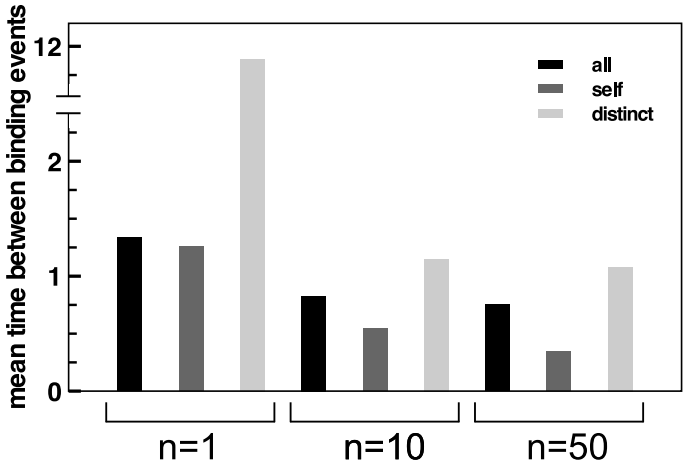

Fig. 4. The time spent by ligand molecules between two consecutive binding events was saved for each molecule during simulations. Theses durations were sorted out in two types : the times between rebinding to a distinct receptor (distinct rebinding) and the times between rebinding to the same receptor (self-rebinding). The mean time between consecutive binding events of such kinds (greyscales) are shown with respect to cluster size n, along with the mean time of consecutive binding when both types are pooled (black).

Receptor clustering seemingly induced a quantitative effect that decreased the global receptor activation by an external ligand. The behavior of the simulated signalling system could be examined in depth. When clustering was imposed to receptors, ligand binding occured more because of ligand molecules rebinding to receptors, at the expense of ligand molecules finding and binding for the first time to a receptor. Not only the crude number of such events was altered in favor of rebinding, the time spent between consecutive binding events also changed. The activation signal of receptors becomes space and time-dependent, showing how a different receptor spatial configuration introduced a shift in the temporal dynamics of the signal transmitted.

This suggests that the peculiar spatial distributions of receptors observed in nature might have a functional role in signalling. This role could possibly be not only quantitative, as the global receptor activation is reduced with clustering, but also qualitative. This study suggests that clustering introduces platforms of aggregated receptors whose activation becomes correlated in time and space, that is, the correlation of receptor position translates into a synchronization of receptor activation. This property is not available in the homogeneous receptor repartition scenario, where receptors are activated randomly in space and time. Making the activation of receptors time and space-dependent could be an advantage in terms of sensitivy, noise reduction and signal robustness. It could also improve signalling-associated cellular processes such as receptor trafficking, recycling, and interaction between parallel pathways. For instance, ligand-induced receptor internalization was observed in different pathways [36, 37], and could be partially relying on harmonization of receptor activation achieved by clustering : activated receptors can be internalized and recycled more efficiently if they

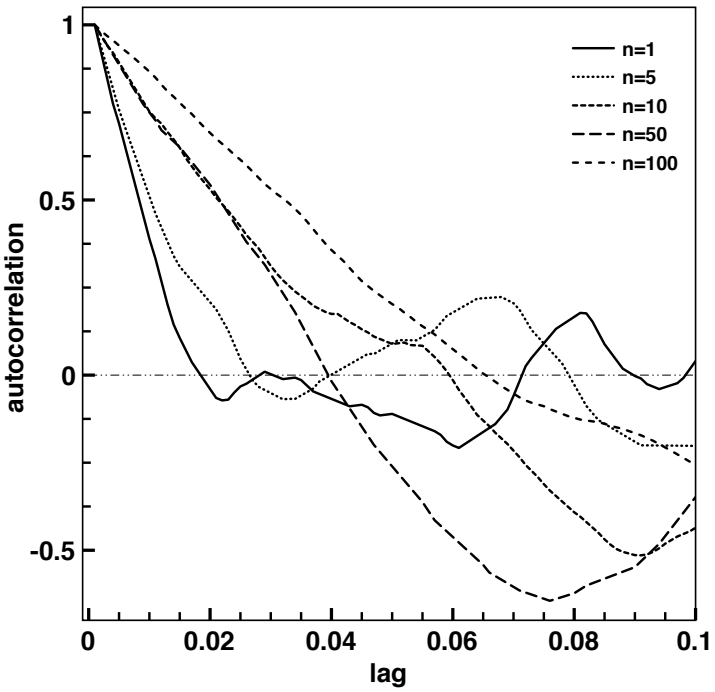

Fig. 5. Autocorrelation functions of the receptor activation signal for various cluster sizes. The binary occupation signal was computed for each receptor and each time step. The average signal of 10 neighboring receptors was used to perform an autocorrelation computation. Autocorrelation functions for clustered receptors show a longer exponential decay, suggesting that the spatial correlation between receptors translated into a temporal correlation.

are already grouped together, rather than spread ramdomly on the cell surface. The question remains to be investigated in studies integrating the spatial and temporal characteristics of such processes, using both modelling and biological experiments.

Acknowledgments. BC holds a fellowship from la Région Rhône-Alpes. We gratefully acknowledge support from the CNRS/IN2P3 Computing Center (Lyon / Villeurbanne, France), for providing a significant amount of the computing resources needed for this work.

References

[1] Heffetz, D., Zick, Y.: Receptor aggregation is necessary for activation of the soluble insulin receptor kinase. The Journal of Biological Chemistry 261(2), 889–894 (1986)

[2] Flrke, R.R., Schnaith, K., Passlack, W., Wichert, M., Kuehn, L., Fabry, M., Federwisch, M., Reinauer, H.: Hormone-triggered conformational changes within the insulin-receptor ectodomain: requirement for transmembrane anchors

[3] Murray, J.D.: Mathematical Biology: I. An Introduction. Springer, Heidelberg (2002)

[4] Gillespie, D.T.: Stochastic simulation of chemical kinetics. Annual Review of Physical Chemistry 58(1), 35–55 (2007)
[5] Berry, H.: Monte carlo simulations of enzyme reactions in two dimensions: fractal kinetics and spatial segregation. Biophysical Journal 83(4), 1891–1901 (2002)
[6] Kholodenko, B.N., Hoek, J.B., Westerhoff, H.V.: Why cytoplasmic signalling proteins should be recruited to cell membranes. Trends in Cell Biology 10(5), 173–178 (2000)
[7] Berg, H.C., Purcell, E.M.: Physics of chemoreception. Biophysical Journal 20(2), 193–219 (1977)
[8] Goldstein, B., Dembo, M.: Approximating the effects of diffusion on reversible reactions at the cell surface: ligand-receptor kinetics. Biophysical Journal 68(4), 1222–1230 (1995)
[9] Erickson, J., Goldstein, B., Holowka, D., Baird, B.: The effect of receptor density on the forward rate constant for binding of ligands to cell surface receptors. Biophysical Journal 52(4), 657–662 (1987)
[10] Zwanzig, R., Szabo, A.: Time dependent rate of diffusion-influenced ligand binding to receptors on cell surfaces. Biophysical Journal 60(3), 671–678 (1991)
[11] Endres, R.G., Wingreen, N.S.: Accuracy of direct gradient sensing by single cells. Proceedings of the National Academy of Sciences 105(41), 15749–15754 (2008)
[12] Endres, R.G., Wingreen, N.S.: Maximum likelihood and the single receptor. Physical Review Letters 103(15), 158101 (2009); PMID: 19905667
[13] Singer, S.J., Nicolson, G.L.: The fluid mosaic model of the structure of cell membranes. Science 175(23), 720–731 (1972)
[14] Koppel, D.E., Sheetz, M.P., Schindler, M.: Matrix control of protein diffusion in biological membranes. Proceedings of the National Academy of Sciences of the United States of America 78(6), 3576–3580 (1981)
[15] Chung, I., Akita, R., Vandlen, R., Toomre, D., Schlessinger, J., Mellman, I.: Spatial control of EGF receptor activation by reversible dimerization on living cells. Nature 464(7289), 783–787 (2010)
[16] Simons, K., Ikonen, E.: Functional rafts in cell membranes. Nature 387(6633), 569–572 (1997)
[17] Simons, K., Toomre, D.: Lipid rafts and signal transduction. Nature Reviews. Molecular Cell Biology 1(1), 31–39 (2000)
[18] Schuck, S., Simons, K.: Polarized sorting in epithelial cells: raft clustering and the biogenesis of the apical membrane. Journal of Cell Science 117(25), 5955–5964 (2004)
[19] Brown, D.A., London, E.: Functions of lipid rafts in biological membranes. Annual Review of Cell and Developmental Biology 14(1), 111–136 (1998)
[20] Zhang, J., Leiderman, K., Pfeiffer, J.R., Wilson, B.S., Oliver, J.M., Steinberg, S.L.: Characterizing the topography of membrane receptors and signaling molecules from spatial patterns obtained using nanometer-scale electron-dense probes and electron microscopy. Micron. 37(1), 14–34 (2006) (Oxford, England: 1993)
[21] Gustavsson, J., Parpal, S., Karlsson, M., Ramsing, C., Thorn, H., Borg, M., Lindroth, M., Peterson, K.H., Magnusson, K.-E., Strälfors, P.: Localization of the insulin receptor in caveolae of adipocyte plasma membrane. The FASEB Journal 13(14), 1961–1971 (1999)
[22] Parpal, S.: Cholesterol depletion disrupts caveolae and insulin receptor signaling for metabolic control via insulin receptor substrate-1, but not for mitogen-activated protein kinase control. Journal of Biological Chemistry 276(13), 9670–9678 (2000)

[23] Lee, S., Mandic, J., Van Vliet, K.J.: Chemomechanical mapping of ligandreceptor binding kinetics on cells. Proceedings of the National Academy of Sciences of the United States of America 104(23), 9609–9614 (2007)
[24] Lim, K., Yin, J.: Localization of receptors in lipid rafts can inhibit signal transduction. Biotechnology and Bioengineering 90(6), 694–702 (2005)
[25] Vitte, J., Benoliel, A.-M., Eymeric, P., Bongrand, P., Pierres, A.: Beta-1 integrin-mediated adhesion be initiated by multiple incomplete bonds, thus accounting for the functional importance of receptor clustering. Biophysical Journal 86(6), 4059–4074 (2004)
[26] Bray, D., Levin, M.D., Morton-Firth, C.J.: Receptor clustering as a cellular mechanism to control sensitivity. Nature 393, 85–88 (1998)
[27] Mello, B.A., Shaw, L., Tu, Y.: Effects of receptor interaction in bacterial chemotaxis. Biophysical Journal 87(3), 1578–1595 (2004)
[28] Mahama, P.A., Linderman, J.J.: A monte carlo study of the dynamics of g-protein activation. Biophysical Journal 67(3), 1345–1357 (1994)
[29] Wanant, S., Quon, M.J.: Insulin receptor binding kinetics: modeling and simulation studies. Journal of Theoretical Biology 205(3), 355–364 (2000)
[30] Shea, L.D., Omann, G.M., Linderman, J.J.: Calculation of diffusion-limited kinetics for the reactions in collision coupling and receptor cross-linking. Biophysical Journal 73(6), 2949–2959 (1997)
[31] Shea, L.D., Linderman, J.J.: Compartmentalization of receptors and enzymes affects activation for a collision coupling mechanism. Journal of Theoretical Biology 191(3), 249–258 (1998)
[32] Gopalakrishnan, M.: Effects of receptor clustering on ligand dissociation kinetics: Theory and simulations. Biophysical Journal 89(6), 3686–3700 (2005)
[33] Ghosh, S., Gopalakrishnan, M., Forsten-Williams, K.: Self-consistent theory of reversible ligand binding to a spherical cell. Physical Biology 4(4), 344–354 (2008)
[34] Fallahi-Sichani, M., Linderman, J.J.: Lipid Raft-Mediated regulation of G-Protein coupled receptor signaling by ligands which influence receptor dimerization: A computational study. PLoS ONE 4(8), e6604 (2009)
[35] Caré, B.R., Soula, H.A.: Impact of receptor clustering on ligand binding. BMC Systems Biology 5(1), 48 (2011)
[36] Carpentier, J.L., Paccaud, J.P., Gorden, P., Rutter, W.J., Orci, L.: Insulin-induced surface redistribution regulates internalization of the insulin receptor and requires its autophosphorylation. Proceedings of the National Academy of Sciences of the United States of America 89(1), 162–166 (1992)
[37] Giudice, J., Leskow, F.C., Arndt-Jovin, D.J., Jovin, T.M., Jares-Erijman, E.A.: Differential endocytosis and signaling dynamics of insulin receptor variants IR-A and IR-B. Journal of Cell Science 124(Pt 5), 801–811 (2011)

III.3 Discussion

The chapters II and this current one constitute a combined analysis of the effect of clustering on the first stage of a signalling pathway : the extracellular ligand-receptor interaction. Heterogeneous spatial distributions, reproduced as clusters of immobile receptors, induced a decrease of the apparent affinity of the receptors illustrated in the chapter II. This chapter confirmed the subsequent intuition that clustering induces a redistribution of binding events, and favors rebinding at the expense of initial binding. Less ligand molecules were involved in the generation of the response, which was increasingly due to a smaller set of molecules rebinding multiple times as the degree of spatial correlation increased. The modification of the relative contributions of these two types of events was not only observed in crude numbers. The spatial correlation of receptor positions induced a temporal correlation measured as a longer-lasting autocorrelation of neighbouring receptors.

The results presented in these two chapters remain to be better related to the quantitative spatial characteristics of the simulated heterogeneous spatial distributions. The redistribution of binding events could be more effectively related to geometrical parameters such as receptor density, inter-cluster and intra-cluster distances, in conjunction with diffusion and reaction rates. This task would be greatly improved by directly using the empirical distributions of binding, rebinding and search times rather than their averages. Notably, Mugler et al. provided a similar analysis and characterized the effect of clustering using scaled parameters putting in perspective all these aspects [Mugler 2012], which could be transposable to different pathways as better estimations of their spatial and kinetics parameters will be provided.

The question of the potential beneficial role of clustering remains elusive, as our work depicts heterogeneous receptor spatial distributions as severely impairing signal transduction – at least at the reception stage. A first aspect to consider is that, although doses-responses curves exhibit a decreased apparent affinity, clustering seems to linearize the shape of the curve. This suggests that heterogeneous spatial distributions could improve the dynamic range of the signalling pathway, as doses near the boundaries of the range are better discriminated. More generally, modifying the spatial distribution of the receptors could be an effective mechanism by which the sensitivity of a pathway could be adapted, or modified dynamically. However, this may not hold when considering that the input/output function characterizing the dose-response relationship is also determined by the downstream structure of the pathway.

The results of this chapter illustrate another potentially beneficial effect of clustering, that is the temporal correlation that arises from the spatial correlation. The surface of the cell would be composed of signalling platforms of receptors activated in a coordinated way, rather than covered by equally distant, randomly activated isolated receptors. This property could be crucial when additionnal cellular processes come into play, such as recycling, trafficking, and more generally processes assuring the maintenance of the cell's signalling apparatus. This possibility could be supported by the observation of ligand-incuded receptor recycling [Carpentier 1992,Kublaoui 1995], and the role of microdomains in endocytosis [Fagerholm 2009]. It becomes more efficient to treat clusters rather than isolated receptors, from this perspective.

The study presented so far only consider the initial reception stage. Our global study of signalling protein spatial heterogeneity continues at the next stop in the signalling pathway, the transduction stage between membrane receptors and membrane intracellular signalling proteins.

Chapter IV

Receptor clustering in the membrane transduction stage

Contents

Highlights

► Activation of intracellular membrane signalling proteins by receptors in fixed heterogenous distributions (clusters), both on a 2-d membrane. ► Clustering decreases the amplitude of the response, but increases the apparent affinity of the system. ► Waiting times between reactions are redistributed towards short time scales.

IV.1 Introduction

This chapter focuses on the next stage in our canonical signalling pathway, the transduction of a signal by receptors activating membrane-bound intracellular signalling proteins, which follows the ligand-receptor interaction examined previously.

IV.1.1 Outline

Receptors are the pivotal components of signalling pathways, set at the frontier between the extracellular medium and the cytoplasm. We explored the effects of heterogeneous spatial distributions of receptor on signal reception

on the extracellular side of the membrane, the present chapter now investigates the implications of these distributions on the transduction stage on the intracellular side of the membrane.

The dynamics of the transduction reaction between receptors and membrane-bound intracellular signalling proteins differs from the ligand-receptor binding reversible reaction. As seen in I.1.2, in the two principal families of signalling systems, RTK-based pathways and GPCR-based pathways, the signal is transduced by receptors that activate "relay" proteins. Such relay proteins continue to diffuse once activated, and activate downstream signalling proteins located elsewhere on the membrane or in the cytoplasm. An example of RTK-based signalling system using this mechanism is the Insulin Receptor-Insulin Receptor Substrate 1 (IRS1) transduction process, where IRS1 is attached on the membrane by a GPI-anchor [Stenkula 2007]. GPCR-based signal are transduced by G-Proteins, which are anchored to the membrane by adjunction of lipidic chains [Wedegaertner 1995]. In this chapter, we explored the effect of clustering on this transduction process that is functionally different from the reversible ligand-receptor binding mechanism. In particular, contrary to the ligand-receptor reaction, the response measured in terms of relay proteins activation is not limited by the number of receptors. Another notable difference susceptible to generate unexpected results is that the receptors and their signalling partners share the reaction environment, the membrane.

We restricted our study to immobile receptors and diffusing membrane-bound relay proteins. They are respectively referred to as R and G in their inactive forms in the publication 3 presented hereafter, and labelled C and H in their active forms. Here, G does not refer exclusively to G-proteins, but to any membrane-bound signalling protein activated according to the transduction process previously described. We adopted a similar approach to the one used in the previous chapters : we used the classical ODE formalism for transduction (as seen in I.2.1.1) as a reference to which the dynamics of the simulated transduction process are compared. We reproduced the transduction stage process in a individual-based computational model that allows for heterogeneous receptor distributions, measuring the activation of G at equilibrium and keeping track of the binding history data.

We excluded the ligand as an explicit component of our transduction process, and replaced it with constant rates of receptor activation/deactivation. This gives a set of reactions very similar to equations I.6 presentend in publication 3 section II.A page 2. This was done in order to restrict our study of the effect of clustering on the C-G interaction : if we were to model explicit ligand

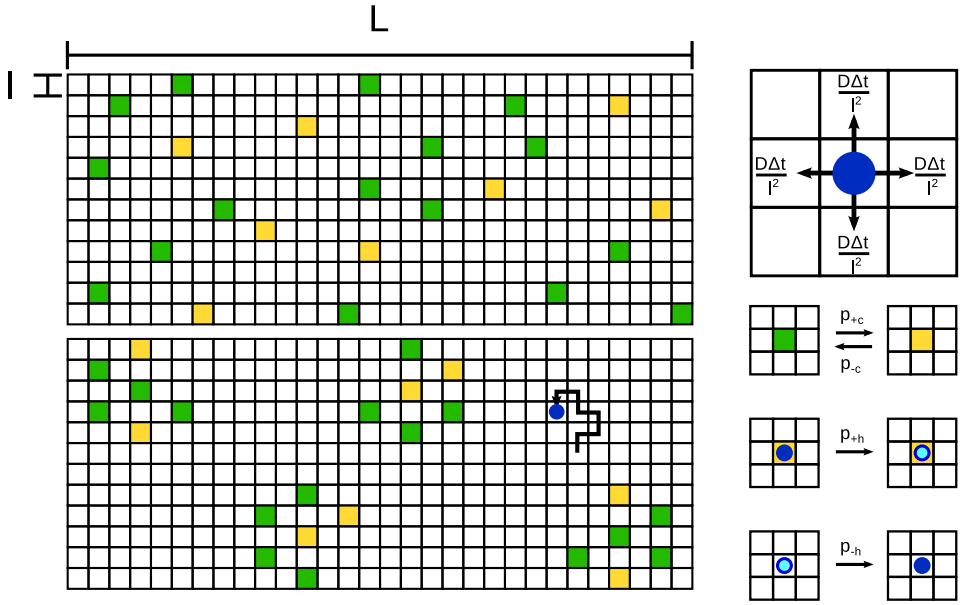

Figure IV.1 – Illustration of the lattice simulation framework. Green square and yellow squares are nodes occupied respectively by deactivated and activated receptors. A homogeneous distribution (up) and a distributio in clusters (down) are shown. The dark blue disc is a deactivated G molecule, the light blue disc is an activated G molecule. Diffusion is the same for activated and deactivated G molecules.

molecules, the effect of clustering on the reception stage could interfere with the effect on the transduction stage, by introducing the phenomena observed in the previous chapters. In this chapter, receptor activation is completely uncorrelated in time and space. Thus, only the spatial correlation of receptors position will explain the potential divergence observed between dynamics in the homogeneous case and the heterogeneous case.

The resulting equation for activation of G at equilibrium (in particular equation 6 in the publication 3) shows that the parameter κ determines the shape of the corresponding dose-response curve, but contrary to the reception stage, κ defines simultaneously the saturation plateau and the half maximal efficient dose. In the homogeneous case, this gives two equivalent methods to estimate the the apparent affinity from the simulated doses-responses curves. In publication 3 figure 1.B, we will see that clustering breaks this equivalence by influencing differently the half-maximal ligand stimulation ratio and the saturation plateau.

In addition to the study of clustering alone, we introduced a potentially compensatory mechanism in receptor activation (presented in publication 3

section III.B). Intermolecular transactivation of the insulin receptor was observed for RTK-based pathways [Lammers 1990,Hayes 1991] as well as GPCR-based systems [Ji 2002, Monnier 2011]. Transactivation refers to the ability of an activated receptor intracellular domain to activate the intracellular domain of a neighbouring receptor, which becomes activated although it is unoccupied by a ligand molecule. Such mechanism was proposed as a transduction amplification mechanism induced by clustering. We implemented this mechanism in simulation. We used the microscopic lattice framework illustrated in I.2.3.2 for this study, presented in detail in publication 3 in section II.B, for which an illustration of the core steps of the simulation is also presented on figure IV.1.

Publication 3

Receptor clustering affects signal transduction at the membrane level in the reaction-limited regime

Bertrand R. Caré and Hédi A. Soula
submitted to *Physical Review E*, 2012

Receptor clustering affects signal transduction at the membrane level in the reaction-limited regime.

Bertrand R Caré[1, 2, 3, *] and Hédi A Soula[3, 2]

[1] *Université de Lyon, LIRIS UMR 5205 CNRS-INSA, F-69621, Villeurbanne, France*
[2] *EPI Beagle, INRIA Rhône-Alpes, F-69603, Villeurbanne, France*
[3] *Université de Lyon, Inserm UMR1060, F-69621 Villeurbanne, France*

(Dated: December 19, 2012)

Many types of membrane receptors are found to be organized as clusters on the cell surface. We investigate the potential effect of such receptor clustering on the intracellular signal transduction stage. We consider a canonical pathway with a membrane receptor (R) activating a membrane-bound intracellular relay protein (G). We use Monte Carlo simulations to recreate biochemical reactions using different receptor spatial distributions and explore the dynamics of the signal transduction. Results show that activation of G by R is severely impaired by R clustering, leading to an apparent blunted biological effect compared to control. Paradoxically, this clustering decreases the half maximal effective dose (ED50) of the transduction stage increasing the apparent affinity. We study an example of inter-receptor interaction in order to account for possible compensatory effects of clustering and observed the parameter range in which such interactions slightly counterbalance the loss of activation of G. The membrane receptors spatial distribution affects the internal stages of signal amplification, suggesting a functional role for membrane domains and receptor clustering independently of proximity-induced receptor-receptor interactions.

I. INTRODUCTION

Signalling is the process by which an external chemical signal is perceived by the cell via membrane proteins called receptors. These receptors when activated trigger a biochemical cascade inside the cell. Two important families of signalling systems are associated with two particular type of receptors: the Receptor Tyrosine Kinase (RTK) [1] and the G-protein coupled receptor (GPCR) [2, 3]. Both systems share the same common functional features. In both cases, membrane receptors, once activated by an external ligand molecule, acquire the ability to activate directly several intracellular membrane-bound proteins that relay the signal further into the cytoplasm.

Contemporary cell biology acknowledges that, among other membrane components, receptors of different signalling pathways are not homogeneously dispatched on the membrane but are oftentimes organized in clusters [4–8], possibly due to the structuration of the membrane in lipid rafts and caveolae [9–11]. According to several recent works, receptor clustering seems to play a important role in cell signalling, and influences regulatory processes such as bacteria chemical sensitivity, chemotaxis, or G-protein signalling [12–14]. Literature however does not come to a consensus regarding the effect of clustering on receptor-ligand binding dynamics and afterwards cell response. When receptors are packed together, signal-enhancing phenomena can occur, such as ligand receptor switching [15], or improved ligand-receptor and receptor-effector encounter probabilities [16–18]. Within the context of diffusion-limited reactions, Goldstein [19] argues that clustering reduces the ligand-receptor binding forward rate constant whereas Gopalakrishnan [17] proposes that clustering increases the ligand-receptor rebinding probability, and thus the cell response. However, in a previous work using individual based-model, we showed that receptor clustering induces an attenuating effect on ligand-receptor binding and leads to a decreased apparent receptor affinity [20, 21], in agreement with a recent study [22]. However, the step further:the effect of clustering on signal transduction at equilibrium, directly downstream of the reception stage, remains relatively unexplored.

In this work, we determine the impact of heterogeneous (and correlated) spatial receptors distributions on the dynamics of a simple canonical pathway at the transduction stage. Since such dynamics are generally studied using mean-field models articulating averaged densities of molecules using the law of mass action, it rests on the well-mixed assumption [23, 24]. This approach is not directly applicable when considering clustering which, by definition, imposes heterogeneous receptor distributions. We propose a simple individual-based computational model to explore the dynamics of a canonical signal transduction stage between a receptor R and its downstream membrane-bound protein substrate G, akin to RTK and GPCR signalling systems. This computational framework allows for the simulation of transduction by heterogeneously distributed receptors, reproducing spatial distributions on the membrane observed in living cells.

* corresponding author:bertrand.care@insa-lyon.fr

II. MODELS

We consider a canonical transduction pathway, described by the following reactions:

$$R \underset{k_{-c}}{\overset{k_{+c}}{\rightleftharpoons}} C \tag{1}$$

$$C + G \xrightarrow{k_{+h}} C + H \tag{2}$$

$$H \xrightarrow{k_{-h}} G \tag{3}$$

where G is a deactivated intracellular relay protein and H its activated form. The activation of G is induced by a activated receptor C whereas R is its deactivated form.
In this simple model, receptor activation/deactivation is performed by an implicit ligand at constant rates : k_{+c} and k_{-c} respectively. This means that the model only considers the phosphorylation state of the receptor intracellular subunit, regardless of possible cooperation mechanisms due to the dimeric structure of the receptor [25, 26]. The response is evaluated by measuring the number of activated G molecules (H).

A. ODE for transduction dynamics at equilibrium

The reaction set can be expressed as a system of ODE describing the evolution of the amounts of species (denominated as lowercase letters) using the law of mass action [23, 26, 27]. The equilibrium of such system yielding $c^\star$ of the number of activated receptor c to the total receptor number $r_0 = r + c$ is well known

$$c^\star = \frac{c}{r_0} = \frac{k_{+\mathrm{c}}}{k_{\text{-c}} + k_{+\mathrm{c}}} = \frac{\rho}{1+\rho} \tag{4}$$

with $\rho = \dfrac{k_{+\mathrm{c}}}{k_{\text{-c}}}$.

The ratio ρ thus represents the implicit ligand stimulus applied to the system.

Activation of G molecules occurs at a rate proportional to $k_{+\mathrm{h}}c$, and deactivation at a constant rate $k_{\text{-h}}$. The fraction of activated $h^\star$ (ratio of h to $g_0 = g + h$) is at equilibrium

$$h^\star = \frac{h}{g_0} = \frac{r_0}{r_0 + (1 + \dfrac{1}{\rho})\kappa} \tag{5}$$

with $\kappa = \dfrac{k_{\text{-h}}}{k_{+\mathrm{h}}}$.
Both Eq. (4) and (5) exhibit several measurable values that relates to dose-responses curves. First let's rewrite Eq. 5 as

$$h^\star = \frac{\dfrac{r_0}{r_0 + \kappa}\rho}{\rho + \dfrac{\kappa}{\kappa + r_0}} \tag{6}$$

which expresses another Michaelian-like equation but with a new saturation plateau $h^\star_{\max}$ – whenever $\rho \mapsto \infty$ – and the half maximal efficient ligand stimulation (often referred to as the ED50) which is in our case the ratio ρ_{50} that generates half of the maximal G activation – namely $h^\star_{\max}/2$. Assuming we can measure both values from dose-responses, we can extract an equation for the reaction affinity κ derived from either the maximal G activation

$$\kappa_{\mathrm{hmax}} = r_0\,(1/h^*_{\max} - 1) \tag{7}$$

This relation is obtained from Eq. 6 by letting $\rho \mapsto \infty$ and rearranging to obtain κ from $h^\star_{\max}$. The other options is by measuring ρ_{50} the value of ρ that yields $h^\star_{\max}/2$ that is

$$\rho_{50} = \frac{\kappa}{\kappa + r_0} \tag{8}$$

and with rearranging yields

$$\kappa_{\rho 50} = \frac{\rho_{50} r_0}{1 - \rho_{50}} \tag{9}$$

Note that both κ should be equal provided that the reaction dynamics obeys Eq. 5. Please also note that, in both cases, the greater the κ, the more ligand stimulation needed to generate a given response, so the parameter κ is inversely proportional to the transduction reaction affinity.
Since ODE model is non-spatial it does not take into account receptor clustering. However, we will compare the theoretical dynamics of a well mixed transduction pathway with the ones obtained in simulation for heterogeneous receptors distributions which should coincide.

B. Monte Carlo microscopic lattice model

We developed a computational model that recreates the canonical transduction pathway described above, using a classical Monte Carlo microscopic lattice framework. The membrane is modelled as a 2D square lattice with periodic boundary conditions. We will assume that receptors are fixed at specific discrete locations on the lattice and do not impair the diffusion of G molecules. Receptors are set at the start of the simulation either uniformly (homogeneous distribution), or arranged in hexagonal clusters located randomly on the lattice (clustering). Additionally, crowding is ignored – several G molecules can reside on the same lattice at any given time step, but not receptors. These assumptions are imposed in order to restrict the study of receptor clustering to the effect of spatial correlation only, and avoid the interference of steric hindrance aspects such as macromolecular crowding and fractal diffusion [28, 29] in the observed effect of clustering.
The diffusion is a discrete-time random walk on the lattice. Each G or H molecule has a probability $p_D =$

$D\Delta t/l^2$ to jump to each of the four adjacent lattice node, D being the molecule diffusion coefficient, l the lattice spacing and Δt the time step. A reaction event characterized macroscopically by a rate k occurs during a time step with a probability

$$p = \frac{k\Delta t}{\mathcal{A}V_n} \tag{10}$$

where $\mathcal{A}$ is Avogadro's number,V_n is the volume of a lattice node [30]. The bimolecular reaction $C+G$ occurs according to this probability between two molecules located on the same node, where as unimolecular reactions are performed independently of the location of the molecule with a probability $p = k\Delta t$. Notably, although receptors are correlated in space, their activation is a stochastic process independent of their position or their neighborhood.
A simulation using an homogeneous receptor repartition should yield dose-response curves following Eq. 4 and Eq. 5. The effects of clustering can then be measured by positioning adequately receptors and relaunch the simulations with identical parameters.

III. RESULTS

Parameters were defined considering a typical eukaryotic cell of radius 10μm ($\sim$ 1.2 $10^3\mu$m^2) with 10^4 receptors (yielding a concentration of 8 receptors per μm^2) [23], and 20 times more intracellular signalling relay proteins, consistent with typical signalling systems such as the insulin pathway [26] or the β-adrenergic pathway [31]. Taking a smaller membrane patch of 800×800 2D-lattice, with a spacing $l = 10nm$ close to the typical membrane receptor diameter [32, 33], which gives $r_0 \sim 512$ receptors – converted down to $r_0 = 500$ for simplicity – and $g_0 = 10^4$ G molecules. We set the jump probability to each of the 4 adjacent lattice nodes $p_D = 1/4 = \frac{D\Delta t}{l^2}$, so each G molecule moves to another lattice node at each time step. With $\Delta t = 10^{-6}$s, this gives a diffusion coefficient $D = 2.5 \times 10^{-7}$cm^2.s^{-1} consistent with the fastest diffusion regime for GPI-anchored proteins on the membrane [34, 35].

Dose-responses curves were obtained by simulating different levels of ligand stimulation, reproduced by varying the parameter $k_{\text{-c}}$ and using a fixed rate $k_{+\text{c}} = 10^{-2}$. The higher the value of the parameter ρ, the higher the average number of activated receptors at equilibrium. These parameters were used for each simulation used in this work.
The rate $k_{+\text{h}}$ for the reaction $C + G \rightarrow C + H$ was defined so activation of G is in the reaction-limited regime to limit the effect of diffusion on the reaction rates. The regime of the reaction was set using a ratio $r_0 k_{+\text{h}}/k_t \geq 1$, k_t being the rate of the transport of G molecules to R molecules [23]. For our parameters, this gives the condition $k_{+\text{h}} \geq 10^6\text{M}^{-1}.\text{s}^{-1}$. Therefore we set the activation reaction probability $p_{+\text{h}} = 0.1$ (per Δt) for a G molecule located on the same lattice node as a C molecule, which gives $k_{+\text{h}} = 6.10^7\text{M}^{-1}.\text{s}^{-1}$. We reproduced different G activation affinities $\kappa = k_{\text{-h}}/k_{+\text{h}}$ by fixing $k_{+\text{h}}$ and varying $k_{\text{-h}}$ between 10^1s^{-1}s and 10^3s^{-1}, which translates into probabilities of deactivation per time step p_{-c} between 10^{-3} and 10^{-5}.

All receptors were initialized as deactivated. Clustering is achieved by assigning fixed position for the receptors on the grid. First a number n of receptors per cluster is defined, and the number of clusters is derived. Then the center of all clusters are positioned randomly, forbidding overlap. When the center of the cluster is positioned, all receptors of this cluster are set in a hexagonal tiling, spiralling around the center, which imposes an approximately disc-like shape although the lattice is square. Each cluster is randomly rotated on itself so no privileged orientation exists for non-symmetrical clusters. Note that when the cluster size is 1 – no clusters – receptors are positioned randomly on the membrane. On the other hand, a cluster size of 500 is one disc whose center is set randomly. Finally, initial positions for G molecules are set randomly, each G in a initially deactivated state.

A. Clustering decreases the activation of G.

For several values of ρ ranging from 0.01 to 20 and for two cluster size ($n = 1$, $n = 5$ and $n = 10$ – see Fig. 1 A) the equilibrium fraction of activated G – $h^\star$ – was retrieved. At equal receptor stimulation, clustering induces a dramatic decrease in G activation at equilibrium, for all values of ρ. Even when fully and constantly activated, receptors distributed in clusters of 5 and 10 activated less G than when randomly spread and separated.

This decreasing response effect is more pronounced the higher the clustering. As a way of quantifying this effect, we estimated the apparent affinity of the reaction $C + G \rightarrow C + H$ by calculating the parameter κ using the two different methods describe in Models. We first obtain the information of the saturation plateau $h^\star_{\text{max}}$ by taking the equilibrium values for very high ρ, averging the value of h for the last 100 time steps of 10 simulation runs at equilibrium. We retrieved the half maximal efficient ligand stimulation ρ_{50} by non-linear fitting of the equation $h = h_{\text{max}}\rho/(\rho_{50} + \rho)$ on dose-response curves that were obtained for 10 simulations runs. Using Eq.7 we derive κ_{hmax} and using Eq. 9 we get $\kappa_{\rho 50}$ as in to Fig. 1 B.

Surprisingly, although both estimation methods were derived from Eq. 5, they exhibit an opposite behavior with increased clustering : whereas κ_{hmax} increases up to 2 orders of magnitude, $\kappa_{\rho 50}$ decreases

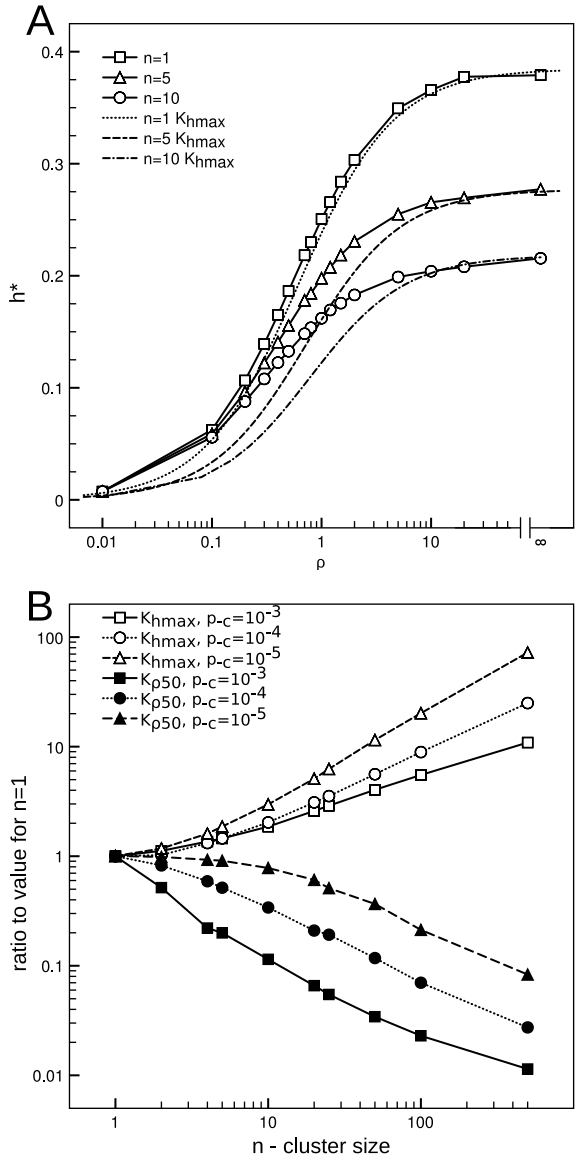

FIG. 1. A. Dose-response curves obtained in simulation for n=1 (no cluster, open squares), n=5 (clusters of 5 receptors, open triangles) and n=10 (open circles), all simulation parameters remaining equal ($p_{+\mathrm{h}} = 0.1, p_{-\mathrm{h}} = 10^{-4}$). Increasing levels of receptor stimulation are achieved by tuning the value of $\rho = p_{+\mathrm{c}}/p_{-\mathrm{c}}$, with fixed $p_{+\mathrm{c}} = 0.01$ and $p_{-\mathrm{c}}$ varying. $\rho \mapsto \infty$ was obtained by setting $p_{+\mathrm{c}} = 1.0$ and $p_{-\mathrm{c}} = 0$. Data points were obtain by averaging h at equilibrium for the last 100 time steps of 10 simulation runs. Theoretical curves (dashed lines) were obtained using Eq. 5 and $\kappa = \kappa_{\mathrm{hmax}}$ estimated from the saturation plateau (Eq. 7). B. Values of κ computed from the saturation plateau (κ_{hmax}) or from the half maximal efficient dose ($\kappa_{\rho 50}$ as in Eq. 9). For each curve, values were normalized on the estimate obtain for $n = 1$.

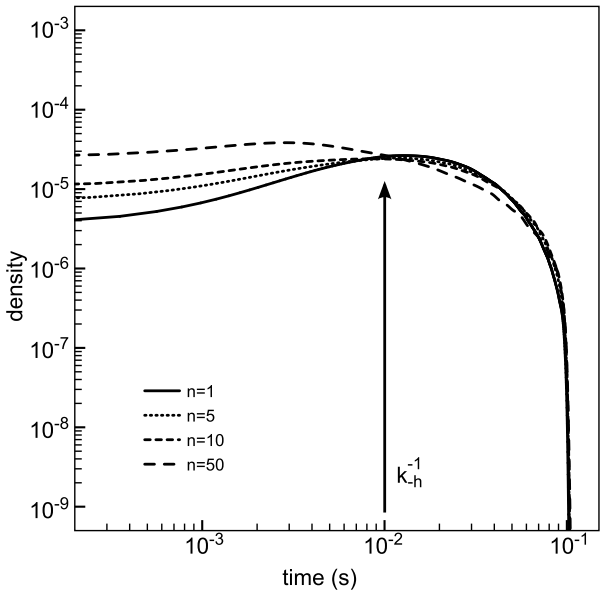

FIG. 2. Empirical densities of times between consecutive activation events of the same G molecule, using the same set of parameters $p_{+\mathrm{c}} = p_{-\mathrm{c}} = 0.01$, $p_{+\mathrm{h}} = 0.1$, $p_{-\mathrm{h}} = 10^{-4}$, for various cluster sizes n. The mean activated time for G molecules is $1/k_{-\mathrm{h}} = 10^{-2}$ s.

down to 2 orders of magnitude. This phenomenon can be seen on dose-response curves : they have a lower saturation plateau, but it is reached sooner in terms of ligand stimulation. Theoretical dose-response curves using Eq. 5 and $\kappa = \kappa_{\mathrm{hmax}}$ are compared to simulated dose-response in Fig. 1 A to illustrate this phenomenon. The deterring effect of clustering is somewhat mitigated by an apparent increase in sensitivity (less ligand stimulation is required) compared to its respective maximal response (which is lower than for the homogeneous case anyway). In other words the overall response is blunted whereas its sensitivity is increased.

This impact of receptor clustering can be further assessed by inspecting waiting times between activation events of the same G molecule. In previous works with ligand-receptor binding, it was shown that the rebinding time decreased with clustering while the time before first binding increased [20–22]. Due to the nature of the problem – most ligand bound then got back to the medium – the time before first binding was a dominating feature. As such, both effects counterbalanced each other but the depleting effect of clustering on the time before first binding was eventually stronger. In this case, the distribution of the times between two activation events are displayed on Fig. 2 A for various cluster sizes. Clustering induces a redistribution of the times between consecutive activations events of the same G molecule. In the highly clustered case, most reactivation events occur on a very short time scale. At times near the average time before

deactivation and larger, less reactivation events occurred. This explains the impairment of the response provoked by clustering: in this model, an activated particle can cover a lot of membrane area before deactivation. Essentially, it means that after being activated, the position where a molecule can be reactivated is anywhere on the membrane, and decorrelated from the starting position. This strongly favors the non-clustered case in terms of signal amplitude, but the clustering case in terms of response sharpness.

B. Impact of transactivation as a compensatory mechanism

The activation of an individual receptor was previously decorrelated in time and space from the activation of other receptors. We explored the effect of transactivation [36–39] as an example of receptor-receptor interaction that introduces a spatio-temporal correlation in receptor activation. Within this mechanism, an activated receptor intracellular domain has the ability to activate another receptor intracellular domain located in its vicinity. It can be introduced naturally in the computational model by setting a probability p_ϕ to activate a receptor located less than 2 lattice nodes away from an activated receptor. With the hexagonal tiling used for clusters, this amounts to only the 6 closer receptors for the first step propagation.

In simulations, as expected, increasing cluster size leads to an increasing activation of R, since larger clusters make transactivation more efficient. Transactivation can propagate itself to a larger number of receptors. In the homogeneous case, the number of activated receptors remained globally unchanged. Fig. 3 A shows the impact of transactivation on G activation as a function of the cluster size, for two distinct ligand stimulations levels ρ. Compared to the unclustered case, the addition of transactivation slightly compensates the deterring effect of clustering for small to intermediate cluster sizes. Thus, for a given stimulation, there is an optimal cluster size that maximizes G activation. However, since the maximal receptor activation (at maximum stimulation) remains unchanged via transactivation, for high ligand stimulation clustering still strongly impairs the overall G activation (see Fig. 3 B). However, the sensitivity (the stimulation needed to elicit half of the relative maximal response) is increased via transactivation, reshaping dose-response curves towards a more "on/off" profile.

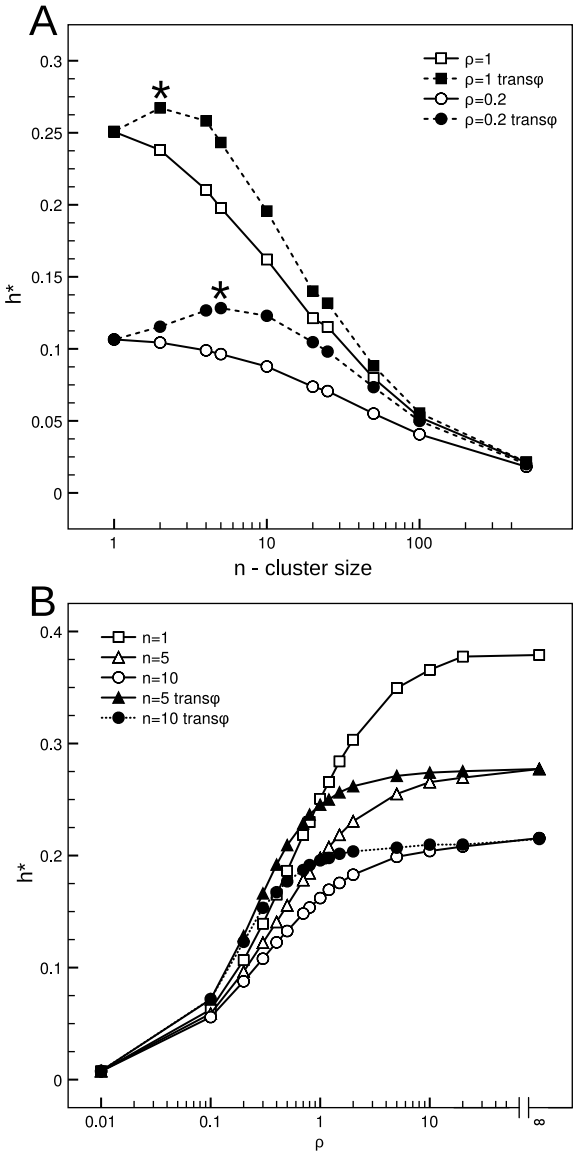

FIG. 3. A. Fraction of activated G at equilibrium $h^\star$ for $\rho = 1$ (squares) and $\rho = 0.2$ (circles) versus various cluster sizes – transactivation is disabled (open symbols) or enabled (closed symbols). Optimal cluster sizes were marked with *. Parameters : $p_\phi = p_{+\mathrm{c}} = 0.01$ and $p_{\text{-h}} = 10^{-4}$. B. Dose-responses curves from simulation for $n = 1$ (squares), 5 (triangles) and 10 (circles). Ligand stimulation was reproduced G activation probabilities were $p_{+\mathrm{h}} = 0.1$ and $p_{\text{-h}} = 10^{-4}$. Open symbols are for simulations without transactivation whereas closed symbols are when transactivation is enabled with $p_\phi = p_{+\mathrm{c}} = 0.01$.

IV. DISCUSSION

We developed a simple individual-based spatially-resolved computational model in which heterogeneous receptor distributions could be reproduced. The simulation of a canonical signalling pathway showed how the heterogeneous distributions of signalling proteins observed in cells can have an effect on the dynamics of transduction. A divergence with classical ODE models was observed without invoking complex protein-protein interaction mechanisms, but simply by changing the spatial distribution of receptors.

The activation of a membrane intracellular signalling protein by receptors in clusters is dramatically decreased whereas the number of available activated receptors is the same. Although the maximal amplitude of the signal was reduced, clustering decreased the half maximal efficient ligand stimulation, producing steeper dose-response curves. Since spatial clustering is available in our individual-base model framework, spatial inter-receptor interactions such as transactivation can be naturally introduced. Such correlating compensatory mechanism in receptor activation did not recover the maximal response, but accentuated the steepness of dose-response curves. The deterring effect of clustering was partially explained by a redistribution of the waiting times between consecutive activations of the same molecule, which favored short-time reactivation at the expense of mean-time reactivation.

To investigate the effect of clustering in the least favorable conditions, this work was done in the context of the reaction-limited regime. However membrane-bound intracellular proteins also exhibit a slow diffusion regime [35]. Our previous results suggest that slower diffusion regimes would reinforce the effect of clustering [20]. The model assumes that receptor diffusion is extremely slow compared to membrane-bound intracellular protein diffusion [40], so receptors are immobile throughout simulation. Allowing receptor mobility would require the use of a dynamical clustering mechanism, possibly ligand-dependent or diffusion-dependent [41–43]

The observed transduction dynamics suggests that clustering could be a simple, effective way of modulating the response of a signalling pathway, as observed in [44]. By adapting the distribution of receptors, the dynamic range and the sensitivity can be adjusted. Our results also support the possibility that clustering is a pathway-tuning mechanism *per se* without invoking complex protein-protein interactions such as oligomerization, crosstalk or trafficking. The qualitative and quantitative divergences between the classical ODE system and the simulated dose-response curves also indicates that accurate estimations of reaction rates *in vivo* could not be achieved without taking into account the heterogeneous spatial distributions of reactants, especially for signalling systems.

ACKNOWLEDGMENTS

BC holds a fellowship from la Rgion Rhne-Alpes. We gratefully acknowledge support from the CNRS/IN2P3 Computing Center (Lyon/Villeurbanne - France), for providing a significant amount of the computing resources needed for this work.

[1] M. A. Lemmon and J. Schlessinger, Cell, **141**, 1117 (2010), ISSN 1097-4172, PMID: 20602996.

[2] W. M. Oldham and H. E. Hamm, Nature reviews. Molecular cell biology, **9**, 60 (2008), ISSN 1471-0080, PMID: 18043707.

[3] R. Nygaard, T. M. Frimurer, B. Holst, M. M. Rosenkilde, and T. W. Schwartz, Trends in pharmacological sciences, **30**, 249 (2009), ISSN 0165-6147, PMID: 19375807.

[4] M. Karlsson, H. Thorn, A. Danielsson, K. G. Stenkula, A. Öst, J. Gustavsson, F. H. Nystrom, and P. Strålfors, European Journal of Biochemistry, **271**, 2471 (2004), ISSN 1432-1033.

[5] S. J. Plowman, C. Muncke, R. G. Parton, and J. F. Hancock, Proceedings of the National Academy of Sciences of the United States of America, **102**, 15500 (2005), ISSN 0027-8424, PMID: 16223883.

[6] S. Lee, J. Mandic, and K. J. Van Vliet, Proceedings of the National Academy of Sciences of the United States of America, **104**, 9609 (2007), ISSN 0027-8424, PMID: 17535923 PMCID: 1887608.

[7] M. Scarselli, P. Annibale, and A. Radenovic, The Journal of Biological Chemistry (2012), ISSN 1083-351X, doi: 10.1074/jbc.M111.329912, PMID: 22442147.

[8] A. N. Bader, E. G. Hofman, J. Voortman, P. M. P. v. B. en Henegouwen, and H. C. Gerritsen, Biophysical Journal, **97**, 2613 (2009), ISSN 1542-0086, PMID: 19883605.

[9] K. Simons and D. Toomre, Nature Reviews. Molecular Cell Biology, **1**, 31 (2000), ISSN 1471-0072, PMID: 11413487.

[10] D. Lingwood and K. Simons, Science, **327**, 46 (2010), ISSN 0036-8075, 1095-9203.

[11] V. L. Reeves, C. M. Thomas, and E. J. Smart, Advances in Experimental Medicine and Biology, **729**, 3 (2012), ISSN 0065-2598, PMID: 22411310.

[12] D. Bray, Annual Review of Biophysics and Biomolecular Structure, **27**, 59 (1998), ISSN 1056-8700, PMID: 9646862.

[13] B. A. Mello, L. Shaw, and Y. Tu, Biophysical journal, **87**, 1578–1595 (2004), ISSN 0006-3495.

[14] M. Fallahi-Sichani and J. J. Linderman, PLoS ONE, **4**, e6604 (2009), ISSN 1932-6203.

[15] P. A. Mahama and J. J. Linderman, Biophysical Journal, **67**, 1345 (1994), ISSN 0006-3495, PMID: 7811949.

[16] L. D. Shea and J. J. Linderman, Journal of Theoretical Biology, **191**, 249 (1998), ISSN 0022-5193.

[17] M. Gopalakrishnan, Biophysical Journal, **89**, 3686 (2005), ISSN 00063495.

[18] S. Ghosh, M. Gopalakrishnan, and K. Forsten-Williams, Physical Biology, **4**, 344 (2008), ISSN 1478-3975.

[19] B. Goldstein and M. Dembo, Biophysical Journal, **68**, 1222 (1995), ISSN 0006-3495, PMID: 7787014 PMCID: 1282020.

[20] B. R. Caré and H. A. Soula, BMC Systems Biology, **5**, 48 (2011), ISSN 1752-0509, PMID: 21453460.

[21] B. R. Caré and H. A. Soula, in *Information Processing in Cells and Tissues*, Vol. 7223 (Springer Berlin Heidelberg, Berlin, Heidelberg, 2012) pp. 50–61, ISBN 978-3-642-28791-6, 978-3-642-28792-3.

[22] A. Mugler, A. G. Bailey, K. Takahashi, and P. Rein ten Wolde, Biophysical Journal, **102**, 1069 (2012), ISSN 0006-3495.

[23] D. A. Lauffenburger and J. Linderman, *Receptors: Models for Binding, Trafficking, and Signaling* (Oxford University Press, USA, 1996) ISBN 0195106636.

[24] D. T. Gillespie, Annual Review of Physical Chemistry, **58**, 35 (2007), ISSN 0066-426X.

[25] S. Wanant and M. J. Quon, Journal of Theoretical Biology, **205**, 355 (2000), ISSN 0022-5193, PMID: 10882558.

[26] A. R. Sedaghat, A. Sherman, and M. J. Quon, American Journal of Physiology - Endocrinology And Metabolism, **283**, E1084 (2002).

[27] J. Murray, *Mathematical biology: I. An introduction* (Springer, 2005).

[28] R. Kopelman, Science, **241**, 1620 (1988), ISSN 0036-8075, 1095-9203.

[29] H. Berry, Biophysical journal, **83**, 1891–1901 (2002), ISSN 0006-3495.

[30] L. Boulianne, S. A. Assaad, M. Dumontier, and W. J. Gross, BMC Systems Biology, **2**, 66 (2008), ISSN 1752-0509.

[31] S. R. Post, R. Hilal-Dandan, K. Urasawa, L. L. Brunton, and P. A. Insel, Biochemical Journal, **311**, 75 (1995).

[32] D. W. Banner, A. D'Arcy, W. Janes, R. Gentz, H. J. Schoenfeld, C. Broger, H. Loetscher, and W. Lesslauer, Cell, **73**, 431 (1993), ISSN 0092-8674, PMID: 8387891.

[33] K. Parang, J. H. Till, A. J. Ablooglu, R. A. Kohanski, S. R. Hubbard, and P. A. Cole, Nature structural biology, **8**, 37 (2001), ISSN 1072-8368, PMID: 11135668.

[34] A. Pralle, P. Keller, E.-L. Florin, K. Simons, and J. K. H. Hörber, The Journal of Cell Biology, **148**, 997 (2000), ISSN 0021-9525, 1540-8140.

[35] A. Nohe, E. Keating, M. Fivaz, F. G. van der Goot, and N. O. Petersen, Nanomedicine: nanotechnology, biology, and medicine, **2**, 1 (2006), ISSN 1549-9642, PMID: 17292110.

[36] R. Lammers, E. Van Obberghen, R. Ballotti, J. Schlessinger, and A. Ullrich, Journal of Biological Chemistry, **265**, 16886 (1990).

[37] G. R. Hayes, L. D. Lydon, and D. H. Lockwood, Diabetes, **40**, 300 (1991), ISSN 0012-1797, PMID: 1991577.

[38] I. Ji, C. Lee, Y. Song, P. M. Conn, and T. H. Ji, Molecular endocrinology (Baltimore, Md.), **16**, 1299 (2002), ISSN 0888-8809, PMID: 12040016.

[39] C. Monnier, H. Tu, E. Bourrier, C. Vol, L. Lamarque, E. Trinquet, J.-P. Pin, and P. Rondard, The EMBO journal, **30**, 32 (2011), ISSN 1460-2075, PMID: 21063387.

[40] O. Thoumine, E. Saint-Michel, C. Dequidt, J. Falk, R. Rudge, T. Galli, C. Faivre-Sarrailh, and D. Choquet, Biophysical Journal, **89**, L40 (2005), ISSN 00063495.

[41] T. Duke and I. Graham, Progress in Biophysics and Molecular Biology, **100**, 18 (2009), ISSN 1873-1732, PMID: 19747931.

[42] H. A. Soula, A. Coulon, and G. Beslon, BMC biophysics, **5**, 6 (2012), ISSN 2046-1682, PMID: 22546236.

[43] B. R. Caré and H. A. Soula, in *4th International Conference on Bioinformatics and Computational Biology (BICoB)* (2012) ISBN 9781618397461.

[44] Taufiq-Ur-Rahman, A. Skupin, M. Falcke, and C. W. Taylor, Nature, **458**, 655 (2009), ISSN 0028-0836, PMID: 19348050 PMCID: 2702691.

IV.3 Discussion

In this chapter we have seen how clustering reduces the response of a pathway taken at the transduction stage. Unlike the ligand-receptor binding stage, clustering decreased the saturation plateau – the maximal response – but increased the apparent affinity of the transduction reaction. A redistribution of the waiting times between consecutive activation of the same G molecule was also observed, and clustering favored short times over medium to long times reactivations. A compensatory mechanism such as transactivation enhanced the apparent affinity, but the saturation plateau remained identical, diminishing the amplification potential of the transduction stage.

Receptor activation was not correlated in time nor space, however our previous results suggested that clusters could act as coherent signalling platforms. Clustering could be investigated in a model combining reception and transduction by heterogeneously distributed receptors. This would help us understand how the effects of clustering on both the reception stage and the transduction stage combine.

We explored a different reaction scheme than the reversible binding reaction seen in chapters II and III, where a relay protein continues its diffusion after activation. The deactivation rate dictates the mean time a relay protein will spend activated before returning to the inactive state, which calls for a better investigation of the relation between the mean time a relay protein remains activated and the inter-cluster distances.

The fact that both receptors and relay proteins are membrane-bound raises the question of clustering mechanisms. In particular, if both these protein types are membrane-bound, does the mechanism inducing receptor clustering also affect the relay signalling proteins ? If so, what impact could it have on the signalling pathway ? We have seen in I.1.3.2 that membrane-bound intracellular relay proteins also present heterogeneous distributions. In the next chapter, we implement a dynamical clustering mechanism based on non-homogeneous diffusion designed to investigate this question.

Chapter V

Dynamical clustering by non-homogeneous diffusion and signal transduction at the membrane

Contents

Highlights

► Activation of membrane-bound relay proteins by receptors, in a 2-d membrane with low-diffusivity patches that overconcentrate molecules in localized zones. ► If both reaction partners are slowed down in localized patches, transduction is amplified, whereas if only receptors are slowed down, transduction is attenuated.

V.1 Introduction

This chapter still investigates the effect of heterogeneous signalling proteins distributions on the transduction stage, but under a dynamical clustering mechanism with mobile receptors, contrary to the static heterogeneous distributions seen previously.

V.1.1 Outline

In I.1.3.2, we saw that not only receptors were distributed heterogeneously, but also were membrane-bound proteins, notably GPI-anchored proteins [Bader 2009, Sharma 2004, Goswami 2008]. This present chapter still uses an individual-based lattice model, but with mobile receptors undergoing a dynamical clustering mechanism : space-dependent non-homogeneous diffusion [Soula 2012]. Instead of setting the positions of fixed receptors in clusters, heterogeneous distributions were obtained by defining delimitated zones of the membrane where the diffusion coefficient was decreased. The publication 4 is set in the context of insulin signalling, where transduction is achieved by the insulin receptor (IR) and its principal membrane-bound relay protein, the Insulin Receptor Substrate 1 (IRS1), both of which exhibit heterogeneous distributions on the membrane [Gustavsson 1999, Karlsson 2004, Stenkula 2007].

The present study consisted in comparing two scenarios : either the slow diffusion zones affect only the motion of IR, or the slow diffusion zones affect simultaneously the motion of IR and the motion of IRS1. In each of these cases, the response of the pathway was measured at the transduction stage as the activation of IRS1 in function of increasing ligand stimulation, and compared with the third scenario : an homogeneous distribution of both molecular species.

V.1.2 Non-homogeneous diffusion : a dynamical clustering mechanism

The lipid composition of membrane rafts, notably cholesterol and spinhoglipids, alters the diffusivity of proteins in microdomains by locally increasing the viscosity of the membrane. We present the non-homogeneous diffusion clustering mechanism as implemented in simulation, derived from the observation of space-dependent diffusion of membrane proteins [Dietrich 2002, Wang 2008], and its ability to create heterogeneous distributions of diffusing molecules [Soula 2012].

The simulated environment consists of a regular lattice of discrete positions, as seen in the previous chapter and in I.2.3.2. The reaction scheme is identical to the one previously used in chapter IV. A diffusing molecule (be it IR or IRS1) can randomly jump to one of the 4 adjacent nodes – each assigned a identical probability – or stay in the same node for the time step being. The probability to stay in place, referred to as p in publication 4, page 2 section

2.1, relates to the diffusion coefficient D by the relationship $4D\Delta t/l^2 = 1 - p$ (consistently with I.2.3.2). A notable difference is that collision of receptors is forbidden in this simulation scheme : two receptors cannot occupy the same lattice node, although IRS1 molecules are allowed to. This was implemented in order to maintain the same effective coverage of the membrane by the receptors in each spatial distribution recreated.

A fraction λ of the total surface is defined with a slow diffusion coefficient D_s, and divided into squares of n nodes. These slow diffusion zones can affect only IR (NHD IR in publication 4), IR and IRS1 (NHD IR+IRS), or neither (HD). In these square zones, molecules affected by the slower diffusion will accumulate, as explained in [Soula 2012]. Thus, clusters of fixed receptors were replaced by slow diffusion zones where IR, IRS1, or both are overconcentrated, hence creating dynamical clusters. Different degrees of spatial correlation were simulated by varying the parameters D_s and n, and the resulting activation of IRS1 compared.

Let us characterize how molecule density is affected by space-dependent diffusion coefficients. In the case of molecules undergoing a continuous Brownian motion, whose diffusion coefficient $D(x, y)$ depends on the position (x, y), one has :

$$\begin{pmatrix} dX_t \\ dY_t \end{pmatrix} = \begin{pmatrix} \sqrt{D(x,y)} & 0 \\ 0 & \sqrt{D(x,y)} \end{pmatrix} \circ \begin{pmatrix} dZ_1 \\ dZ_2 \end{pmatrix} \tag{V.1}$$

The motion is set in a square of area $[-L; L]^2$, and , dZ_i/dt $(i = 1, 2)$ is the classical Brownian noise (with zero mean and unit variance). The Fokker-Planck equation for the density function can be derived either using the Itô formalism, or the Stratonovich formalism. In the simulation scheme described above, the correct formalism is Itô's one : the amplitude of the jump of a molecule only depends on its origin, not its destination. So a molecule located in a low-diffusivity zone can jump out ot the zone, but the mean amplitude of the jump will be determined by the slow diffusion coefficient. In these conditions, the associated Fokker-Planck equation for molecule density probability function $\rho(x, y)$ is :

$$\frac{\partial \rho(x, y, t)}{\partial t} = \mathrm{div}(\nabla(D\rho)) \tag{V.2}$$

This yields the equilibrium density distribution :

$$\rho(x, y) = \frac{\Omega}{D(x, y)} \tag{V.3}$$

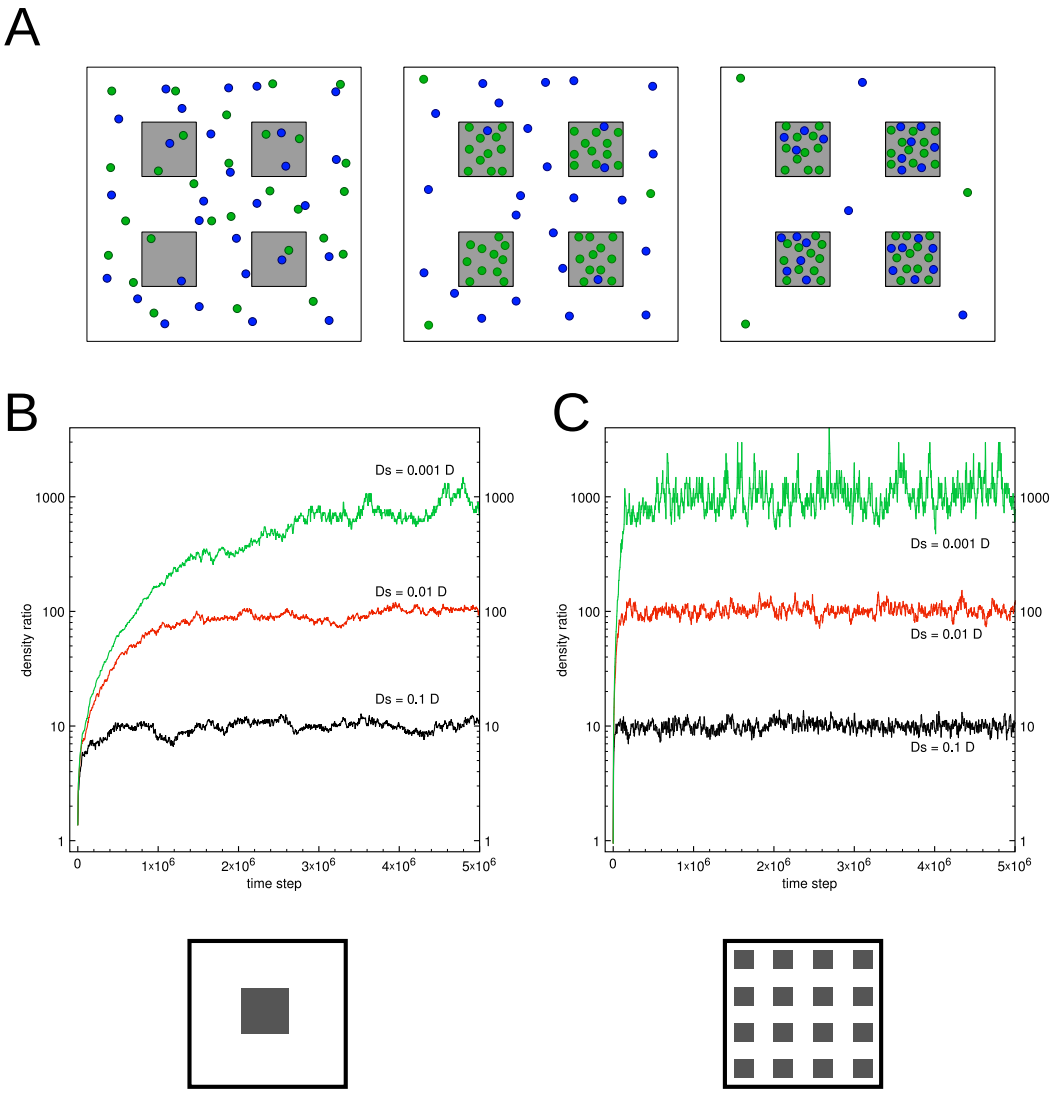

Figure V.1 – ***A.*** The three classes of spatial distributions : homogeneous distribution (left), IR (green) non-homogeneous diffusion only (middle) and IR+IRS1 (green+blue) non-homogeneous diffusion. Slow difffusion patches are in gray. ***B.*** Evolution of the ratio of molecule density inside the slow diffusion patches to outside for $\lambda = 0.2$, distributed in $n = 1$ single patch or $n = 16$ patches (***C.***).

with $\Omega = \left[\int\int_{[-L;L]^2} \frac{dxdy}{\sqrt{D(x,y)}}\right]^{-1}$ a normalizing constant for density. The key property is that the overconcentration is inversely proportionnal to the diffusion coefficient. Using the Stratonovich formalism (which is anyway not suitable for our simulation scheme) would have yield a overconcentration inversely proportional to the square root of the diffusion coefficient [Soula 2012].

The publication 4 page 2 section 2.1 presents the derivation of the overconcentration obtained in slow diffusion patches, in the discrete space case. A patch with a slow diffusion constant $D_s < D$ will contain a density D/D_s times greater than outside where diffusion is D, thus recreating clusters as overconcentrated zones.

Publication 4

Impact of receptor clustering on the membrane-based stage of a signalling pathway

Bertrand R. Caré and Hédi A. Soula

Proceedings of the 4th ISCA International Conference on Bioinformatics and Computational Biology, 2012

Impact of receptor clustering on the membrane-based stage of a signalling pathway

Bertrand R. Caré
Beagle LIRIS CNRS U5205, INRIA
Université de Lyon
F-69621 VILLEURBANNE

Hédi A. Soula
CaRMeN Inserm U1060
Université de Lyon
F-69621 VILLEURBANNE

Abstract

Individual-based Monte Carlo simulations naturally introduce spatial-based constraints on simulated binding kinetics. As far as the membrane is concerned, these spatial constraints may have an important impact on the signalling cascade. Indeed, several works have shown that membrane receptors distribution is not uniform. Some membrane structures known as domains can contain several copies of a particular receptor. Additionally, the disruption of these structures widely affects the pathway. We propose here to simulate one particular pathway – the first stage of the membrane part of the insulin-dependent glucose uptake cascade. By using a simple mechanism of space-dependent diffusion, we are able to create dynamical receptor clusters. We show that adjusting the diffusion regime can modify drastically the resulting response.
Keywords: signalling, receptor clustering, kinetics, computational biology.

1 Introduction

Cells have the ability to respond to external stimuli by the means of membrane receptors. When activated, the receptor propagates the signal inside the cell by activating internal effectors [1]. Membrane receptors diffuse on the cell membrane which is in fluid-phase [2]. Under such conditions, one would expect a homogeneous receptor spatial distribution on the cell membrane. However, several studies show that receptors spatial distribution is far from uniform [3, 4, 5] for different receptor and cell types [6, 7], and that membrane receptors form clusters.

This spatial configuration of receptors must be taken into account in systems biology approaches. Indeed, all models assume mass-action kinetics, hereby implying a well-stirred medium and space-independent behavior of species. In that case, the spatial characteristics of the system of interest are ignored.

As receptor clustering was studied in different signalling systems, no clear consensus can be extracted regarding its functional impact for cell signalling [8, 9]. In a previous work, our results suggested that, at binding equilibrium, receptor clustering leads to a decrease in the apparent receptor affinity, and thus diminishes cell response at equal stimulation [10].

We propose to go further and study the impact of clustering in a later signalling stage that is restricted in the membrane. For this problem, insulin pathway presents some interesting characteristics that makes it a particulary suitable target. Firstly, insulin, the main hormone enabling the metabolic regulation of glucose, is able to bind to its cognate receptor (IR) which can then phosphorylate tyrosine residues of intracellular signal mediators [11]. The membrane-bound insulin receptor substrate 1 (IRS1) protein is the principal internal effector of insulin-induced cell response [12]. Secondly, insulin receptors are known to be localized in clusters on the membrane – inside structures known as caveolae [13]. When caveolae are disrupted, clusters unfold and IR redistribute themselves uniformly, and the cell response to an insulin stimulus seems significantly affected [14, 15].

In this work, we propose to investigate the effect of receptor clustering on the early internal stage of insulin signalling, that is, the IRS1 activation by IR. A Monte Carlo individual-based computational framework was developed in order to recreate the IR-IRS1 interaction under different IR and IRS1 spatial configurations.

In order to impose such spatial constraints, we chose a diffusion-based mechanism. By introducing a space-dependent diffusion, we are able to create dynamical clusters of either species. This space-dependent process known as non-homogeneous diffusion will be applied selectively to IRS1, allowing the simulation of insulin-induced cell response under experimentally relevant spatial configurations: an homogeneous distribution of IRS1 in the membrane or a colocalized with IR distribution of IRS1.

2 Model

The exact mechanism leading to receptors clustering remains unclear. Several models have accounted for a non-homogeneous spread of membrane molecules [16, 17]. In essence, most models include a specific static zone where the diffusion of species is constrained (see e.g [18]). One the simplest, yet non readily explored, is a non-homogeneous space-dependent diffusion as we will describe below.

2.1 Non-Homogeneous Diffusion

Throughout this paper, simulations will be perform on a lattice where particles (both IR and IRS1) will undergo a simple 2d random walk using toric boundary conditions. In addition, in order to be able to simulate various diffusion constants, we added a probability p to stay in place. A particle at position (x, y) at time t will have:

$$\begin{cases} x+1, y & \text{at} & t+1 & \text{with probability} & (1-p)/4 \\ x, y+1 & \text{at} & t+1 & \text{with probability} & (1-p)/4 \\ x-1, y & \text{at} & t+1 & \text{with probability} & (1-p)/4 \\ x, y-1 & \text{at} & t+1 & \text{with probability} & (1-p)/4 \\ x, y & \text{at} & t+1 & \text{with probability} & p \end{cases}$$

Basically, each particle has a probability $(1-p)/4$ to jump on an adjacent lattice cell at each time step. One can easily show that the resulting movement will be a classical diffusion process with $D = 1 - p$. If we hypothesize that membrane diffusion is not constant, that is $p(x, y)$ is a non-constant function of the position, we will obtain a simple particle clustering process. Indeed, let us assume – in the 1d case for the sake of simplicity – a constant-by-part dependence of the diffusion coefficient $D(x) = D_1$, $\forall x \in [a, b]$ and $D(x) = D_2$ outside $[a, b]$ (where $[a, b]$ is a more viscous zone in the membrane – $D_1 < D_2$). Considering a single molecule, its probability $\pi(x, t)$ to be located at position x at time t is:

$$\begin{aligned} \pi(x, t+\delta t) = & \quad p(x)\pi(x,t) \\ & + \quad \pi(x-\delta x, t)\left(1-p(x-\delta x)\right)/2 \\ & + \quad \pi(x+\delta x, t)\left(1-p(x+\delta x)\right)/2 \end{aligned}$$

where $p(x)$ is our probability to stay in place at each time step and is defined, using the jump probability $q(x) = 2\delta t/(\delta x)^2 D(x)$ above, as $p(x) = 1 - q(x)$. Noting $g(x, t) = (1 - p(x))\pi(x, t)/2$ and developing $g(x \pm \delta x, t)$ in series of x, one obtains at order 2:

$$\begin{aligned} \pi(x, t+\delta t) & = p(x)\pi(x,t) + 2g(x) + (\delta x)^2 \partial_{xx} g(x) \\ & = \pi(x,t) + (\delta x)^2 \partial_{xx} g(x,t) \end{aligned} \quad (1)$$

Dividing by δt, taking the limit $\delta t \to 0$, and setting $\delta t/(\delta x)^2 = 1$, one gets:

$$\partial_t \pi(x,t) = \partial_{xx}\left(D(x)\pi(x,t)\right) \quad (2)$$

where we used the expression of $p(x)$ above to define $D(x)$. Noting $u(x, \infty)$ the density of molecules at x at equilibrium, one expects from eq.(2) $D(x)u(x, \infty) = A$, where A is a constant. Now, using the constant-by-part function for $D(x)$ expressed above, this yields $u(x, \infty) = A/D_1$ $\forall x \in [a, b]$ and $u(x, \infty) = A/D_2$ outside. The equilibrium concentration inside the $[a, b]$ patch equals the one outside the patch times the ratio D_2/D_1. Hence the larger the slowdown of the Brownian diffusion inside the patch, the larger the accumulation inside it at equilibrium.

This mechanism will serve as a simple mean to obtain dynamical clusters. We will therefore make the assumption that the stability of such diffusion gradients will be greater than the typical equilibrium time constants of all the reactions described below.

2.2 Spatial simulation of Insulin pathway

In order to test the impact of receptor clustering at the membrane level, we will consider the very first steps of the insulin signalling pathway.

$$IR \underset{a_{-1}}{\overset{a_1}{\rightleftharpoons}} IR^\star \quad (3)$$

$$IRS1 + IR^\star \xrightarrow{k_1} IR^\star + IRS1^\star \quad (4)$$

$$IRS1^\star \xrightarrow{m_1} IRS \quad (5)$$

where $IRS1$ is the non-phosphorylated form of IRS1 molecule and $IRS1^\star$ its phosphorylated form. The phosphorylation of IRS1 is induced by a phosphorylated insulin receptor $IR^\star$ whereas IR is its non-phosphorylated form.

In this simple model, receptor activation/deactivation is simulated using constant rates: a_1 and a_{-1} respectively. We do not explicitely model insulin ligand particles. Receptor activation is done every time step with probability a_1 when a receptor is not activated and a_{-1} in the other case (see Eq.3). Similarly, all phosphorylated IRS1 will have a probability m_1 to spontaneously dephosphorylate itself at each time step (Eq.5). The reaction itself in Eq.4 will occur with probability k_1 for each unphosphorylated IRS1 particle that resides on the same lattice cell as an activated IR.

Receptors will undergo a Brownian motion on the membrane using the space-dependent diffusion $D(x, y)$ as described in the section above. In all simulations, diffusion will be 1 everywhere except on the domains where diffusion will be lower D_s. These domains will

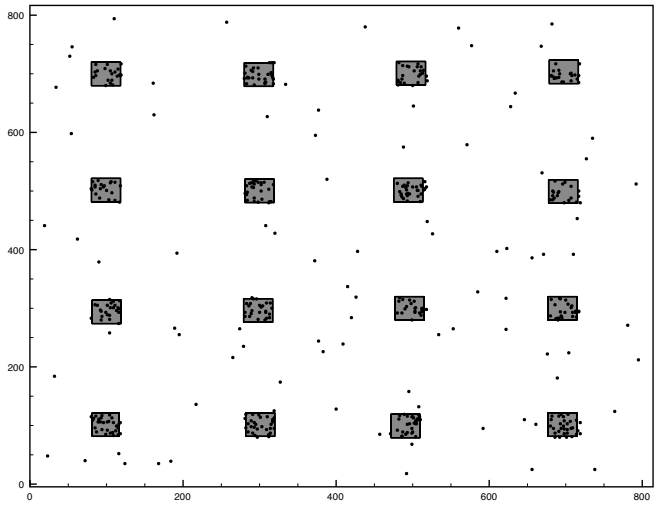

Figure 1: Receptor map at equilibrium. Black dots are receptors positions while grey squares are zones of slow diffusion $D_s < 1$. Parameters: $n = 2^4$, $D_s = 10^-2$ and total time is $T = 10^6$ steps.

be n squares (with $n = 1, 2^2, 2^4, 2^8$) positioned on an evenly spaced grid and whose sizes are such that the covered space is constant and equal to λS with S being the whole surface.

As such, a situation where $n = 1$ is a large slow patch which will accumulate all the particles and will describe an extremely clustered case for the receptors. Concerning the diffusion of IRS1 we will study two scenarios: one where IRS1 diffusion is not altered by the domain - $D_{irs} = 1$ everywhere on the lattice will be called $HD - IRS1$. In the second scenario, the IRS1 diffusion function will be equal to the IR diffusion one – $NHD - IRS1$. In the first scenario, the equilibrium distribution of IRS1 will cover homogeneously the whole membrane, whereas in the second scenario IR and IRS1 equilibrium distribution will coincide.

3 Results

Several situations were studied. At first, we can manipulate the equilibrium numbers of $IR^\star$ simulating various insulin stimulation. This yields dose-response functions of phosphorylated IRS1 versus stimulation. This is the obvious biological effect at this stage of the pathway. In all simulations the number of receptors (of any form) on the membrane will be $N_R = 500$ and the total IRS1 (of any form) will be $N_I = 10,000$. The initial distribution of both species is uniform on the membrane which is a 800×800 grid.

We tested several values of $D_s \in \{1, 10^{-1}, 10^{-2}, 10^{-3}\}$. Note that $D_s = 1$ stands as the control situation where all particles undergo the same Brownian motion. Simulations were performed on 10^6 time steps to ensure equilibrium.

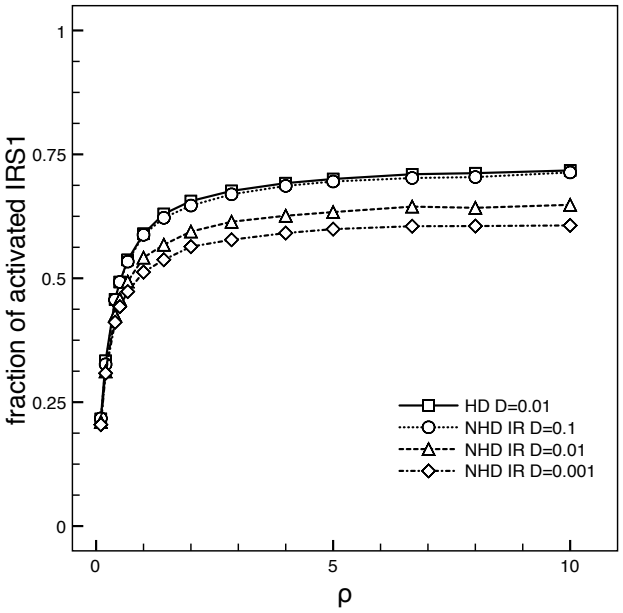

Figure 2: Dose-response of HD-IRS1: number of $IRS1^\star$ versus stimulation (ratio $\rho = a_1/a_{-1}$) for various diffusion coefficients in the slow zone $D_s = 1$ ($\square$), $D_s = 10^{-1}$ ($\bigcirc$), $D_s = 10^{-2}$ ($\triangle$) and $D_s = 10^{-3}$ ($\diamond$). All curves reach a plateau: a maximum amplification that decreases with the clustering, i.e. with lower D_s. As an indication of clustering, note that the equilibrium map of receptors in Fig. 1 is for $D_s = 10^{-2}$ here. Parameters: $n = 2^4$ and $T = 10^6$. Values are averaged over the last 10^4 time steps and over 3 different runs.

In order to assess the clustering effect of the non-homogeneous diffusion, a map of receptors at the equilibrium of a typical simulation $n = 2^4$ and $D_s = 10^{-2}$ is displayed on Figure 1. Note that this is a screenshot taken at a single time step and that all receptors keep on diffusing.

3.1 IRS1 diffuse homogeneously – HD-IRS1

In this section, IRS1 diffusion is not altered by the domains. We will suppose for simplicity's sake that its diffusion is the same for the phosphorylated form and is equal to the 'fastest' receptor diffusion ($D = 1$). In this case, we can have an insight of the result by noticing that unsphosphorylated IRS1

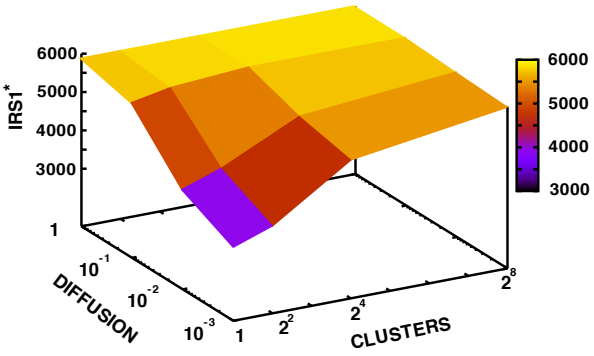

Figure 3: Maximal response for HD-IRS1 for all parameters: $n \in \{1, 2^2, 2^4, 2^8\}$ and $D_s \in \{1, 10^{-1}, 10^{-2}, 10^{-3}\}$. Note that the control cases are either $D = 1$ or $n = 0$ (not shown) and yield identical values ~ 5800. The maximal values were taken using the $\rho = a_1/a_{-1} = 10$ stimulation for the last 10^4 times step and for 3 runs.

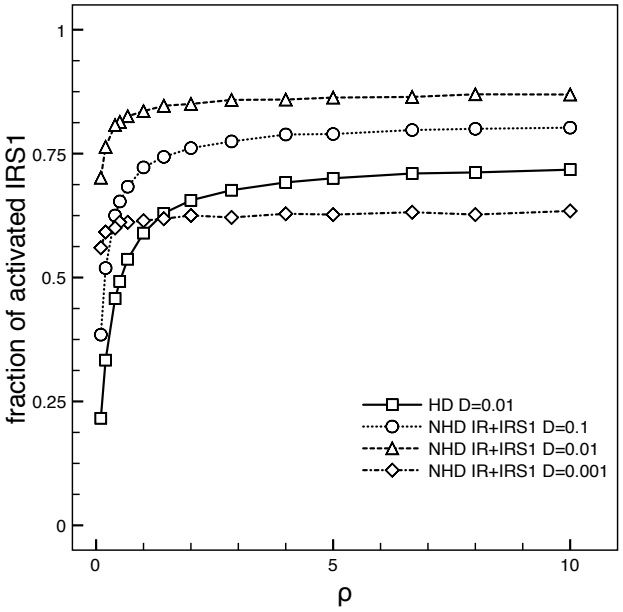

Figure 4: Dose-response of NHD-IRS1: number of $IRS1^\star$ versus stimulation (ratio $\rho = a_1/a_{-1}$) for various diffusion coefficients in the slow domain $D_s = 1$ ($\square$), $D_s = 10^{-1}$ ($\bigcirc$), $D_s = 10^{-2}$ ($\triangle$) and $D_s = 10^{-3}$ ($\diamond$). All curves reach a plateau: a maximum amplification that decreases with the clustering i.e. with lower D_s. As an indication of the clustering, note that the equilibrium map of receptors in Fig. 1 corresponds to $D_s = 10^{-2}$ here. Parameters: $n = 2^4$ and $T = 10^6$. Values are averaged over the last 10^4 time steps and over 3 different runs.

will have a harder time to find heavily clustered receptors. Moreover when a receptor is found and a IRS1 molecule is phosphorylated, the latter will have ample time to return to a receptor-free zone. We can expect this effect to be stronger with clustering: that is with n close to 1 and $D \ll 1$.

We display on Figure 2 the results of such simulations. The dose-response - the number of $IR^\star$ versus the ratio $\rho = a_1/a_{-1}$ – for three different diffusion $D_s \in \{10^{-1}, 10^{-2}, 10^{-3}\}$ for $n = 2^4$. Note that when $D = 10^{-2}$ the receptors clustering is as in Figure 1. As expected, there is a important decrease in the response – the number of phosphorylated IRS1 – versus the stimulation. By decreasing D_s we obtain less loose clusters and therefore less IRS1 activation. We can predict at this stage that this decrease will be sharper with bigger clusters, i.eI with $n = 1$ or $n = 2^2$.

Indeed, by compiling maximal responses for various diffusion values and profiles, one obtains the results on Figure 3. All maximal values are below the control case ($D_s = 1.0$) for all n. The worst case scenario is for the lowest diffusion ($D_s = 10^{-3}$) and the big square ($n = 1$) where $IRS1^\star$ maximal stimulation is almost 50% of the control.

In essence, we showed that deep clustering decreases the biological effect of insulin stimulation on the first phase of amplification. The main hypothesis here is that $IRS1$ are membrane bound and not colocalized with IR. We explore next the scenario where $IRS1$ is colocalized with the insulin receptors.

3.2 IRS1 diffuse non-homogeneously – NHD-IRS1

By submitting $IRS1$ to the same non-homogeneous diffusion mechanism as IR, we expect the opposite effect happening. Indeed, now both species will be colocalized in the same area and the reaction should come easier. However the picture is not as straightforward as it seems. Indeed as Figure 4 shows it, for $n = 2^4$. For $D = 10^{-1}$ and 10^{-2}, there are more $IRS1^\star$ compared to the control (squares). However for $D = 10^{-3}$, the reaction is severely downgraded.

Additionally, clustering also affects the results. Indeed and contrary to the previous scenario, the more there are clusters (higher n), the more there is an effect on the pathway. As displayed on Figure 5, the maxi-

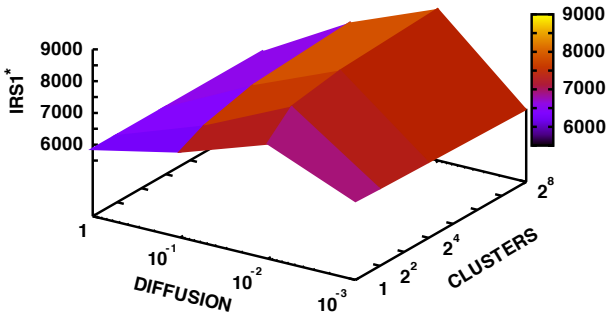

Figure 5: Maximal response as a function of diffusion and clustering in the case of NHD-IRS1: $n \in \{1, 2^2, 2^4, 2^8\}$ and $D_s \in \{1, 10^{-1}, 10^{-2}, 10^{-3}\}$. Note that the control case are either $D = 1$ or $n = 0$ (not shown) and yields identical values ~ 5800. The maximal values were taken using the $\rho = a_1/a_{-1} = 10$ stimulation for the last 10^4 times step and for 3 runs.

mal responses are higher for intermediate diffusion and small, sparse clustering (almost a 50% increase in the maximal response compared to the control). Note that as in the first scenario, controls were made for all diffusion coefficients without clustering and were identical.

4 Conclusion

As growing pieces of evidence suggest that membrane components are clustered into domains, functional properties of this clustering remain elusive. In the case of receptors, we previously showed using a simple individual-based model that ligand binding was hindered because of clustering [10]. In essence, ligand molecules spend more time in receptor-free zones than they would if receptors were spread homogeneously on the membrane.

By introducing a simple mechanism of non-homogeneous diffusion, we are able to simply create clusters of receptors while maintaining diffusion. In addition, this scheme allows us to create identical clusters for any other membrane species. In a signalling pathway such as the insulin one, the next step after receptor activation involves a diffusing membrane species: IRS1. Therefore we needed to consider two scenarios: either IRS1 is clustered with insulin receptor or not. Both cases are simply obtained by hindering the diffusion of IRS1 the same way as IR or not.

When IRS1 diffusion is not hindered and IRS1 position distribution is homogeneous – as this seems to be the case at least in human cells [15] – the effect of clustering is important: the phosphorylation of the insulin receptor substrate IRS1 is dramatically decreased with equal stimulation. This effect is stronger with high, dense clustering. Therefore we can conclude that the pathway is severely impaired by the clustering.

In the second scenario, the non-homogeneous diffusion apply to all species creating co-clustering between IRS1 and IR on the membrane. In that case, we showed that the pathway is upgraded and more phosphorylated IRS1 are available with small, sparse clustering. The effect of diffusion on the results is not monotonic and the effect is stronger with small clustering [18, 19].

Note that we ignored in our simulation an important mechanism pertaining to insulin receptors: transphosphorylation. Receptors can be activated by an already phosphorylated nearby receptor. This hereby can potentially increase the overall phosphorylated receptor pool and even more so in case of clustering. This feature should be added in a future version of the model.

This type of individual-based simulations allows to introduce spatial constraints naturally. We showed that these spatial constraints can drastically modify a simple pathway. Spatial and diffusion constraints will therefore be an important issue in the field of systems biology.

Acknowledgements

BC holds a fellowship from la Région Rhône-Alpes. We gratefully acknowledge support from the CNRS/IN2P3 Computing Center (Lyon/Villeurbanne - France), for providing a significant amount of the computing ressources needed for this work.

References

[1] Linderman JJ, Lauffenburger DA: *Receptors: models for binding, trafficking, and signaling*. Oxford University Press 1993.

[2] Singer SJ, Nicolson GL: **The fluid mosaic model of the structure of cell membranes**. *Science (New York, N.Y.)* 1972, **175**(23):720–731.

[3] Simons K, Ikonen E: **Functional rafts in cell membranes**. *Nature* 1997, **387**(6633):569–572.

[4] Parpal S, Karlsson M, Thorn H, Stralfors P: **Cholesterol Depletion Disrupts Caveolae and Insulin Receptor Signaling for Metabolic Control via Insulin Receptor Substrate-1, but Not for Mitogen-activated Protein Kinase Control**. *Journal of Biological Chemistry* 2000, **276**(13):9670–9678.

[5] Zhang J, Leiderman K, Pfeiffer JR, Wilson BS, Oliver JM, Steinberg SL: **Characterizing the topography of membrane receptors and signaling molecules from spatial patterns obtained using nanometer-scale electron-dense probes and electron microscopy**. *Micron (Oxford, England: 1993)* 2006, **37**:14–34.

[6] Almqvist N, Bhatia R, Primbs G, Desai N, Banerjee S, Lal R: **Elasticity and adhesion force mapping reveals real-time clustering of growth factor receptors and associated changes in local cellular rheological properties**. *Biophysical Journal* 2004, **86**(3):1753–1762.

[7] Lee S, Mandic J, Van Vliet KJ: **Chemomechanical mapping of ligandreceptor binding kinetics on cells**. *Proceedings of the National Academy of Sciences of the United States of America* 2007, **104**(23):9609–9614.

[8] Goldstein B, Dembo M: **Approximating the effects of diffusion on reversible reactions at the cell surface: ligand-receptor kinetics.** *Biophysical Journal* 1995, **68**(4):1222–1230.

[9] Gopalakrishnan M: **Effects of Receptor Clustering on Ligand Dissociation Kinetics: Theory and Simulations**. *Biophysical Journal* 2005, **89**(6):3686–3700.

[10] Caré BR, Soula HA: **Impact of receptor clustering on ligand binding**. *BMC Systems Biology* 2011, **5**:48.

[11] White MF, Kahn CR: **The insulin signaling system**. *The Journal of Biological Chemistry* 1994, **269**:1–4.

[12] Boura-Halfon S, Zick Y: **Phosphorylation of IRS proteins, insulin action, and insulin resistance**. *American Journal of Physiology. Endocrinology and Metabolism* 2009, **296**(4):E581–591.

[13] Gustavsson J, Parpal S, Karlsson M, Ramsing C, Thorn H, Borg M, Lindroth M, Peterson KE Kajsa Holmgren anMagnusson, Stralfors P: **Localization of the insulin receptor in caveolae of adipocyte plasma membrane**. *The FASEB Journal* 1999, **13**(14):1961 –1971.

[14] Karlsson M, Thorn H, Danielsson A, Stenkula KG, st A, Gustavsson J, Nystrom FH, Strlfors P: **Colocalization of insulin receptor and insulin receptor substrate1 to caveolae in primary human adipocytes**. *European Journal of Biochemistry* 2004, **271**(12):2471–2479.

[15] Stenkula KG, Thorn H, Franck N, Hallin E, Sauma L, Nystrom FH, Strlfors P: **Human, but not rat, IRS1 targets to the plasma membrane in both human and rat adipocytes**. *Biochemical and Biophysical Research Communications* 2007, **363**(3):840–845.

[16] Kusumi A, Nakada C, Ritchie K, Murase K, Suzuki K, Murakoshi H, Kasai RS, Kondo J, Fujiwara T: **Paradigm shift of the plasma membrane concept from the two-dimensional continuum fluid to the partitioned fluid: high-speed single-molecule tracking of membrane molecules**. *Annu. Rev. Biophys. Biomol. Struct.* 2005, **34**:351–78.

[17] Burrage K, Hancock J, Leier A, Nicolau Jr DV: **Modelling and simulation techniques for membrane biology**. *Briefings in bioinformatics* 2007.

[18] Shea LD, Linderman JJ: **Compartmentalization of Receptors and Enzymes Affects Activation for a Collision Coupling Mechanism**. *Journal of Theoretical Biology* 1998, **191**(3):249–258.

[19] Fallahi-Sichani M, Linderman JJ: **Lipid Raft-Mediated Regulation of G-Protein Coupled Receptor Signaling by Ligands which Influence Receptor Dimerization: A Computational Study**. *PLoS ONE* 2009, **4**(8):e6604.

V.3 Discussion

The results of publication 4 showed how two qualitatively opposite behaviors of the same transduction system can emerge only by introducing a non-homogeneous diffusion mechanism, summarized in figure V.2. If the two components of the transduction stage were affected by slow diffusion zones, the response was amplified. If only receptor diffusion was impaired by low-diffusivity patches, the response was decreased in a manner similar to our previous results.

Both these opposite effects were modulated by the distribution of the total low-diffusivity surface. This suggests that the observed effect on the transduction kinetics was not only due to the overconcentration induced by non-homogeneous diffusion. If slow diffusion was set for the same fraction of the surface, but decomposed in a higher number of smaller slow diffusion patches, the effect observed in the NHD IR situation was attenuated, and the response returned to its control value. On the contrary, in the NHD IR+IRS1 situation, a higher number of patches accentuated the amplificating effect observed on the response.

The overconcentration resulting from non-homogeneous diffusion is highly dependent on the implementation of diffusion in simulation. At the frontier between low-diffusivity and high-diffusivity membrane domains, the probability to jump from one domain to another determines the effective flux of molecules, and condition the resulting overconcentration. In our simulation scheme, the jump probability only depends on the starting point, which leads to the Itô calculus, and a density ratio inverserly proportional to the ratio of diffusion coefficients. This generates highly overconcentrated clusters, whereas a jumping probability calculated from, for instance, the mean of the diffusion coefficients in and outside the domain, would lead to the Stratonovich formalism. As illustrated in [Soula 2012], it would result in a density ratio inversely proportional to the ratio of the square roots of diffusion coefficients, and therefore less overconcentrated clusters. Beyond the numerical divergence, this illustrates how two different modelling assumptions can lead to drastically different reproductions of the same system.

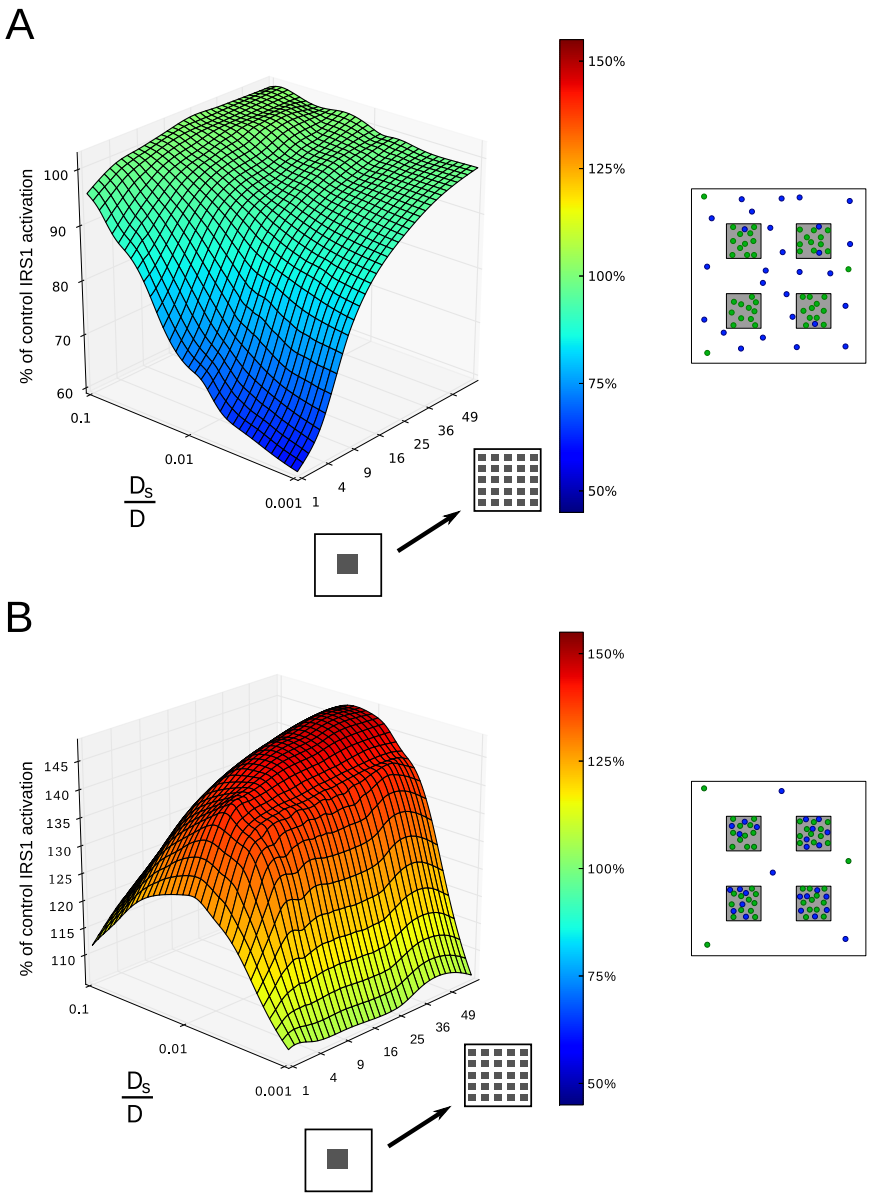

Figure V.2 – Figures 3 and 5 from the publication 4, with additionnal data interpolated by cubic splines. ***A.*** Activation of IRS1 (fraction of activation in the homogeneous control case) in function of the diffusion ratio and the number of patches, at equal low-diffusivity surface, for the NHD IR scenario. Increasing the number of patches, and therefore the number of effective clusters, decreases the response at equilibrium. ***B.*** Activation of IRS (fraction of control) for the NHD IR+IRS scenario. Clustering induces an amplification effect, characterized by an optimal diffusion ratio and a bell-shaped curve.

Discussion

The signalling proteins relaying a signal from the extracellular medium towards the cytoplasm exhibit different degrees of spatial heterogeneity. The spatial distributions of signalling proteins dictate the frequency and the location of these collisions at the microscopic level. The observation of heterogeneous signalling protein distributions in signalling systems of different types and purposes suggest that spatiality plays a functional role in signalling. We undertook the investigation of the effect of heterogeneous spatial distributions on the dynamics of a canonical signalling pathway. This pathway was representative of the core functional structure of signalling systems, built on a reception stage followed by a transduction stage. We excluded complex biochemical interactions from our field of investigation to focus uniquely on the effect of spatial heterogeneity on a simple linear pathway, consisting of a ligand, a membrane receptor, and a membrane-bound intracellular relay protein.

Compared to a homogeneous distribution, clustering decreased the response measured in terms of receptor occupation for the reception stage, and measured in terms of intracellular membrane-bound protein activation for the transduction stage. The two different dynamics of these successive stages were however affected differently. For the reception stage which was a reversible ligand-receptor binding reaction, clustering only reduced the apparent affinity of the system, the maximal response being not determined by the reaction rates, but only by the total number of available receptors. In the transduction stage composed of an activate-and-go reaction that does not immobilize the relay proteins after activation, the reaction rates determine not only the affinity, but also the maximal response. In this case, clustering broke this duality, and increased the apparent affinity of the reaction while paradoxically decreasing the maximal response.

The effect of clustering was caused by a spatio-temporal redistribution of activation events, as clustering favored short-time scale reactivation at the expense of initial activation events. This was also observed in the number of distinct ligand molecules generating binding events, the set of unique binding contributors being drastically reduced with clustering. However, since the reactivation events are dependent of initial activation events, the global outcome is a decreased number of total reaction events. This defavorable imbalance is maintained even at equilibrium. The temporal distributions of reaction events and waiting times are closely related to the first passage time distribution of

a molecule searching for a reaction partner. In classical spatially homogeneous models such as ODE and the stochastic CME, the next reaction time distribution is assumed to be exponential, implicitly for ODE, explicitly for the CME. The principal trait of this distribution is its "memorylessness" [Dobrzynski 2008] : the probability of the next reaction time is independent of the reaction history of molecules. The physical basis for this memorylessness is diffusion of reaction partners that are homogeneously distributed. With heterogeneous distributions, this memoryless diffusion principle does not hold if the diffusion regime is not fast enough compared to the inter-cluster distances, the mean time spent activated and the activation rate.

The introduction of a dynamical clustering mechanism demonstrated that the attenuating effect of clustering could be turned into an amplification phenomenon, if both receptors and relay proteins are overconcentrated within the same microdomains. In the NHD IR only scenario, splitting the low-diffusivity surface in smaller patches cancelled the decreasing effect of clustering, which was consistent with the effect of clustering on the ligand-receptor reaction. In the NHD IR+IRS1 scenario, an amplification effect was observed. Non-homogeneous diffusion induces localized overconcentrated zones, which is a first way to understand its amplificating effect on the transduction reaction in the NHD IR+IRS1 scenario. However, if the same fraction of low-diffusivity surface was splitted in more smaller patches, this amplification effect was increased, althoug the same overall surface contained the same density of molecules at equilibrium. Moreover, increasing the surconcentration by slowing down diffusion in these patches did not result in an increased amplification, although it did result in stronger overconcentration. The resulting response exhibited a bell-shaped curve centered on an optimal diffusion ratio, and we have yet to explain this peculiarity. We can add that, although splitting the same low-diffusivity surface in smaller patches does preserve the global fraction of membrane where diffusion is slowed down, it also dramatically increases the perimeter of the low-diffusivity and high-diffusivity domains frontier, which is where fluxes of molecule from one domain to the other occur. The examination of these fluxes could lead to a better understanding of the effect of non-homogeneous diffusion on the response.

We have seen that the effect of clustering on the dynamics of the pathway is conditionned by the relative magnitude of various parameters : the inter-cluster distance, the activation and deactivation rates, the diffusion coefficients. Our study lacks the thorough examination of the combinations of such parameters that lead to a functional divergence between homogeneous and heterogeneous distributions. We have yet to find the quantitative rules

that would allow one to determine whether a specific pathway, given its reaction, diffusion and geometrical parameters, is susceptible to have dynamics that diverge from those predicted by classical homogeneous models. The high computational resource consumption and the difficulty to find biologically accurate parameters also limit the extent of our conclusions.

We focused our study on a simple linear pathway, where the response is the output of a increasing monotonous function whose input is the ligand stimulation, and had a simple, single equilibrium. All reactions were positive activation ones, and we excluded inhibitory reactions. In this context, clustering only decreased or increased the response, but globally preserved the monotonous function of the pathway. There are however many biochemical networks that have more complex topologies, resulting in non-monotonous dynamics, bi-stability, bifurcations determined by intrinsic parameters, or oscillatory behaviors. In our simple linear pathway, clustering modified the effective value of intrinsic parameters. Our work raises the question of what could be the implications of spatial heterogeneity in pathways exhibiting complex topologies, feedback loops and inhibitory reactions. Notably, in systems presenting bifurcations, spatial heterogeneity could lead to effective values of critical parameters that lead to qualitatively different dynamics. Such systems could switch between dynamics by changing the spatial distribution of reactants or their diffusion coefficients, even though the intrinsic reaction rates remain the same. A dedicated study remains to be undertaken on this matter.

By simulating individual molecules at the microscopic scale and measuring the effect spatial heterogeneity at the macroscopic scale, computational models can help the derivation of macroscopic formalisms that account for heterogeneous molecule distributions. More specifically, the exponential probability distributions of activation events could be replaced by distributions obtained in simulation with clustering in a stochastic simulation algorithm. Once the effect of clustering on these distributions will have been thoroughly determined, it could be possible to extract this effect and reintroduce it in non-spatial models that are less computationally expensive than individual-based spatially resolved models. Eventually, the equivalent of the law of mass action in heterogeneous conditions could result in ODE equations accounting for spatiality in signalling, characterized by parameters easily relatable to doses-responses curves obtained in wet experimentation.

Membrane microdomains are sometimes presented as signalling platforms concentrating membrane-bound interacting proteins in rafts, thus facilitating the operation of the pathway. Our results suggest that the decreasing effect

of clustering would still affect the relay of the signal by proteins in clusters to the cytoplasmic signalling effectors. Changing the spatial distribution of signalling proteins suffices to modulate signal transduction, in amplitude and in sensitivity. Response modulation could be achieved simply by tuning the geometrical parameters of protein distributions. This speculative response-tuning ability could be comparatively less energy and resource-consuming than maintaining different versions of signalling proteins characterized by different intrinsic affinities. We have only explored one putative clustering mechanism in our study, non-homogeneous diffusion. It is unlikely that this mechanism would affect differently receptors and their membrane-bound substrate, as a locally higher viscosity should affect the diffusion of both species. Other mechanisms proposed to explain heterogeneous distributions could be better candidates for a response-tuning mechanism : receptor aggregation, ligand-induced oligomerization, anomalous diffusion induced by obstacles, or specific lipids acting as picket or fences. It remains to be determined if clustering has a real biological advantage. We would have to measure the spatial organization of homologuous pathways from different species and cell lineages – together with the kinetics parameters of the corresponding pathways and the diffusion coefficients – to identify biological situations where clustering present an advantage.

This work constitutes another step towards the acknowledgement that spatiality plays a crucial role in cellular processes. Understanding how these processes operate cannot be achieved by only considering the interactome, the genome or the proteome characterizing a given cell, and requires the integration of knowledge from various disciplines to be integrated in coherent models that simultaneously account for the physical, biochemical and spatial aspects of cell biology. Computational models are a particularly suitable framework in which cellular processes can be reproduced including insights from statistical physics and biophysics. Hypothesis that are difficult to test in wet experimentation can be investigated in a controlled experimental environment. In this context, individual-based models are also particularly suitable for the exploration of macroscopic emergent properties arising from the interaction of populations of components at the microscopic scale.

Bibliography

[Aderem 2005] Alan Aderem. *Systems Biology: Its Practice and Challenges.* Cell, vol. 121, no. 4, pages 511–513, May 2005. (Cited on pages 15 and 16.)

[Alberts 2002] Bruce Alberts, Alexander Johnson, Julian Lewis, Martin Raff, Keith Roberts and Peter Walter. *Molecular Biology of the Cell, fourth edition.* Garland Science, 2002. (Cited on pages 20 and 22.)

[Almqvist 2004] N Almqvist, R Bhatia, G Primbs, N Desai, S Banerjee and R Lal. *Elasticity and adhesion force mapping reveals real-time clustering of growth factor receptors and associated changes in local cellular rheological properties.* Biophysical Journal, vol. 86, no. 3, pages 1753–1762, March 2004. PMID: 14990502. (Cited on page 29.)

[Andrews 2004] Steven S Andrews and Dennis Bray. *Stochastic simulation of chemical reactions with spatial resolution and single molecule detail.* Physical biology, vol. 1, no. 3-4, pages 137–151, December 2004. PMID: 16204833. (Cited on page 49.)

[Andrews 2010] Steven S. Andrews, Nathan J. Addy, Roger Brent and Adam P. Arkin. *Detailed Simulations of Cell Biology with Smoldyn 2.1.* PLoS Comput Biol, vol. 6, no. 3, page e1000705, March 2010. (Cited on page 49.)

[Andrews 2012] Steven S Andrews. *Spatial and stochastic cellular modeling with the Smoldyn simulator.* Methods in molecular biology (Clifton, N.J.), vol. 804, pages 519–542, 2012. PMID: 22144170. (Cited on page 49.)

[Arjunan 2010] Satya Nanda Vel Arjunan and Masaru Tomita. *A new multicompartmental reaction-diffusion modeling method links transient membrane attachment of E. coli MinE to E-ring formation.* Systems and synthetic biology, vol. 4, no. 1, pages 35–53, March 2010. PMID: 20012222. (Cited on page 47.)

[Bader 2009] Arjen N Bader, Erik G Hofman, Jarno Voortman, Paul M P van Bergen en Henegouwen and Hans C Gerritsen. *Homo-FRET imaging enables quantification of protein cluster sizes with subcellular resolution.* Biophysical Journal, vol. 97, no. 9, pages 2613–2622, November 2009. PMID: 19883605. (Cited on pages 29 and 110.)

[Barabási 2004] Albert-László Barabási and Zoltán N Oltvai. *Network biology: understanding the cell's functional organization.* Nature reviews. Genetics, vol. 5, no. 2, pages 101–113, February 2004. PMID: 14735121. (Cited on page 15.)

[Becskei 2000] A Becskei and L Serrano. *Engineering stability in gene networks by autoregulation.* Nature, vol. 405, no. 6786, pages 590–593, June 2000. PMID: 10850721. (Cited on page 15.)

[Berg 1977] H C Berg and E M Purcell. *Physics of chemoreception.* Biophysical Journal, vol. 20, no. 2, pages 193–219, November 1977. PMID: 911982. (Cited on page 43.)

[Berg 2002] Jeremy Berg, John Tymockzo and Lubert Stryer. Biochemistry - NCBI bookshelf. W H Freeman, New York, 5th édition, 2002. (Cited on pages 20 and 21.)

[Bergner 2005] Andreas Bergner and Judith Günther. *Structural Aspects of Binding Site Similarity: A 3D Upgrade for Chemogenomics.* In Hugo Kubinyi and Gerhard Müller, editeurs, Chemogenomics in Drug Discovery, page 97–135. Wiley-VCH Verlag GmbH & Co. KGaA, 2005. (Cited on page 22.)

[Berry 2002] H. Berry. *Monte Carlo simulations of enzyme reactions in two dimensions: fractal kinetics and spatial segregation.* Biophysical journal, vol. 83, no. 4, page 1891–1901, 2002. (Cited on page 47.)

[Boulianne 2008] Laurier Boulianne, Sevin Al Assaad, Michel Dumontier and Warren J. Gross. *GridCell: a stochastic particle-based biological system simulator.* BMC Systems Biology, vol. 2, no. 1, page 66, July 2008. (Cited on page 47.)

[Burrage 2011] Kevin Burrage, Pamela M. Burrage, André Leier, Tatiana Marquez-Lago and Dan V. Nicolau. *Stochastic Simulation for Spatial Modelling of Dynamic Processes in a Living Cell.* In Heinz Koeppl, Gianluca Setti, Mario di Bernardo and Douglas Densmore, editeurs, Design and Analysis of Biomolecular Circuits, pages 43–62. Springer New York, New York, NY, 2011. (Cited on page 48.)

[Campbell 2007] Neil Campbell, Jane Reece, Lisa Urry, Michael Cain, Steven Wasserman, Peter Minorsky and Robert Jackson. Biology. Pearson International, 8th édition, 2007. (Cited on page 20.)

[Carpentier 1992] J L Carpentier, J P Paccaud, P Gorden, W J Rutter and L Orci. *Insulin-induced surface redistribution regulates internalization of the insulin receptor and requires its autophosphorylation.* Proceedings of the National Academy of Sciences of the United States of America, vol. 89, no. 1, pages 162–166, January 1992. PMID: 1729685. (Cited on page 94.)

[Cedersund 2008] Gunnar Cedersund, Jacob Roll, Erik Ulfhielm, Anna Danielsson, Henrik Tidefelt and Peter Strålfors. *Model-Based Hypothesis Testing of Key Mechanisms in Initial Phase of Insulin Signaling.* PLoS Comput Biol, vol. 4, no. 6, page e1000096, June 2008. (Cited on page 25.)

[Changeux 2006] J. P Changeux and S. J Edelstein. *Allosteric receptors after 30 years.* Rendiconti Lincei, vol. 17, no. 1, page 59–96, 2006. (Cited on page 23.)

[Cowan 2012] Ann E Cowan, Ion I Moraru, James C Schaff, Boris M Slepchenko and Leslie M Loew. *Spatial modeling of cell signaling networks.* Methods in cell biology, vol. 110, pages 195–221, 2012. PMID: 22482950. (Cited on page 46.)

[Dietrich 2002] Christian Dietrich, Bing Yang, Takahiro Fujiwara, Akihiro Kusumi and Ken Jacobson. *Relationship of lipid rafts to transient confinement zones detected by single particle tracking.* Biophysical journal, vol. 82, no. 1 Pt 1, pages 274–284, January 2002. PMID: 11751315. (Cited on page 110.)

[Dobrzynski 2008] Maciej Dobrzynski, Gauges, R., Kummer, U., Pahle, J. and Willy, P.M. *When do diffusion-limited trajectories become memoryless?* Logos Verlag Berlin, January 2008. (Cited on pages 39 and 126.)

[Dudko 2004] Olga K. Dudko, Alexander M. Berezhkovskii and George H. Weiss. *Rate constant for diffusion-influenced ligand binding to receptors of arbitrary shape on a cell surface.* The Journal of Chemical Physics, vol. 121, no. 3, page 1562, 2004. (Cited on page 49.)

[Duke 2009] Thomas Duke and Ian Graham. *Equilibrium mechanisms of receptor clustering.* Progress in Biophysics and Molecular Biology, vol. 100, no. 1-3, pages 18–24, October 2009. PMID: 19747931. (Cited on page 29.)

[Elf 2004] J Elf and M Ehrenberg. *Spontaneous separation of bi-stable biochemical systems into spatial domains of opposite phases.* Systems biology, vol. 1, no. 2, pages 230–236, December 2004. PMID: 17051695. (Cited on page 46.)

[Erban 2009] Radek Erban and S Jonathan Chapman. *Stochastic modelling of reaction–diffusion processes: algorithms for bimolecular reactions.* Physical Biology, vol. 6, no. 4, page 046001, August 2009. (Cited on pages 36, 49 and 54.)

[Fagerholm 2009] Siri Fagerholm, Unn Örtegren, Margareta Karlsson, Iida Ruishalme and Peter Strålfors. *Rapid Insulin-Dependent Endocytosis of the Insulin Receptor by Caveolae in Primary Adipocytes.* PLoS ONE, vol. 4, no. 6, page e5985, June 2009. (Cited on page 94.)

[Fallahi-Sichani 2009] Mohammad Fallahi-Sichani and Jennifer J. Linderman. *Lipid Raft-Mediated Regulation of G-Protein Coupled Receptor Signaling by Ligands which Influence Receptor Dimerization: A Computational Study.* PLoS ONE, vol. 4, no. 8, page e6604, August 2009. (Cited on page 47.)

[Feinberg 1987] Martin Feinberg. *Chemical reaction network structure and the stability of complex isothermal reactors—I. The deficiency zero and deficiency one theorems.* Chemical Engineering Science, vol. 42, no. 10, pages 2229–2268, 1987. (Cited on page 35.)

[Feinberg 1989] Martin Feinberg. *Necessary and sufficient conditions for detailed balancing in mass action systems of arbitrary complexity.* Chemical Engineering Science, vol. 44, no. 9, pages 1819–1827, 1989. (Cited on page 35.)

[Fisher 2000] M J Fisher, G Malcolm and R C Paton. *Spatio-logical processes in intracellular signalling.* Bio Systems, vol. 55, no. 1-3, pages 83–92, February 2000. PMID: 10745112. (Cited on page 17.)

[Foster 2003] Leonard J. Foster, Carmen L. de Hoog and Matthias Mann. *Unbiased quantitative proteomics of lipid rafts reveals high specificity for signaling factors.* Proceedings of the National Academy of Sciences, vol. 100, no. 10, pages 5813–5818, May 2003. (Cited on page 28.)

[Gillespie 1977] Daniel T. Gillespie. *Exact stochastic simulation of coupled chemical reactions.* The Journal of Physical Chemistry, vol. 81, no. 25, pages 2340–2361, December 1977. (Cited on page 37.)

[Gillespie 2007] Daniel T. Gillespie. *Stochastic Simulation of Chemical Kinetics.* Annual Review of Physical Chemistry, vol. 58, no. 1, pages 35–55, May 2007. (Cited on page 39.)

[Goldstein 1995] B Goldstein and M Dembo. *Approximating the effects of diffusion on reversible reactions at the cell surface: ligand-receptor kinetics.* Biophysical Journal, vol. 68, no. 4, pages 1222–1230, April 1995. PMID: 7787014 PMCID: 1282020. (Cited on page 43.)

[Goswami 2008] Debanjan Goswami, Kripa Gowrishankar, Sameera Bilgrami, Subhasri Ghosh, Riya Raghupathy, Rahul Chadda, Ram Vishwakarma, Madan Rao and Satyajit Mayor. *Nanoclusters of GPI-anchored proteins are formed by cortical actin-driven activity.* Cell, vol. 135, no. 6, pages 1085–1097, December 2008. PMID: 19070578. (Cited on pages 29 and 110.)

[Graham 2005] Ian Graham and Thomas Duke. *The logical repertoire of ligand-binding proteins.* Physical biology, vol. 2, no. 3, pages 159–165, September 2005. PMID: 16224121. (Cited on page 17.)

[Gustavsson 1999] J Gustavsson, S Parpal, M Karlsson, C Ramsing, H Thorn, M Borg, M Lindroth, K H Peterson, K E Magnusson and P Strålfors. *Localization of the insulin receptor in caveolae of adipocyte plasma membrane.* FASEB journal: official publication of the Federation of American Societies for Experimental Biology, vol. 13, no. 14, pages 1961–1971, November 1999. PMID: 10544179. (Cited on pages 29, 30 and 110.)

[Hanzal-Bayer 2007] Michael F. Hanzal-Bayer and John F. Hancock. *Lipid rafts and membrane traffic.* FEBS Letters, vol. 581, no. 11, pages 2098–2104, May 2007. (Cited on page 28.)

[Hattne 2005] Johan Hattne, David Fange and Johan Elf. *Stochastic reaction-diffusion simulation with MesoRD.* Bioinformatics, vol. 21, no. 12, pages 2923–2924, June 2005. (Cited on page 45.)

[Hayes 1991] G R Hayes, L D Lydon and D H Lockwood. *Intermolecular phosphorylation of insulin receptor as possible mechanism for amplification of binding signal.* Diabetes, vol. 40, no. 2, pages 300–303, February 1991. PMID: 1991577. (Cited on page 98.)

[Held 2011] Martin Held, Philipp Metzner, Jan-Hendrik Prinz and Frank Noé. *Mechanisms of Protein-Ligand Association and Its Modulation by Pro-*

tein Mutations. Biophysical Journal, vol. 100, no. 3, pages 701–710, February 2011. (Cited on page 23.)

[Higham. 2001] Desmond J. Higham. *An Algorithmic Introduction to Numerical Simulation of Stochastic Differential Equations.* SIAM Rev., vol. 43, no. 3, page 525–546, March 2001. (Cited on page 48.)

[Hlavacek 2003] William S Hlavacek, James R Faeder, Michael L Blinov, Alan S Perelson and Byron Goldstein. *The complexity of complexes in signal transduction.* Biotechnology and bioengineering, vol. 84, no. 7, pages 783–794, December 2003. PMID: 14708119. (Cited on page 25.)

[Holcman 2008] D Holcman and Z Schuss. *Diffusion escape through a cluster of small absorbing windows.* Journal of Physics A: Mathematical and Theoretical, vol. 41, no. 15, page 155001, April 2008. (Cited on page 72.)

[Horn 1972] F. Horn and R. Jackson. *General mass action kinetics.* Archive for Rational Mechanics and Analysis, vol. 47, no. 2, pages 81–116, 1972. (Cited on page 35.)

[Hurtley 2009] Stella Hurtley. *Location, Location, Location.* Science, vol. 326, no. 5957, pages 1205–1205, November 2009. (Cited on page 17.)

[Ji 2002] Inhae Ji, ChangWoo Lee, YongSang Song, P Michael Conn and Tae H Ji. *Cis- and trans-activation of hormone receptors: the LH receptor.* Molecular endocrinology (Baltimore, Md.), vol. 16, no. 6, pages 1299–1308, June 2002. PMID: 12040016. (Cited on page 98.)

[Jordan 2000] J.Dedrick Jordan, Emmanuel M Landau and Ravi Iyengar. *Signaling Networks: The Origins of Cellular Multitasking.* Cell, vol. 103, no. 2, pages 193–200, October 2000. (Cited on page 17.)

[Juska 2008] Alfonsas Juska. *Minimal models of multi-site ligand-binding kinetics.* Journal of Theoretical Biology, vol. 255, no. 4, pages 396–403, December 2008. PMID: 18851980. (Cited on pages 53 and 72.)

[Karlsson 2004] Margareta Karlsson, Hans Thorn, Anna Danielsson, Karin G Stenkula, Anita Öst, Johanna Gustavsson, Fredrik H Nystrom and Peter Strålfors. *Colocalization of insulin receptor and insulin receptor substrate-1 to caveolae in primary human adipocytes.* European Journal of Biochemistry, vol. 271, no. 12, pages 2471–2479, June 2004. (Cited on pages 29 and 110.)

[Kerr 2008] Rex A. Kerr, Thomas M. Bartol, Boris Kaminsky, Markus Dittrich, Jen-Chien Jack Chang, Scott B. Baden, Terrence J. Sejnowski and Joel R. Stiles. *Fast Monte Carlo Simulation Methods for Biological Reaction-Diffusion Systems in Solution and on Surfaces.* SIAM J. Sci. Comput., vol. 30, no. 6, page 3126–3149, October 2008. (Cited on page 49.)

[Kholodenko 2006] Boris N Kholodenko. *Cell-signalling dynamics in time and space.* Nature Reviews. Molecular Cell Biology, vol. 7, no. 3, pages 165–176, March 2006. PMID: 16482094. (Cited on pages 17 and 42.)

[Kholodenko 2009] Boris N Kholodenko. *Spatially distributed cell signalling.* FEBS Letters, vol. 583, no. 24, pages 4006–4012, December 2009. PMID: 19800332. (Cited on page 42.)

[Kiskowski 2009] Maria A. Kiskowski, John F. Hancock and Anne K. Kenworthy. *On the Use of Ripley's K-Function and Its Derivatives to Analyze Domain Size.* Biophysical Journal, vol. 97, no. 4, pages 1095–1103, August 2009. (Cited on page 29.)

[Koshland 2002] Daniel E. Koshland. *The Seven Pillars of Life.* Science, vol. 295, no. 5563, pages 2215–2216, March 2002. (Cited on page 20.)

[Kublaoui 1995] B Kublaoui, J Lee and P F Pilch. *Dynamics of signaling during insulin-stimulated endocytosis of its receptor in adipocytes.* The Journal of Biological Chemistry, vol. 270, no. 1, pages 59–65, January 1995. PMID: 7814420. (Cited on page 94.)

[Kusumi 1993] A Kusumi, Y Sako and M Yamamoto. *Confined lateral diffusion of membrane receptors as studied by single particle tracking (nanovid microscopy). Effects of calcium-induced differentiation in cultured epithelial cells.* Biophysical Journal, vol. 65, no. 5, pages 2021–2040, November 1993. PMID: 8298032. (Cited on page 29.)

[Kusumi 2005] Akihiro Kusumi, Chieko Nakada, Ken Ritchie, Kotono Murase, Kenichi Suzuki, Hideji Murakoshi, Rinshi S Kasai, Junko Kondo and Takahiro Fujiwara. *Paradigm shift of the plasma membrane concept from the two-dimensional continuum fluid to the partitioned fluid: high-speed single-molecule tracking of membrane molecules.* Annual review of biophysics and biomolecular structure, vol. 34, pages 351–378, 2005. PMID: 15869394. (Cited on page 29.)

[Lammers 1990] R Lammers, E Van Obberghen, R Ballotti, J Schlessinger and A Ullrich. *Transphosphorylation as a possible mechanism for insulin and epidermal growth factor receptor activation.* Journal of Biological Chemistry, vol. 265, no. 28, pages 16886 –16890, October 1990. (Cited on page 98.)

[Lauffenburger 1996] Douglas A. Lauffenburger and Jennifer Linderman. Receptors: Models for binding, trafficking, and signaling. Oxford University Press, USA, January 1996. (Cited on pages 32 and 42.)

[Lazebnik 2002] Yuri Lazebnik. *Can a biologist fix a radio?—Or, what I learned while studying apoptosis.* Cancer Cell, vol. 2, no. 3, pages 179–182, September 2002. (Cited on page 16.)

[Leach 2001] Andrew Leach. Molecular modelling: Principles and applications. Prentice Hall, 2 édition, April 2001. (Cited on page 23.)

[Lee 2007] Sunyoung Lee, Jelena Mandic and Krystyn J. Van Vliet. *Chemomechanical mapping of ligand–receptor binding kinetics on cells.* Proceedings of the National Academy of Sciences of the United States of America, vol. 104, no. 23, pages 9609–9614, June 2007. PMID: 17535923 PMCID: 1887608. (Cited on page 29.)

[Lingwood 2009] Daniel Lingwood, Hermann-Josef Kaiser, Ilya Levental and Kai Simons. *Lipid rafts as functional heterogeneity in cell membranes.* Biochemical Society transactions, vol. 37, no. Pt 5, pages 955–960, October 2009. PMID: 19754431. (Cited on page 28.)

[Lingwood 2010] Daniel Lingwood and Kai Simons. *Lipid Rafts As a Membrane-Organizing Principle.* Science, vol. 327, no. 5961, pages 46–50, January 2010. (Cited on page 28.)

[Mahama 1994] P A Mahama and J J Linderman. *A Monte Carlo study of the dynamics of G-protein activation.* Biophysical Journal, vol. 67, no. 3, pages 1345–1357, September 1994. PMID: 7811949. (Cited on page 47.)

[Milo 2002] R Milo, S Shen-Orr, S Itzkovitz, N Kashtan, D Chklovskii and U Alon. *Network motifs: simple building blocks of complex networks.* Science (New York, N.Y.), vol. 298, no. 5594, pages 824–827, October 2002. PMID: 12399590. (Cited on page 15.)

[Monnier 2011] Carine Monnier, Haijun Tu, Emmanuel Bourrier, Claire Vol, Laurent Lamarque, Eric Trinquet, Jean-Philippe Pin and Philippe

Rondard. *Trans-activation between 7TM domains: implication in heterodimeric GABAB receptor activation.* The EMBO journal, vol. 30, no. 1, pages 32–42, January 2011. PMID: 21063387. (Cited on page 98.)

[Montroll 1956] Elliot W. Montroll. *Random Walks in ultidimensional Spaces, Especially on Periodic Lattices.* Journal of the Society for Industrial and Applied Mathematics, vol. 4, no. 4, page 241, 1956. (Cited on page 72.)

[Morelli 2008] Marco J Morelli and Pieter Rein ten Wolde. *Reaction Brownian Dynamics and the effect of spatial fluctuations on the gain of a push-pull network.* arXiv:0804.4125, April 2008. (Cited on page 49.)

[Mugler 2012] Andrew Mugler, Aimee Gotway Bailey, Koichi Takahashi and Pieter Rein ten Wolde. *Membrane Clustering and the Role of Rebinding in Biochemical Signaling.* Biophysical Journal, vol. 102, no. 5, pages 1069–1078, March 2012. (Cited on page 93.)

[Neves 2009] Susana R. Neves and Ravi Iyengar. *Models of Spatially Restricted Biochemical Reaction Systems.* Journal of Biological Chemistry, vol. 284, no. 9, pages 5445–5449, February 2009. (Cited on page 17.)

[Plimpton 2005] SJ Plimpton and A Slepoy. *Microbial cell modeling via reacting diffusing particles.* Journal of Physics: Conference Series, vol. 15, pages 305–309, 2005. (Cited on page 49.)

[Plowman 2005] Sarah J Plowman, Cornelia Muncke, Robert G Parton and John F Hancock. *H-ras, K-ras, and inner plasma membrane raft proteins operate in nanoclusters with differential dependence on the actin cytoskeleton.* Proceedings of the National Academy of Sciences of the United States of America, vol. 102, no. 43, pages 15500–15505, October 2005. PMID: 16223883. (Cited on page 29.)

[Prior 2003] I. A. Prior. *Direct visualization of Ras proteins in spatially distinct cell surface microdomains.* The Journal of Cell Biology, vol. 160, no. 2, pages 165–170, January 2003. (Cited on page 29.)

[Ripley 1979] BD Ripley. *Tests of randomness for spatial point patterns.* J. Roy. Statist. Soc., pages 368–374, 1979. (Cited on page 29.)

[Rosenfeld 2011] Simon Rosenfeld. *Mathematical descriptions of biochemical networks: Stability, stochasticity, evolution.* Progress in Biophysics and Molecular Biology, vol. 106, no. 2, pages 400–409, August 2011. (Cited on page 16.)

[Scarselli 2012] Marco Scarselli, Paolo Annibale and Aleksandra Radenovic. *CCell-type-specific ?2 adrenergic receptor clusters identified using photo-activated localization microscopy are not lipid raft related, but depend on actin cytoskeleton integrity.* The Journal of Biological Chemistry, March 2012. PMID: 22442147. (Cited on page 29.)

[Schaff 1997] J. Schaff, C. C. Fink, B. Slepchenko, J. H. Carson and L. M. Loew. *A general computational framework for modeling cellular structure and function.* Biophysical Journal, vol. 73, no. 3, page 1135, September 1997. (Cited on page 45.)

[Schaff 2000] J C Schaff, B M Slepchenko and L M Loew. *Physiological modeling with virtual cell framework.* Methods in enzymology, vol. 321, pages 1–23, 2000. PMID: 10909048. (Cited on page 45.)

[Scott 2009] J. D. Scott and T. Pawson. *Cell Signaling in Space and Time: Where Proteins Come Together and When They're Apart.* Science, vol. 326, no. 5957, pages 1220–1224, November 2009. (Cited on page 17.)

[Sharma 2004] Pranav Sharma, Rajat Varma, R C Sarasij, Ira, Karine Gousset, G Krishnamoorthy, Madan Rao and Satyajit Mayor. *Nanoscale organization of multiple GPI-anchored proteins in living cell membranes.* Cell, vol. 116, no. 4, pages 577–589, February 2004. PMID: 14980224. (Cited on pages 29 and 110.)

[Shea 1998] Lonnie D. Shea and Jennifer J. Linderman. *Compartmentalization of Receptors and Enzymes Affects Activation for a Collision Coupling Mechanism.* Journal of Theoretical Biology, vol. 191, no. 3, pages 249–258, April 1998. (Cited on page 47.)

[Shoup 1982] D Shoup and A Szabo. *Role of diffusion in ligand binding to macromolecules and cell-bound receptors.* Biophysical Journal, vol. 40, no. 1, pages 33–39, October 1982. PMID: 7139033 PMCID: PMC1328970. (Cited on page 43.)

[Simons 1997] K Simons and E Ikonen. *Functional rafts in cell membranes.* Nature, vol. 387, no. 6633, pages 569–572, June 1997. PMID: 9177342. (Cited on page 28.)

[Simons 2000] K Simons and D Toomre. *Lipid rafts and signal transduction.* Nature Reviews. Molecular Cell Biology, vol. 1, no. 1, pages 31–39, October 2000. PMID: 11413487. (Cited on page 28.)

[Simons 2010] Kai Simons and Mathias J Gerl. *Revitalizing membrane rafts: new tools and insights.* Nature reviews. Molecular cell biology, vol. 11, no. 10, pages 688–699, October 2010. PMID: 20861879. (Cited on page 28.)

[Singer 1972] S J Singer and G L Nicolson. *The fluid mosaic model of the structure of cell membranes.* Science (New York, N.Y.), vol. 175, no. 23, pages 720–731, February 1972. PMID: 4333397. (Cited on page 27.)

[Soula 2012] Hedi A Soula, Antoine Coulon and Guillaume Beslon. *Membrane microdomains emergence through non-homogeneous diffusion.* BMC biophysics, vol. 5, no. 1, page 6, April 2012. PMID: 22546236. (Cited on pages 29, 110, 111, 113 and 123.)

[Stenkula 2007] Karin G. Stenkula, Hans Thorn, Niclas Franck, Elisabeth Hallin, Lilian Sauma, Fredrik H. Nystrom and Peter Strålfors. *Human, but not rat, IRS1 targets to the plasma membrane in both human and rat adipocytes.* Biochemical and Biophysical Research Communications, vol. 363, no. 3, pages 840–845, November 2007. (Cited on pages 27, 96 and 110.)

[Stiles 2001] Joel Stiles, Thomas Bartol and Erik Schutter. *Monte Carlo Methods for Simulating Realistic Synaptic Microphysiology Using MCell.* In Computational neuroscience: realistic modeling for experimentalists. CRC Press, 2001. (Cited on page 49.)

[Tomita 1999] M. Tomita, K. Hashimoto, K. Takahashi, T. S. Shimizu, Y. Matsuzaki, F. Miyoshi, K. Saito, S. Tanida, K. Yugi, J. C. Venter and C. A. Hutchison. *E-CELL: software environment for whole-cell simulation.* Bioinformatics, vol. 15, no. 1, pages 72–84, January 1999. (Cited on page 47.)

[Wang 2008] Q. Wang, X. Zhang, L. Zhang, F. He, G. Zhang, M. Jamrich and T. G. Wensel. *Activation-dependent Hindrance of Photoreceptor G Protein Diffusion by Lipid Microdomains.* Journal of Biological Chemistry, vol. 283, no. 44, pages 30015–30024, August 2008. (Cited on page 110.)

[Wedegaertner 1995] Philip B. Wedegaertner, Paul T. Wilson and Henry R. Bourne. *Lipid Modifications of Trimeric G Proteins.* Journal of Biological Chemistry, vol. 270, no. 2, pages 503–506, January 1995. (Cited on page 96.)

[Weng 1999] Gezhi Weng, Upinder S. Bhalla and Ravi Iyengar. *Complexity in Biological Signaling Systems.* Science, vol. 284, no. 5411, pages 92–96, February 1999. (Cited on page 16.)

[Wiley 1988] H S Wiley. *Anomalous binding of epidermal growth factor to A431 cells is due to the effect of high receptor densities and a saturable endocytic system.* The Journal of cell biology, vol. 107, no. 2, pages 801–810, August 1988. PMID: 3262110. (Cited on page 43.)

[Zhang 2006] Jun Zhang, Karin Leiderman, Janet R Pfeiffer, Bridget S Wilson, Janet M Oliver and Stanly L Steinberg. *Characterizing the topography of membrane receptors and signaling molecules from spatial patterns obtained using nanometer-scale electron-dense probes and electron microscopy.* Micron (Oxford, England: 1993), vol. 37, no. 1, pages 14–34, 2006. PMID: 16081296. (Cited on pages 29 and 30.)

[Zwanzig 1991] R Zwanzig and A Szabo. *Time dependent rate of diffusion-influenced ligand binding to receptors on cell surfaces.* Biophysical Journal, vol. 60, no. 3, pages 671–678, September 1991. PMID: 1657231. (Cited on page 43.)

FOLIO ADMINISTRATIF

THÈSE SOUTENUE DEVANT L'INSTITUT NATIONAL DES SCIENCES APPLIQUÉES DE LYON

NOM : **CARÉ** DATE de SOUTENANCE : 26 novembre 2012

Prénoms : **Bertrand Roland René**

TITRE :

Modèles individu-centrés de l'impact fonctionnel des hétérogénéités de diffusion et de distribution spatiale des protéines de signalisation cellulaire

NATURE : Doctorat Numéro d'ordre : 2012ISAL0123

Ecole doctorale : École Doctorale Informatique et Mathématiques (ED512)

Spécialité : Informatique

RÉSUMÉ :

Les voies de signalisation cellulaires permettent aux cellules de percevoir et d'échanger de l'information sous la forme de signaux chimiques. Un tel signal génère une réponse de la cellule au travers des étapes cruciales de réception, transduction et amplification. Différents types de protéines sont organisés dans une cascade de réactions de proche en proche qui relaient le signal de l'extérieur vers l'intérieur de la cellule, notamment au travers de la membrane. Les protéines de signalisation sont restreintes à des compartiments avec des degrés de liberté différents, et diffusent soit dans la membrane cellulaire qui est bidimensionnelle, soit dans le cytoplasme qui est en trois dimension. De plus, au sein même de ces espaces, leurs distributions respectives sont hétérogènes. Or l'étude de la dynamique des voies de signalisation repose classiquement sur des modèles mathématiques supposant une homogénéité de distribution.

Nous avons développé des modèles de réactions biochimiques entre populations de molécules où l'état et la position de chaque molécule sont caractérisés. La diffusion et les interactions entre molécules simulées sont reproduits sur la base de processus stochastiques issus de la biophysique. Ceci permet de recréer des distributions spatiales et des modes de diffusion hétérogènes tels qu'observés en biologie et d'étudier leur effet sur la dynamique de la signalisation en simulation.

L'exploitation des modèles a été menée sur les différentes étapes de signalisation. Premièrement, l'étude a porté sur l'interaction entre un ligand dans le milieu extracellulaire et des récepteurs membranaires fixes. Lorsque les récepteurs forment des grappes au lieu d'être répartis uniformément, cela provoque une perte de sensibilité globale de l'étage de réception. Deuxièmement, l'analyse a été poursuivie au niveau de l'étage de transduction entre les récepteurs et un effecteur au niveau de la membrane. Là aussi, une distribution en grappe plutôt qu'uniforme des récepteurs provoque une perte de sensibilité. Enfin, l'étude s'est portée sur un modèle intégrant un mécanisme de diffusion non-homogène en mettant en interaction des récepteurs mobiles et leur substrat membranaire. Lorsque des zones restreintes de diffusion ralentie sont définies sur la membrane, deux effets opposés apparaissent sur la dynamique de transduction : un phénomène d'amplification si le ralentissement affecte les deux protéines, et un phénomène de perte de sensibilité si seul les récepteurs sont ralentis. Globalement, les résultats illustrent comment les hétérogénéités spatiales modifient les distributions de collision et d'évènements de réaction dans le temps et l'espace à l'échelle microscopique, et comment cela se traduit par un effet sur la dynamique globale de la voie de signalisation à l'échelle macroscopique.

MOTS-CLÉS :

signalisation, modèle individu-centré, diffusion, marche aléatoire, simulation,
méthodes de Monte Carlo, équation différentielle ordinaire

Laboratoire (s) de recherche :

Laboratoire d'Informatique en Image et Systèmes d'information
LIRIS CNRS UMR5205

Directeur de thèse:

Dr. Christophe RIGOTTI et Dr. Hédi SOULA

Président de jury :

Pr. Guillaume BESLON

Composition du jury :

Pr. Carson C. CHOW, Rapporteur
Dr. Dirk DRASDO, Rapporteur
Pr. Ovidiu RADULESCU, Examinateur
Dr. Christophe RIGOTTI, Directeur de thèse
Dr. Hédi SOULA, Directeur de thèse
Pr. Guillaume BESLON, Examinateur